Tomosyn-1 is a Novel Molecular Target of the Ubiquitin-Proteasome System and Underlies Synaptic Architecture

by

Johnny J. Saldate, Jr.

A dissertation submitted in partial fulfillment
of the requirements for the degree of
Doctor of Philosophy
(Neuroscience)
in The University of Michigan
2018

Doctoral Committee:

Professor Edward L. Stuenkel, Chair
Assistant Professor Asim A. Beg
Professor Richard I. Hume
Associate Professor Michael A. Sutton
Professor Michael D. Uhler

“There was truth and there was untruth, and if you clung to the truth even against the whole world, you were not mad.”

— George Orwell, *1984*

“‘It seems very pretty,’ she said when she had finished it, ‘but it’s *rather* hard to understand!’ (You see she didn’t like to confess, even to herself, that she couldn’t make it out at all.) ‘Somehow it seems to fill my head with ideas – only I don’t exactly know what they are!’”

— Lewis Carroll, *Through the Looking-Glass*

Johnny J. Saldate, Jr.

jsaldate@umich.edu

ORCID iD: 0000-0003-4912-6299

DEDICATION

To my family:

You truly are an inexhaustible source of support and encouragement. This work is dedicated to you, as I could not have accomplished it in the absence of your even greater dedication to me.

ACKNOWLEDGEMENTS

First and foremost, I must acknowledge my thesis advisor and dissertation chair Dr. Edward Stuenkel for his unwavering support of my scientific and professional development and success. Ed is far more than an academic advisor, he has gradually, if not unceremoniously, become a genuine personal mentor and friend. The past six years in his lab, at times working alongside Victor Cazares, Kumar Subramani, Woody Hoerauf, Meredith Njus, Amanda Manly, Jason Shiau, Sam Wing, Simon David, Joe Richards, Nicole Xu, and Erwin Arias-Hervert, have provided countless memorable moments and made my time at the University of Michigan even more fulfilling.

I would also like to acknowledge the following funding sources which have enabled me to undertake these studies, and live comfortably while doing so; The Pre-doctoral Ruth L. Kirschstein National Research Service Award – National Institutes of Health (NIH NRSA, NINDS Grant F31NS087883); Rackham Merit Fellowship, Pre- and Candidate Student Research Grants – Rackham School of Graduate Studies, University of Michigan; Early Stage Training in the Neurosciences – National Institutes of Health (NIH Training Grant T32NS076401); Neuroscience Scholars Fellowship – Society for Neuroscience (SfN); MBL Woods Hole Scholarship – Marine Biological Laboratory (MBL), Conference Travel Grant – Society for Advancing Chicano and Native Americans in Science (SACNAS); Without this support, I feel a significant level of focus on my studies and lab work may have suffered, in part due to financial strain. Furthermore, the non-lab-based professional experiences these opportunities also afforded me ensured that my graduate training was one of substantial growth.

Thank you to each of my dissertation committee members for their continuous consideration and valuable advice; Drs. Michael Sutton, Michael Uhler, Richard Hume, and Asim Beg. Your distinctive strengths have contributed to my success.

Chapter 2 of this dissertation is published in the Journal of Biological Chemistry (https://www.ncbi.nlm.nih.gov/pubmed/29269412), copyrighted by and used with permission from The American Society for Biochemistry and Molecular Biology, Inc. 2017. The following are contributing authors; Jason Shiau, Victor Cazares, and Edward Stuenkel. This study was supported by National Institutes of Health Grants R01NS097498 to Edward Stuenkel and F31NS087883 to myself. We thank Drs. Michael Sutton, Alan Attie, and Uri Ashery for valuable research discussion. We also thank Dr. Christina Whiteus for helpful comments on the manuscript. This research made use of the following University of Michigan core facilities: Vector, DNA

Sequencing, Microscopy and Image Analysis. Thank you all for helping me accomplish my research objectives.

I offer my sincere appreciation to those professional and personal mentors who have contributed to my advancement in both concrete and intangible ways; Drs. Gina Poe, Geoff Murphy, Jill Becker, Phil Esposito, and Pedro Lowenstein. Thank you for your direction, intellectual encouragement, and personal investment.

I am fortunate to have had membership or association with the following University of Michigan student-centered organizations, which expanded my academic and professional worldviews; Rackham Summer Institute, Program in Biomedical Sciences (PIBS), Neuroscience Graduate Program (NGP) Graduate Student Organization, Graduate Employees Organization, Association of Multicultural Scientists, Alliance for Graduate Education and the Professoriate, and Undergraduate Research Opportunities Program.

A special thank you goes out to my University of Michigan NGP and PIBS incoming cohorts of 2011, my MBL Neurobiology student and instructor summer cohort of 2014, as well as the students and staff of the NGP and the Molecular and Integrative Physiology Department. Friends made within these groups are among the best I have ever had.

Another note of love and appreciation is due to my family; Mom, Dad, Krissy Savanna, Evelyn, Grandma and Grandpa, Oma, Gramps and Granny, and so on… You each played a role in getting me here and in my success. I can only hope to make you proud in return for what you have provided me.

Lastly, I must acknowledge the unique and absolutely irreplaceable support of my significant other Dr. Kristin Bradley. You have celebrated, commiserated, and otherwise tolerated the highs, lows, and everything in betweens – by my side, every step of the way. For this reason, you know better than anyone what it has taken for me to reach this milestone in my life, and I am truly grateful that you have maintained such an integral position throughout the process. Your dedication continually inspires me and I love you for it.

TABLE OF CONTENTS

LIST OF FIGURES

FIGURE

ABSTRACT

The efficacy of information transfer at synaptic contacts between excitatory central neurons undergoes continual modification in response to neuronal activity and physiological state. This plasticity in synaptic transmission may involve changes in presynaptic release probability, postsynaptic receptor number and sensitivity, and/or synaptic morphology. The molecular mechanisms influencing these distinctive targets are an investigative focus given their importance in learning, memory, and cognitive function. Much attention has focused on transcriptional and translational regulation of the synapse, but post-translational modification and directed turnover of specific protein components is also recognized as critical. Central to targeted protein degradation is the ubiquitin-proteasome system (UPS). While an increasing number of synaptic proteins are known to be susceptible to activity-dependent regulation by the UPS, relatively little has focused on the action of the UPS on known negative regulators of synaptic function. The SNARE protein Tomosyn-1 (Tomo-1) directly inhibits evoked release at central synapses, but it is also present post-synaptically, where no known function has been identified. It was recently discovered that the related Tomosyn-2 protein is subject to ubiquitination and degradation in neuroendocrine pancreatic beta cells, suggesting their secretory activity may be under control of the UPS. The general hypothesis of this

dissertation is that a central mechanism underlying modulation of the synapse is the targeted degradation of Tomo-1.

This dissertation made use of a series of complementary biochemical, molecular, and imaging technologies in hippocampal neuronal culture. We demonstrate that Tomo-1 protein level, independently of its SNARE domain, positively correlates with postsynaptic dendritic spine density *in vivo*. The data also indicate that the UPS regulates steady-state Tomo-1 level and function. Immunoprecipitated Tomo-1 was ubiquitinated and co-precipitated the E3 ligase HRD1, and both effects dramatically increased upon proteasome inhibition. The interaction was also found *in situ*, via fixed-cell proximity ligation assay. *In vitro* reactions indicated direct, HRD1 concentration-dependent Tomo-1 ubiquitination. Furthermore, we demonstrated that neuronal HRD1 knockdown increased Tomo-1 level, and consequently, dendritic spine density. This effect was abrogated by concurrent knockdown of Tomo-1, strongly suggesting a direct HRD1/Tomo-1 effector relationship. We confirmed Tomo-1 is a UPS substrate by identifying 12 lysine residues which are ubiquitinated by HRD1 and generated a non-ubiquitinateable Tomo-1 mutant. Finally, we performed Tomo-1 isoform and homologue comparisons, protein structure modeling, and antibody-based domain targeting of Tomo-1 in neuronal lysates to identify four lysine residues which are highly likely to be ubiquitinated *in vivo*. In summary, the results of this dissertation indicate that the UPS participates in tuning synaptic efficacy via the precise regulation of neuronal Tomo-1 and spine density. These findings implicate Tomo-1 as a prime target of UPS mediated degradation in the implementation of morphological plasticity in central neurons.

CHAPTER I

Introduction: The proteostasis of synaptic proteins modulates neurotransmission

1.1 Fundamental units: The physiology of synapses

Chemical neurotransmission, namely neurotransmitter release and reception at the synapse, serves an integral function in the efficient transfer of information within the brain. Consequently, the synapse can be viewed as a foundational unit for information encoding in central and peripheral nervous systems. The cellular and molecular mechanisms which underlie synaptic physiology, including both the fusion of neurotransmitter-containing presynaptic vesicles and the resultant activation of postsynaptic neurotransmitter receptors, coalesce to govern interneuronal signaling. Neuronal communication among networks is at least in part responsible for sensory perception, motor function, organismal homeostasis, memory formation and stability, and cognition. Therefore, examination of the diverse regulatory mechanisms which dictate the availability and activity of synaptic proteins is crucial to understanding neuronal biology in health and disease, notably including Alzheimer's and Parkinson's Diseases and Autism Spectrum Disorder.

Calcium-synchronized evoked release

Neurons are highly specialized cells which communicate with exceptional spatial and temporal fidelity to meet a wide range of physiological demands. Upon action potential (AP) initiation at the axon initial segment and orthodromic propagation down the axon, a complex system of biochemical interactions is employed in a step-wise, but extremely rapid fashion at presynaptic terminals (1). This process ultimately results in the fusion of neurotransmitter (NT)-containing synaptic vesicles (SVs) at the active zone (AZ) of the presynaptic membrane, which is directly apposed to the NT receptor-rich postsynaptic density across the synaptic cleft. Amazingly, the extensive biophysical conformational changes and protein interactions required for SV fusion all occur within the timescale of a millisecond (2). The SV fusion process is primarily mediated by cycling interactions of soluble NSF (N-ethylmaleimide-sensitive fusion protein) attachment protein receptor (SNARE) and Sec1/Munc18-like (SM) and Munc13 family proteins (3). These proteins function as biomolecular nanomachines and are driven by AP-mediated presynaptic calcium influx through voltage-gated Ca^{2+}-channels (4). The channels are tethered in close proximity to vesicle release sites by Rab3-interacting molecule (RIM), considered to be a central organizer of the AZ, the small GTPase Rab3, and the exocytosis-essential Munc13 in addition to RIM-binding proteins (5). Rab3 is a member of a large superfamily of GTPase proteins that regulate intracellular membrane trafficking, including of SVs, via membrane associations dependent upon GDP/GTP-cycling (6). This multi-protein module of RIM, Rab3, and Munc13 is reported to facilitate the voltage-gated Ca^{2+}-channels to rapidly conduct calcium ions directly into the presynaptic terminal within hundreds of microseconds (7). Pore opening drastically

increases the calcium concentration within the first ≈ 50 nanometers of the channel, facilitating synchronous neurotransmitter release, which then rapidly drops within the first few hundred nanometers and may contribute to asynchronous release (8). Increased [Ca^{2+}] activates regulatory proteins including the complexins, which act as clamps on release by binding the SNARE core complex, and the calcium sensor family of proteins termed the synaptotagmins, which physically bind calcium via their C2 domains to regulate fusion of the SV with the presynaptic plasma membrane (PM) at the AZ (9). It is to these release sites that the SVs have been recruited or locally recycled. Indeed many are anchored or "docked" in close proximity to the PM via the SM Munc18 (10), which like Munc13, is absolutely essential for neuronal exocytosis. Only a small number of docked SVs are completely fusion-competent or morphologically "primed" (11), awaiting presynaptic terminal depolarization-induced calcium influx. This coupling affords the cell minimal delay in translating an AP to vesicle fusion, ultimately presenting the synaptic cleft with their NT content.

SNARE-mediated vesicle fusion at the active zone

The detailed molecular mechanisms underlying SV fusion with the PM have been extensively investigated over the past three decades, a process in which SNARE-family proteins are essential. SNAREs execute many functions within eukaryotic cells, but are primarily responsible for mediating membrane fusion with target organelles and are most well-studied in neurons in the context of SV targeting and fusion with the presynaptic plasma membrane. There are now upwards of 35 identified SNARE

proteins in humans, which share an evolutionarily conserved motif of 60-70 amino acids, termed the SNARE domain (12). The most well-characterized SNARE proteins in the context of vesicle fusion are the VAMPs (vesicle-associated membrane proteins, also known as synaptobrevins), which span the membranes enclosing synaptic vesicles (so-called v-SNAREs for vesicular, or R-SNAREs for an arginine at the 0 core of the SNARE motif), and the syntaxins and SNAP25, which are also membrane delimited, but are integrated into the PM (t-SNAREs for target, or Q-SNAREs for a glutamine at the 0 core of the SNARE motif) rather than that of the SV (13). VAMP and Syntaxin proteins contain a C-terminal membrane anchor, while SNAP25 contains a cysteine-rich palmitoylated domain between its two SNARE domains which act as pivot points during SV priming, allowing a heterotrimeric trans-SNARE complex comprising four SNARE domains to form between the three proteins – termed the SNARE core complex. The AAA+-ATPase known as NSF is required to disassemble SNARE complexes post-fusion, thereby exerting a functional role in energizing the formation of core complexes. Trans-SNARE core complexes physically link the SV to the PM and ultimately act as engines to drive fusion. SNARE core complexes are highly stable and comprise the release apparatus alongside other membrane-bound and associated soluble/cytosolic proteins such as Munc18, RIM, and RIM-binding proteins in addition to signaling lipids (14). The SNARE proteins then “zipper” from the N-terminal regions of the core complex’s coiled 4-helix bundle toward their C-terminal membrane anchors, which brings the vesicle in direct apposition to the PM and catalyzes *trans*-fusion of the lipid

bilayers. This lipid fusion is then immediately followed by formation of a fusion pore and consequential initiation of NT release directly into the synaptic cleft (15).

Following full collapse of the vesicle, the membranes of the SV and PM are contiguous, and the now *cis*-SNARE complex is recycled by NSF and its adaptor α-SNAP via ATP-hydrolysis-dependent mechanisms. In contrast to full fusion, "kiss-and-run" fusion has been recognized, particularly in large dense core vesicles, as a more transient fusion pore opening event, whereby the vesicle only briefly fuses with the PM and then reseals, allowing it to forgo the more time- and energy-intensive vesicle recycling pathway prior to SV refilling (16). For example, in the event of full fusion, the SV membrane is extracted from the PM via a physical process termed endocytosis, which is primarily dependent upon clathrin and dynamin for invagination and fission (17, 18). These newly re-formed vesicles are then sorted through an endosomal recycling pathway, or in some cases faster reuse is facilitated by local recycling and refilling with NT. The latter of these routes also bypasses some of the extensive cell biological mechanisms which are implemented during vesicle maturation, targeting, and sorting amongst functionally distinct pools.

Synaptic vesicles and their functional pools

Synaptic vesicles are 35-40nm in diameter and are recognized to contain a dense and heterogeneous population of proteins. Notable among these are transmembrane proteins important for NT-loading (e.g. the vesicular glutamate transporters, or vGluTs, in glutamate-containing SVs) and membrane targeting and

trafficking (e.g. VAMP and synaptotagmin). Also present are various adaptor and other membrane-associated proteins such as the synapsins and Rab GTPases (19). Synapsin, an abundant phospho-protein, cycles on and off the SV membrane depending on its phosphorylation state. It is phosphorylated by Ca^{2+}/calmodulin-dependent protein kinase I (CaMKI) and protein kinase A (PKA), and is reported to contribute to the segregation of SVs into distinct presynaptic pools (20). This occurs primarily via synapsin binding with cytoskeletal actin and the vesicles themselves. Within central terminals SVs are functionally categorized into distinct pools based on their release probability following a single or series of action potentials, hypertonic osmotic challenge, or as morphologically determined based on their physical location. The readily-releasable pool (RRP) is the smallest (typically 5-10 vesicles at cortical and hippocampal synapses, or 0.1-2% of the total primed vesicle number (21)), and this pool is rapidly depleted upon high-frequency stimulation. Though in large dense-core vesicles of chromaffin cells of the adrenal medulla may not completely comprise the pool of docked vesicles, as judged by their location relative to the AZ, vesicles of the RRP are nonetheless considered primed given their rapid time constant of release upon stimulation (10-40μs at [20μM] Ca^{2+}) (11). Therefore, not all RRP vesicles appear docked in all systems. A fraction of the RRP is sometimes also considered “pre-primed” or “rapidly releasing” due to their probability of release following basal physiological conditions (22). Next largest is the recycling pool (RP) at approximately 5-20% of the total, though this proportion varies between synapse types and experimental conditions such as temperature and cell preparation. These vesicles maintain release when

stimulated at moderate physiological frequencies and timescales. Finally, the largest pool (at approximately 80-95%) is known as the reserve or resting pool, which may act to increase or decrease the size of the RP and serves as an SV reservoir to refill the RRP during and following extended high-frequency stimulation or sustained depolarization. There is also what is considered an unprimed pool (UPP), which is comprised of vesicles that reside in the presynaptic terminal and near the AZ, yet are unable to undergo synchronized exocytosis upon calcium influx. Instead vesicles of the UPP are released asynchronously, more slowly and constantly on the timescale of several seconds (23). The summing of each pool's properties gives rise to three kinetic modes of physiological SV exocytosis; a synchronous, a non-synchronous, and a spontaneous phase of release. It is important to note that each pool is dynamically tuned during and following activity via mechanisms that are not entirely understood. However, the local recycling of previously fused vesicles and the delivery and processing of nascent vesicles to the terminal are essential for SV pool maintenance and, consequently, efficient NT release.

Postsynaptic signal reception

The acute increase in neurotransmitter concentration present in the synaptic cleft following presynaptic SV exocytosis, most commonly glutamate in central excitatory synapses, acts directly on postsynaptic NT receptors. This process is more straightforward than vesicle fusion in the sense that activation of ionotropic transmembrane receptors, such as a class of glutamate receptors (GluRs), directly and

non-selectively conduct cations into the postsynaptic terminal. For example, glutamate-sensitive AMPA (α-amino-3-hydroxy-5-methyl-4-isoxazolepropionic acid) receptor (AMPAR) permeability for sodium, potassium, and especially for calcium vary depending upon the channel's subunit composition (24). Kainate (or kainic acid) receptors have similar conductances to AMPARs though they are typically slower and can have a lower conductance for Ca^{2+} in particular. Conversely, NMDA (*N*-methyl-D-aspartate) receptors (NMDARs), which require glycine as a co-agonist and are blocked in the open state by Mg^{2+} at negatively polarized membrane potentials, have a high Ca^{2+} permeability (25). GluRs in most excitatory central neurons are responsible for postsynaptic current production, and with reversal potentials around 0mV, they depolarize the postsynaptic cell toward AP threshold. Their activation also causes postsynaptic intracellular signaling mechanisms which are involved in neuronal maintenance and homeostasis, protein translation, and plasticity induction.

1.2 The adaptive brain: Hebbian and homeostatic plasticities in excitatory neurotransmission

An essential capacity of the brain is the establishment, maintenance, and reactivation/recall of use-dependent changes in neuronal morphology and activity – termed neuroplasticity. Plasticity is enacted on various scales, from individual subcellular compartments such as dendritic spines and/or presynaptic boutons, to networked ensembles of neurons, to whole brain regions and their interconnections. The most well-studied source of plasticity induction is activity-dependent, whereby a

stimulus modifies the activity of neurons and circuit formation and function, subsequently influencing memory, thought, emotion, and/or behavior. Indeed, converging theories on the physiological basis of memory describe its encoding as dependent upon the synchronized activity of specific spatio-temporal patterns of neural networks. Furthermore, the growing number of pathological cognition, motor function, learning, and memory issues apparent in various forms of neurological disorders and diseases are known to be associated with deficits in neuronal plasticity. For this reason, thorough examination and understanding of the mechanisms underlying plasticity are vital to the advancement of neuroscientific research and human health.

Long-term facilitation and depression

Neuronal plasticity is one of the most extensively studied phenomena of the nervous system. It is categorized into short- and long-term, depending on its persistence (26). Short-term plasticity (STP) lasts milliseconds to minutes and is thought to heavily depend on the acute regulation of ion channel function through post-translational modifications (PTMs) and the parameters of presynaptic Ca^{2+} entry and intracellular [Ca^{2+}], with post-tetanic potentiation also relying in part on presynaptic intracellular [Na^{2+}] (27). Long-term plasticity has been observed to last minutes to years, and is thought to rely on Ca^{2+} signaling, protein kinase activity, and mRNA synthesis and protein translation (25). Feedback-based alterations in the function of neurons are not specific to but are ubiquitously expressed in cortical and sub-cortical structures of vertebrates. These so-called Hebbian forms of plasticity, those which strengthen or

weaken in their efficiency depending on coincident pre- and post-synaptic activity, operate under a positive-feedback system. That is, networks subject to Hebbian plasticity are typically strengthened upon increased coincident activity and dampened following non-correlated. These robust alterations contribute to the reliable and efficient transfer of information while allowing for flexibility to an organism's non-static environment.

For example, long-term potentiation (LTP) is a form of synaptic strengthening originally identified following brief high-frequency stimulation of hippocampal afferents from neocortical areas (28), though it is now recognized to occur in potentially all regions of the brain and across a multitude of species (25). However, if occurring unchecked, LTP would be of no great consequence to the nervous system as a strictly feedforward loop. Not surprisingly, evolution has also afforded the ability for activity-dependent and selective downregulation of the efficacy of neurotransmission. This counterpoint to LTP's increase in presynaptic firing and postsynaptic response is known as long-term depression (LTD). LTD is most well-studied in the Schaffer-collateral synapses of the CA1 region of the hippocampus, where it is reliably induced upon extended low-frequency stimulation (0.5-3Hz) (29). Amazingly however, LTD was originally identified to occur in separate hippocampal inputs following the same stimulus that induced LTP in others (30). LTP and LTD can therefore be conceptualized as more a spectrum than discrete phenomena. Indeed, there are a multitude of sub-categories of LTP and LTD. Those which differ by induction site (i.e. pre- versus post-synaptic) may employ unique mechanisms in their implementation, yet produce the same outcome.

This further supports the hypothesis that an interplay between differential sites of induction is important, a notable example of such is spike-timing dependent plasticity (STDP). STDP results from the association between the timing of presynaptic activation versus that of the postsynaptic response (31). Importantly, STDP determines both the sign and the magnitude of LTP and LTD, potentiation occurring when presynaptic precede postsynaptic spikes and depression occurring when postsynaptic activity precedes presynaptic input. It is therefore concluded that LTP and LTD together, through local and global mechanisms within individual neurons and their networks, exert influence on higher order cognition, including memory. Furthermore, it may be a futile attempt to identify *the* mechanistic crux of memory induction - as there is likely no *single* point of master regulation. Instead, the brain implements an intricate balance of molecular biochemical, cell, and systems level phenomena, each subject to the mathematical principles of chaos and control theories, toward the establishment of complex and emergent physiological properties. Perhaps there are specific circuits or networks that must be specifically temporally or spatially activated to induce the formation, stabilization, or pruning of memories (i.e. those during sleep). Nonetheless, Hebbian forms of use-dependent, associative plasticity are considered to be the putative biological substrates of learning and memory. Relatedly, STP may be critical in affording the circuit temporary up- or down-regulation to drive the induction of LTP or LTD as an ultimate outcome of continuous and transient STP mechanisms. Consequently, examples of Hebbian plasticities, including LTP and LTD, are well-

represented in the examination and evaluation of memory and experimental models thereof.

Homeostatic synaptic plasticity

Comparatively, homeostatic plasticity, the cell-intrinsic stabilization of synaptic activity following persistent deviation from an innate baseline level or "set-point," is hypothesized to retain efficient information transfer capabilities in neurons by maintaining a dynamic range which encompasses the steady-state baseline activity (32, 33). The homeostatic process may then subsequently allow for acute variation in activity upon demand, for example, during memory induction. The functional activity of neurons, in this case action potential output, appears under constant internal modulation around a point of reference. This set-point is hypothesized to result from the summation of intrinsic parameters including cell size and morphology as well as the complement and subunit composition/individual conductances of various ion channels (34). Existence of a or multiple sensors to monitor cell electrical state is therefore assumed, by which detection of out-of-range electrical activity triggers responsive mechanisms. This feedback control is a hallmark of homeostatic regulation and the subject of intensive research, primarily in relation to cell-intrinsic excitability, presynaptic release, and postsynaptic reception.

Originally identified in electrophysiological studies of cultured neurons, so-called synaptic scaling was observed to occur following extended pharmacological up- or down-regulation of neuronal activity (35). Persistent voltage-gated sodium or $GABA_A$

channel blockade decreased and increased neuronal activity, respectively. What is now recognized as homeostatic plasticity induction then occurred, whereby the postsynaptic cell increased or decreased its reception capabilities accordingly and reestablished intrinsic activity. These types of studies are still used in evaluating the mechanistic underpinnings responsible for resumption of baseline activity. Experimental approaches have also since expanded in scope to explore bidirectional contributions, that is, the pre-to-post anterograde signaling and post-to-pre retrograde signaling mechanisms involved. At mammalian central synapses the two main components hypothesized to facilitate homeostatic induction are presynaptic action potentials and protein translation. Depending on the system, homeostatic regulation is also now known to include effects on DNA transcription, protein translation, receptor trafficking, presynaptic release probability, and post-translational modifications, and may even be differentially enacted in individual synapses or classes of synapses within a single neuron (36). It is important to note that Hebbian and homeostatic forms of plasticity operate concurrently and are thought to exert influence over each other, though their timescales can vary (37, 38). Growing evidence suggests that induction of one form may shift the probability of future induction of the other. This interplay between Hebbian and homeostatic plasticities, maintaining cell adaptability while stabilizing intrinsic activity, is an area of intense investigation termed metaplasticity (39).

Mechanisms of plasticity induction

Hebbian and homeostatic plasticity have been extensively examined through a reductionistic lens to gain insights into their cellular and molecular mechanisms (40, 41). Notable findings from these studies have identified numerous specific proteins, distinct morphological domains, and critical cell biological processes which are required or substantially impact plasticity induction and maintenance. Many of these mechanisms regulate both Hebbian and homeostatic plasticity, however key differences will likely be identified upon more nuanced experimental design in combination with higher precision research tools, such as genetic targeting of light-activated ion channels and specific microRNA and small-molecule-mediated inhibition of target substrates.

Regulation of presynaptic terminal physiology allows for alterations in NT release through multiple mechanisms. The small GTPase Rab3, in addition to crucial effector proteins Rab3GAP and RIM1α, have been shown to influence both Hebbian induction in mice (42) and homeostatic induction in Drosophila (43). Because RIM1 anchors calcium channels in close proximity to the AZ, and is an effector of Rab3 and its activating protein Rab3GAP, which affects SV allocation into/out of the RRP, pool sizes and their related release probability are likely important and currently unappreciated methods of plasticity induction. However, it is at present unclear which homeostatic mechanisms identified at the Drosophila NMJ will be recapitulated with those of mammalian excitatory neurons of the CNS. Relatedly, the microRNA known as miR-458 targets the vesicle protein SV2A in the presynaptic downregulation induced by prolonged increases in activity in dissociated hippocampal culture (44). SV2A is reportedly important for

spontaneous vesicle release from these neurons and has been shown to indirectly influence postsynaptic spine density through this presynaptic mechanism.

Postsynaptic mechanisms are more thoroughly-defined in the context of excitatory synaptic plasticity. The abundance of AMPARs in postsynaptic spines, the direct receivers of presynaptic input from across the synaptic cleft, is controlled via their insertion into or removal from the postsynaptic density (24, 45). The scaling of synaptic strength following homeostatic challenge has been examined in this context, indicating some overlapping AMPAR-related mechanisms as compared with Hebbian induction (46, 47). AMPAR-mediated changes in postsynaptic signal reception are partially controlled by the immediate early gene Arc/Arg3.1, which is involved in the structural and physiological competence of postsynaptic dendritic spines (48) and influences both Hebbian and homeostatic plasticity. Postsynaptic depolarization also repels pore-blocking Mg^{2+} ions from NMDAR channels, increasing Ca^{2+} influx and the internal $[Ca^{2+}]$, which is often required for LTD and LTP induction. However, there is some question as to what extent LTD strictly requires an increase in postsynaptic calcium concentration (169). Furthermore, NMDAR activation upregulates the activity of the abundant kinases PKA, PKC, and CaMKII, triggering the phosphorylation of AMPAR reserves and their insertion into the postsynaptic membrane (49, 50), in addition to influencing their gating and ultimately modulating its intrinsic excitability. A growing body of evidence also highlights the importance of a retrograde signaling molecule, brain derived neurotrophic factor (BDNF), which is prompted by the mechanistic target of rapamycin complex 1 (mTORC1) upon post-synaptic inactivation to induce its local and

rapid translation within postsynaptic dendrites, functionally serving as a retrograde signal to induce compensatory increases in presynaptic function (51-53). It is presently unclear via what presynaptic mechanism compensatory changes are enacted, though the post-translational ubiquitination of proteins including AMPAR subunits within the postsynaptic cell appear important for sustained homeostatic plasticity in the same mammalian hippocampal culture system (54).

The post-translational modification of protein substrates, such as ubiquitination and phosphorylation, in both pre- and post-synaptic compartments is indeed an integral layer of control in the establishment of Hebbian and homeostatic plasticity. Action potentials in the presynaptic neuron trigger the cAMP-dependent protein kinases PKA and PKC, which in turn respond to elevated calcium concentrations and phosphorylate major potassium channels, reducing the rate of membrane repolarization, and other molecular mediators in the exocytotic pathway to enhance glutamate release. Presynaptic PKA is also retrotranslocated to the nucleus, where it activates the transcription factor cAMP response element binding protein-1 (CREB-1) to upregulate protein synthesis and form new synapses. Furthermore, ubiquitin and ubiquitin-like modifiers (ULMs, also known as ubiquitin-like proteins (ULPs)) such as the small ubiquitin-like modifier (SUMO) and NEDD8 proteins are critical in the maintenance of cellular and synaptic physiology (55-60). Ubiquitin modifications are specifically important for the targeted regulation of protein levels, as will be described in detail in the following section.

1.3 A molecular lifetime: Regulated protein turnover in neurons

An extensive literature has focused on the control of protein production and degradation mechanisms and their physiological impact on the development, health, and plasticity demands of the nervous system. Protein homeostasis (proteostasis) is a fine balance between two complementary systems which, together, continuously adjust the production and degradation of proteins within the cell. The functional result of these complex and coupled regulatory networks is the capability to, both globally and locally, preserve the neuronal proteome in a state which meets the current and/or future functional demands of the neuron.

As it is central to the hypothesis of this dissertation, we now focus attention on regulatory mechanisms in neurons related to the turnover of synaptic proteins. Most intracellular proteins are subject to regulated degradation, which can occur on the timescale of minutes, to decrease their levels in a rapid and robust fashion even during continued production of new proteins. The mechanistic understanding of how targeted protein degradation influences their turnover rate and subsequently their abundance has advanced quickly. However, how the regulation of proteostasis via degradation directly impacts downstream neuronal physiology and plasticity, especially in consideration of the synapse, is of significant importance.

Degradative and proteolytic systems

Proteolysis, or the inactivation and enzymatic breakdown of protein and peptide substrates into their constituent amino acid components, is mediated by a variety of proteases which together comprise multiple regulated degradative pathways. Just as

substrate protein populations vary enormously in composition, size, conformation, abundance, subcellular location, and function, the proteases which control their degradation are diverse. The two primary proteolytic systems in eukaryotic cells are the autophagy-lysosome system and the ubiquitin-proteasome system. Both govern protein degradation alongside synthesis to set and maintain the level of proteins within the cell. The UPS appears to regulate 80-90% of all intracellular proteolysis (61), while autophagy is responsible for approximately 10-20% (62, 63), though cell-type and state influence their activities. Autophagy and the UPS act concurrently and both operate using the ubiquitin molecule and ubiquitin-binding domains (UBDs) toward regulated protein degradation. However, autophagy and the UPS are distinct in their mechanism of proteolysis, ultimately operating as unique processes. The autophagy and lysosomal degradation of proteins is primarily a bulk mechanism through microautophagic invagination of the lysosomal membrane and cytoplasmic constituents, though substrate delivery to the lysosome can occur via chaperoning (64). During conditions of cellular stress, such as starvation, the cell may also utilize macroautophagy, whereby non-cytosolic components such as mitochondria and the endoplasmic reticulum (ER) are engulfed into lysosomes. In contrast, the UPS affords more selective targeting of substrates for degradation, including specifically those which are over-abundant, misfolded, aggregated, or otherwise detrimental to the cell (63).

Though the UPS operates in a dynamic fashion, its activity is strictly governed by a functional class of enzymes which act in series and parallel to identify, tag, target, and degrade the majority of intracellular proteins. As such, these UPS components serve as

a “chemical barrier” between active proteases and proteins of the cytosol, a mechanism utilizing specific targeting rather than a physical barrier, such as the membrane separating the acidic and protease-rich internal environment of the lysosome lumen from the protein-containing cytosol. Work in reticulocytes, maturing red blood cells which have expelled their lysosomes, allowed for the controlled examination of non-lysosomal degradative pathways, as it was noted that reticulocytes have the capacity to rapidly and specifically degrade mutated or unassembled hemoglobins (65). This process was later shown to occur in an ATP-dependent manner, and most effectively at a neutral pH (66). This work indicated that non-lysosomal cellular activity was likely responsible for the selective degradation of proteins, which helped to explain the extensive variation (minutes to days) in protein half-lives observed by many cell biologists and biochemists.

Some of the first evidence substantiating selective protein degradation in mammals was discovered by Rose, Hershko, and colleagues in the late 1970s, which challenged the pervasive assumption that most intracellular proteins were long-lived and degraded by the lysosome (67). These studies built upon observations in prokaryotes and eukaryotes from the previous three decades, primarily regarding the growing consensus that proteins operate in a dynamic state as a result of their synthesis and degradation rates. Seminal work in identifying the nature of regulated degradation was carried out by Aaron Ciechanover, as a graduate student in the lab of Avram Hershko, at the Technion Institute in Israel in 1978. The main conclusion of this early work was that proteolysis is not carried out by a single protease, but rather

multiple components which were differentially purified from rabbit reticulocytes (68). This group went on to further discover a small, heat-stable, 76 amino acid protein was covalently conjugated to protein substrates prior to an ATP-dependent process of degradation (69, 70). This ATP-dependent Proteolytic Factor 1 (APF1) was soon identified to be ubiquitin, whose covalent attachment necessarily preceded the ATP-dependent proteolysis of many proteins. It was concluded that the addition of ubiquitin to a substrate protein acted as a "tag", often marking the protein for degradation. This conclusion added a layer of potential specificity to the then-current models of proteolysis in that it afforded a reversible and specific mechanism (ubiquitination) to the irreversible and non-specific (proteolytic scission) framework already in place (71). This early work provided further valid evidence supporting an explanation for how both the mediators and targets of proteolysis coexist and are operable within the same cell compartment of the bulk cytosol in that it comprised a selective barrier. The post-translational modification of protein substrates by covalent addition of ubiquitin molecules and their subsequent degradation by the proteasome, well-known now as the Ubiquitin-Proteasome System (UPS) or the Ubiquitin-Proteasome Pathway (UPP), has since been extensively studied. Furthermore, the foundational research, discovery, and examination of the mechanisms and functions of the UPS by Hershko, Ciechanover, and Rose was awarded the Nobel Prize in Chemistry in 2004.

Introduction to the Ubiquitin-Proteasome System

The UPS is a selective degradation system utilizing the small molecule termed ubiquitin, named as such because it was found to be expressed in all eukaryotes prior to the identification of its function. Many detailed reviews of the general (67, 72-76) and nervous system-specific (77-82) mechanisms and effects of protein ubiquitination and degradation by the UPS exist, and what follows is a brief summary of the current views on this process, with selected findings highlighted based on specific relevance. The substrate selectivity of the system results from its multistep utilization of enzymes and cofactors, commonly referred to as the "enzymatic cascade". The covalent attachment of a ubiquitin moiety to its target substrate is most commonly termed ubiquitination, but also ubiquitylation, and requires upstream activation and downstream handling of the ubiquitin small molecule. The cooperation of three classes of enzymes are primarily responsible for substrate ubiquitination, generally known as ubiquitin-activating enzymes (E1s), ubiquitin-conjugating enzymes (or ubiquitin-transferring enzymes, E2s), and ubiquitin ligases (E3s). These components, and their various identity-specific interdependencies, afford further fine-tuning of substrate selectivity throughout the process. Ubiquitination of a protein with the ultimate intent of degradation often occurs at specifically targeted lysine residues via stereotyped multi-ubiquitin linkages and poly-ubiquitin chains. Using poly-ubiquitin chains as molecular tags, the cell targets the protein for recognition and proteolysis by the large, multi-subunit complex known as the 26S proteasome, whereby the substrate is cleaved into short poly-peptides of between 3-32 amino acids in length and the ubiquitin molecules are recycled for further use.

Following cellular identification of protein substrates for degradation, including those which are terminally misfolded, aggregated, non-functional, and/or damaged, ubiquitination and chaperones are employed for initiation of the UPS toward rectifying the imbalance (83). The ubiquitin molecule is first activated by an E1 through the use of ATP to form ubiquitin adenylate. The ubiquitin molecule is then transferred to an E2 via a thioester bond and prepared for handling alongside an E3. Some E2s directly link ubiquitin to the target protein with or without recruitment of an E3 as a substrate-selective adaptor. In other cases, an E3-ubiquitin thioester intermediate is formed prior to the transfer of ubiquitin from the E2 to the E3, again utilizing the E3 for substrate specificity (72). Each step in this cascade provides for further substrate selectivity and accuracy, as some E3s have varying affinities for different individual or classes of upstream E2s as well as downstream protein substrates. For example, UbcH8, a human E2, interacts with parkin and E6-AP, whereas a similar E2, UbcH5, functions specifically with Rsp5 and BRCA1-BARD1 (84). The honing of substrate specificity is finer at the single protein scale, which have canonical lysine residues which are ubiquitinated under certain conditions and by the action of particular E2-E3 combinations. Amino acid sites of ubiquitination, especially in cases where ubiquitination leads to protein degradation, are overwhelmingly lysines, but also occasionally a serine, threonine, or cysteine (85). A notable example of regulated degradation following ubiquitination of a protein substrate at specific lysine residues occurs by the E3 ligase known as neural precursor cell expressed developmentally down-regulated 4 (Nedd4), which ubiquitinates neuronal glutamate receptors, specifically Lysine-868 of the AMPA-type glutamate receptor

subunit 1 (GluA1) C-terminus, which results in receptor internalization and degradation (86). After initial ubiquitination of a protein substrate, additional ubiquitin moieties can be added to any number of the seven lysine residues of ubiquitin, beginning a poly-ubiquitin chain. Chain elongation primarily occurs via the iterative addition of additional ubiquitin molecules to those which are already linked which, dependent upon the poly-ubiquitin chain structure and length, determines the substrate's fate.

Poly-ubiquitinated proteins, specifically those with multi-ubiquitin chains of K48 and K63 ubiquitin linkages, are then degraded by the 26S proteasome complex. The 26S proteasome contains a catalytically active, cylindrical 20S core apposed on each end by a 19S regulatory particle (87). Molecular catabolism of poly-ubiquitinated proteins occurs by the central 20S core. The 20S core is comprised of two outer rings, each with seven alpha subunits and two inner rings, each with seven beta subunits, three of which (ß1, ß2, and ß5) are required for its catalytic activity. Unfolded substrates are recognized by the 19S regulatory particle and passed through a pore of roughly 13 ångström diameter (88), which is size-restrictive for all but unfolded substrates, into the catalytic core. Evidence most strongly supports protein unfolding is accomplished by 19S ATPases, comprised of six regulatory ATPase subunits (Rpt 1-6) in addition to four non-ATPase subunits (Rpn 1, 2, 10, and 13) (89). Usp14 (or Ubp6) has been shown to reversibly associate with Rpn1 to initiate protein degradation via deubiquitination (90, 91). The poly-ubiquitin chains themselves are not cleaved, but detached and disassembled by one of two classes of deubiquitinating enzymes (DUBs). DUBs are most commonly differentiated by their size and contain varying intrinsic substrate

specificities. Low molecular weight DUBs are also known as ubiquitin C-terminal hydrolases (UCHs), conversely, high molecular weight DUBs are termed ubiquitin-specific proteases (USPs, or UBPs) (84). The lid of the 19S regulatory particle contains nine non-ATPase subunits (Rpn3, 5, 6-9, 11, and 15) (92) and has shown deubiquitinase activity by Rpn11 (Poh1) and 13 (Uch37) during substrate unfolding and insertion into the catalytic chamber through the pore. Furthermore, the proteasome complex is itself subject to post-translational modification in regulation of its activity, including phosphorylation (93).

E3 ubiquitin ligases and target specification of the UPS

The dynamic regulation of cellular function requires targeting of specific protein substrates for ubiquitination and subsequent degradation. Substrate specificity is primarily implemented via a diverse population of E3 ubiquitin ligases. Neuronal E3s are expressed throughout the cell and localize to the nucleus, golgi apparatus, endoplasmic reticulum (ER), dendrites, axons, and synapses. Their subcellular localization is thought to contribute to the recognition of and reaction to intrinsic and extrinsic cues, in some cases allowing for local and rapid regulation. E3s, like other examples of post-translational protein modification, regulate many aspects of cellular physiology, including proper cell proliferation and differentiation, gene expression and DNA repair, apoptosis (81), and importantly, neuronal morphology and synaptic activity and plasticity (77, 79).

E3s can function individually or in protein complexes and either as an intermediate substrate, itself directly catalyzing ubiquitin transfer to the target after accepting it from an E2, or by bringing together an E2-ubiquitin conjugate and its target. The over 800 E3s encoded by the human genome can be categorized into two large classes, which are differentiated by their catalytic domains, and therefore their mechanisms of ubiquitination and degradative control (94). The former, intermediate acting group are termed HECT domain ligases (for homologous to E6-AP carboxyl-terminus), and the latter, E2-to-substrate paring group are known as RING finger ligases (for really interesting new gene). The RING finger E3s alone are represented by over 600 gene products in humans (95), denoting their potential for high target specification in directing protein ubiquitination. Later identified was a third class of E3s with the so-called U-box domain, also referred to as E4s in that they provide ubiquitin chain elongation (96), though these are more often considered to be modified RING-finger domains. Six of these factors were originally identified to be capable of catalyzing the ubiquitination of mammalian substrates with dependence on E1 and various E2s but in the absence of any HECT- or RING-type E3 (97, 98), further implying they have E3 activity. In addition to the extensive number of identified and predicted E3s, many studies have implied further intrinsic E3 specificity results from the distinct subcellular localizations of many E3s throughout neuronal and synaptic development, maturation, and maintenance (81).

Neuronal and synaptic effects of the UPS

It is recognized that E3 ubiquitin ligases are especially important in the function of neuronal cells and signaling, and extensive evidence indicates this includes perturbed physiology and disease states in addition to normal function. For example, HECT domain E3s were discovered to be a class of ubiquitin ligases with a homologous C-terminal region to E6-AP (known as UBE3A in humans), which ubiquitinates the tumor suppressor protein p53 in HPV-infected cells (99) and when defective in humans, causes the neurodevelopmental disorder termed Angelman Syndrome. Patients suffering from Angelman syndrome display severe intellectual disabilities beginning in early development (100, 101), and a mouse model of the disease shows impaired LTP and spatial learning (102) likely due to synaptic ubiquitination of the AMPAR endocytosis and plasticity-related protein Arc (activity-regulated cytoskeleton-associated protein, also known as Arg3.1) (103). RING finger domain E3s can be sub-divided into two classes, based on their containing either a single subunit, for example Mdm2 (for mouse double minute 2), or multiple subunits, such as APC (for anaphase-promoting complex, also known as cyclosome and APC/C). Mdm2 is known to ubiquitinate the synaptic scaffolding protein PSD95 (104) to influence signal reception, and APC plays an important role in the differentiation (105) and size (106) of presynaptic sites, in addition to dendrite morphogenesis (107).

As previously mentioned, the UPS regulates the activity of critical neuronal cell systems, for example, the abundance of PKA regulatory subunits. However, there is also a wealth of evidence indicating more acute control of neuronal proteins which directly influence their neuronal function and activity. The degradation of presynaptic

components is the topic of intensive study, as this process can regulate neurotransmitter release and plasticity. For example, the presynaptic vesicle associated proteins RIM1α and syntaxin1, which are both critically important in neurotransmitter release, are known targets for proteasomal degradation (108, 109). Syntaxin1 is specifically targeted for ubiquitination by the E3 ligase staring, though its physiological significance in living neurons has yet to be evaluated. Additionally, the E3 known as SCRAPPER was shown to regulate the levels of the presynaptic scaffolding protein RIM1α to modulate synaptic transmission by modulating release probability, as measured by miniature excitatory postsynaptic currents (mEPSCs) in culture, and also affecting short-term plasticity in mice (108). It is furthermore hypothesized that activity of the proteasome contributes to the maintenance of synaptic vesicle pools, as their inhibition increases the recycling pool size but not neurotransmitter release probability in cultured neurons (110). This effect was occluded by concurrent pharmacological neuronal activity blockade. Proteasome blockade also increased mEPSC frequency, but not amplitude, indicating an importance for the presynaptic terminal to maintain proper proteostasis via proteasomal degradation in mammalian hippocampal neuronal culture (111). Relatedly, Dunc-13, the drosophila ortholog of mammalian Munc-13, a presynaptic priming protein, is degraded by the proteasome to control the number and output of presynaptic terminals at the drosophila neuromuscular junction (112). It is unclear under what circumstances or physiological states cue the degradation or stabilization of key presynaptic proteins. However, these notable examples of UPS-mediated control over the abundance of crucial proteins involved in presynaptic

physiology indicate the importance of further examining this system for a more comprehensive understanding of changes in protein homeostasis that may affect synaptic morphology, number, and/or function.

There is also significant evidence indicating the degradative regulation of postsynaptic protein levels by the UPS, primarily regarding the regulation of neurotransmitter receptors and related scaffolding proteins (113). Ubiquitination of membrane receptors, most frequently via K63 linkage types, often leads to their internalization and ultimately either; recycling and reinsertion into the postsynaptic membrane following deubiquitination by DUBS (114), sorting and degradation by the lysosome (77), or degradation by the proteasome (72). Simple inhibition of proteasome-mediated degradation via pharmacological blockade in cultured hippocampal neurons indicates an overall decrease in AMPAR internalization (115). Additionally, the postsynaptic scaffolding protein PSD95 is subject to degradation prompted by the UPS, which itself leads to AMPAR internalization (104). Slice culture experiments from the same study indicated a decrease in LTD following pharmacological proteasome blockade. UPS control over postsynaptic physiology and plasticity is not limited to excitatory systems, as GABA (116) and Glycine (117) receptors are also ubiquitinated, internalized, and degraded by the proteasome. Further study into the activity states and cell biological pathways underlying regulated protein turnover in neurons is paramount to a more comprehensive understanding of how the UPS influences neuronal and synaptic physiology.

Regulatory actions of the RING-type E3 ubiquitin ligase HRD1

One mechanism by which neurons, as well as other cell types, regulate misfolded, mutated, or perturbed protein expression levels is via ER-associated degradation (ERAD). ERAD is the crucial process whereby targeted ER, secretory, and related proteins are retro-translocated through the membrane into the cytosol prior to their deubiquitination and degradation by the proteasome. Disturbances in ER protein homeostasis cause ER stress, which activates the unfolded protein response (UPR) to alter the expression of many genes involved in ER quality control. One of those upregulated genes encodes an important RING-type E3 termed HRD1 (also known as Hrd1p, Der3p, and synoviolin), an ER-resident, transmembrane ubiquitin ligase required for ERAD (118). HRD1 serves as the central component of the large, multi-protein complex that facilitates the degradation of ERAD substrates, which are most often misfolded, damaged, or aggregated. Cryoelectron microscopy data support that HRD1 creates an ER-transmembrane pore, likely acting as a protein channel, in complex with the related HRD3 (119). This channel formation may be prompted by HRD1 auto-ubiquitination (120), though a lack of HRD3 is also hypothesized to cause unrestricted self-degradation of HRD1 (121). The catalytic ligase activity of HRD1 emerges from its various interdependent subunits and domains. HRD1 is comprised of an eight-spanning transmembrane domain, a cytosolic RING-finger domain, and an evolutionarily conserved but intrinsically disordered HAF-H domain, which engages co-factors in the cytosol (122).

The HRD1-containing complex also contains SEL1L, which is stabilized by HRD1, whose transmembrane domain may regulate HRD1 function (123). Relatedly, OS-9, a lectin responsible for binding terminally misfolded non-glycosylated proteins and improperly folded glycoproteins, is hypothesized to retain its targets at the ER and transfer them to the HRD1 ubiquitination machinery (124-127). Recently, two major high-molecular-mass complexes containing HRD1 were identified, each with distinct interacting proteins and variable stoichiometries, indicating heterogeneity in the functional units of HRD1-mediated protein degradation (128). The composition and stoichiometry of HRD1-containing complexes are heavily influenced by HRD1 expression levels. As such, HRD1 is itself strictly regulated within the cell. It is a substrate for the DUB known as ubiquitin-specific protease 19 (USP19), which deubiquitinates HRD1 and promotes its stabilization by inhibiting degradation (129). HRD1 is also targeted for degradation by the related E3 GP78 (130).

HRD1 has been shown to specifically ubiquitinate dozens of proteins (131), often having anti-aggregation effects on proteins and an overall anti-apoptotic effect on the cell. Importantly, while HRD1 is well-recognized for regulating biosynthetically ER-targeted proteins, it has also more recently been reported to regulate several cytosolic proteins, presumably due to cytosolic capture and delivery. These include the tumor suppressor protein p53 (132, 133) and optineurin (134), a cytosolic protein involved in the maintenance of the Golgi complex, membrane trafficking, and exocytosis in neuronal cells (135). Furthermore, ER stress causes the aggregation of proteins, most of which are not ER or secretory pathway proteins. Proteomic analysis of aggregated

proteins has revealed enrichment of intrinsically aggregation-prone proteins, rather than those which are affected in a stress-specific manner (136).

HRD1 has several reported regulatory actions that are likely functionally important in neurons. The upregulation of HRD1 expression resulting from ER stress inhibits neurite outgrowth and dendritic arborization in differentiated neurons, and knockdown (KD) of HRD1 abolished these effects (137). Relatedly, HRD1 facilitates the degradation of components of the synaptic proteome, including the Parkin-associated endothelin receptor-like receptor PaeIR (138), and tau and p-tau to promote neuronal survival by inhibiting protein aggregation (139). HRD1 can also target pathogenic poly-glutamine expanded huntingtin protein (httN) for degradation, thereby protecting cells against httN-induced cell death (140). Taken together, these findings highlight the potential for HRD1-mediated control of protein turnover as a critical mechanism of neuronal and synaptic physiology.

Preview to the dissertation: Tomosyn as a prime target for mediating UPS-dependent synaptic plasticity

Activity-dependent alteration of the structure and activity of synapses linking neurons into functional networks is foundational to their capacity for encoding, storing, and relaying information. A balance of local *de novo* protein synthesis and targeted protein degradation within these synapses promotes long-lasting changes in synaptic efficacy that are maintained well-beyond the induction period (77, 141-143). For example, the mTORC1 signaling pathway is induced in postsynaptic dendrites in an

activity-dependent fashion to regulate protein translation (144) and mediate the long-lasting plasticity required for some forms of learning/memory (145, 146) and synaptic adaptations (52, 147). Downstream effects mediate a retrograde signal to retune neurotransmitter release and reception through an unidentified mechanism which is partially dependent upon activity of the proteasome via UPS-mediated degradation (54).

The central hypothesis of this dissertation is that a synaptic molecular mechanism underlying neuronal plasticity is Tomo-1. Furthermore, we hypothesize that this plasticity may result from currently unidentified postsynaptic actions of Tomo-1 following the specific upregulation of Tomo-1 ubiquitination by HRD1 and subsequent proteasomal degradation (see Fig. 1.1). In examination of this hypothesis I test for downstream effects of the newly-identified regulation of Tomo-1 proteostasis by HRD1, including consequential synaptic morphology. Testing this hypothesis allows for significant advancement of the understanding of a central mechanism by which pre- and post-synaptic terminals are functionally integrated and cooperatively implement locally-mediated plasticity. Further informing our comprehension of this process will significantly advance the field by contributing novel mechanistic insight into the molecular underpinnings of these coordinated, trans-synaptic pathways.

Notably, Tomosyn proteins are also correlated with neurological disorders including as autism spectrum disorder (ASD), intellectual disability, and epilepsy (151-153). Tomosyn proteins are encoded by two genes in mammals, Tomosyn-1 and Tomosyn-2, and differentially spliced into seven protein isoforms (154). They are generally considered to be inhibitors of membrane fusion, specifically, evoked vesicle

fusion from neurons and neuroendocrine cells. Indeed, overexpression of Tomo-1 in neuronal cells leads to reduced membrane fusion and secretion (155-158). The prevailing mechanistic model of Tomo-1's inhibitory actions on membrane fusion postulates that its C-terminal, VAMP-like R-SNARE domain competitively inhibits the interaction of VAMP2 and Munc18 with Syntaxin1A (161, 162). Thus, this model proposes Tomosyn functions as a clamp on fusion events via action of its SNARE domain. Another mechanism by which Tomo-1 may negatively regulate fusion has also been identified to result from its N-terminal ß-propeller domains (156, 157, 163-166). These highly structured regions are hypothesized to contribute in reallocating vesicles into a non-releasable pool to decrease or abolish the induction of some forms of synaptic plasticity and memory (158, 167, 168). Additionally, previous work from our lab identified two of the three unstructured loop domains (loop numbers one and three, but not two) emanating from the ß-propeller core of mammalian Tomo-1 to be crucial for its inhibition, but not its binding with Syntxain1A (166). Lastly, PTM of Tomo-1 by the small ubiquitin-like modifier SUMO2/3 within loop number two enhanced its inhibitory actions without affecting its Syntaxin1A binding characteristics. Therefore, the negative regulation of membrane fusion by Tomo-1 is not entirely imposed by its SNARE domain via competitive inhibition of Syntaxin1A binding. Further examination of Tomo-1-dependent effects on synaptic morphology and physiology is needed to elucidate the mechanistic contributions post-translational modifications of Tomo-1 at specific regions to its actions on membrane trafficking/fusion.

Figure 1.1: General hypothesis model.

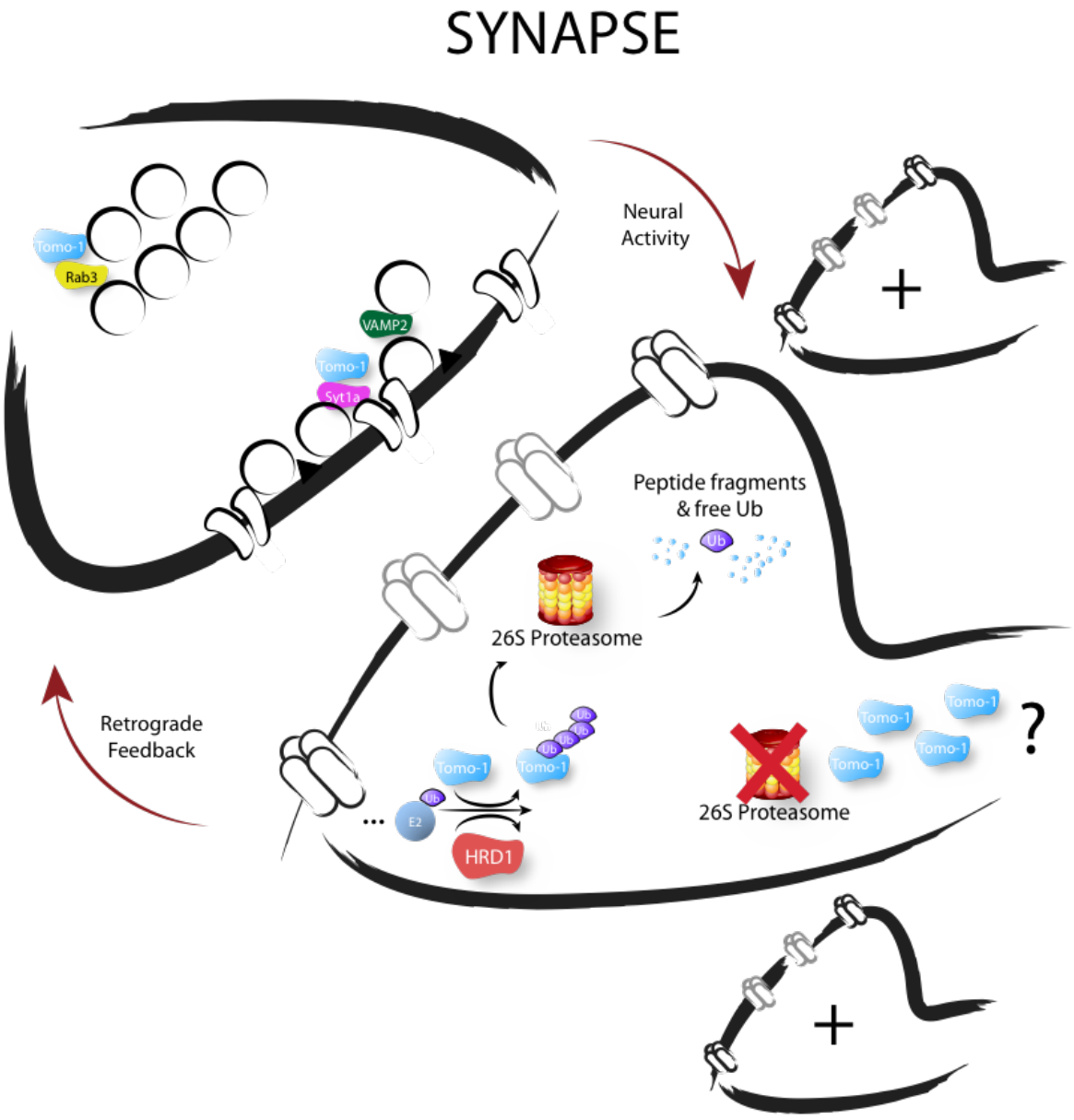

Figure 1.1: General hypothesis model.

A simplified cartoon model outlining our hypothesis that a synaptic molecular mechanism modulating the information encoding capabilities between neurons is the UPS-dependent, specific regulation of Tomo-1 ubiquitination by HRD1 and its subsequent proteasomal degradation. Furthermore, we expect novel neuronal plasticity effects may result from currently unidentified postsynaptic actions of Tomo-1 protein, such as on dendritic spine morphology or number.

1.4 Bibliography

1. Rizo, J., Rosen, M. K., and Gardner, K. H. (2012) Enlightening molecular mechanisms through study of protein interactions. *Journal of Molecular Cell Biology*. **4**, 270–283

2. Südhof, T. C. (2013) Neurotransmitter Release: The Last Millisecond in the Life of a Synaptic Vesicle. *Neuron*. **80**, 675–690

3. Sudhof, T. C., and Rothman, J. E. (2009) Membrane Fusion: Grappling with SNARE and SM Proteins. *Science*. **323**, 474–477

4. Pang, Z. P., and SÃ¼dhof, T. C. (2010) Cell biology of Ca2+-triggered exocytosis. *Current Opinion in Cell Biology*. **22**, 496–505

5. Gandini, M. A., and Felix, R. (2012) Functional interactions between voltage-gated Ca2+ channels and Rab3-interacting molecules (RIMs): New insights into stimulus–secretion coupling. *BBA - Biomembranes*. **1818**, 551–558

6. Jordens, I., Marsman, M., Kuijl, C., and Neefjes, J. (2005) Rab Proteins, Connecting Transport and Vesicle Fusion. *Traffic*. **6**, 1070–1077

7. Sabatini, B. L., and Regehr, W. G. (1999) Timing of synaptic transmission. *Annu. Rev. Physiol.* **61**, 521–542

8. Neher, E., and Sakaba, T. (2008) Multiple Roles of Calcium Ions in the Regulation of Neurotransmitter Release. *Neuron*. **59**, 861–872

9. Chapman, E. R. (2008) How Does Synaptotagmin Trigger Neurotransmitter Release? *Annu. Rev. Biochem.* **77**, 615–641

10. Schoch, S., and Gundelfinger, E. D. (2006) Molecular organization of the presynaptic active zone. *Cell Tissue Res*. **326**, 379–391

11. Becherer, U., and Rettig, J. (2006) Vesicle pools, docking, priming, and release. *Cell Tissue Res*. **326**, 393–407

12. Jahn, R., and Scheller, R. H. (2006) SNAREs — engines for membrane fusion. *Nat Rev Mol Cell Bio*. **7**, 631–643

13. Rizo, J., and Südhof, T. C. (2012) The membrane fusion enigma: SNAREs, Sec1/Munc18 proteins, and their accomplices--guilty as charged? *Annu. Rev. Cell Dev. Biol.* **28**, 279–308

14. Han, J., Pluhackova, K., and Böckmann, R. A. (2017) The Multifaceted Role of SNARE Proteins in Membrane Fusion. *Front. Physiol.* **8**, E1609–17

15. Rizo, J., and Xu, J. (2015) The Synaptic Vesicle Release Machinery. *Annu. Rev. Biophys.* **44**, 339–367

16. Rizzoli, S. O., and Jahn, R. (2007) Kiss-and-run, Collapse and "Readily Retrievable" Vesicles. *Traffic*. **8**, 1137–1144

17. Jung, N., and Haucke, V. (2007) Clathrin-Mediated Endocytosis at Synapses. *Traffic*. **8**, 1129–1136

18. Mettlen, M., Pucadyil, T., Ramachandran, R., and Schmid, S. L. (2009) Dissecting dynamin's role in clathrin-mediated endocytosis. *Biochm. Soc. Trans.* **37**, 1022–1026

19. Takamori, S., Holt, M., Stenius, K., Lemke, E. A., Grønborg, M., Riedel, D., Urlaub, H., Schenck, S., Brügger, B., Ringler, P., Müller, S. A., Rammner, B., Gräter, F., Hub, J. S., De Groot, B. L., Mieskes, G., Moriyama, Y., Klingauf, J., Grubmüller, H., Heuser, J., Wieland, F., and Jahn, R. (2006) Molecular Anatomy of a Trafficking Organelle. *CELL*. **127**, 831–846

20. Bykhovskaia, M. (2011) Synapsin regulation of vesicle organization and functional pools. *Seminars in Cell and Developmental Biology*. **22**, 387–392

21. Rizzoli, S. O., and Betz, W. J. (2005) Synaptic vesicle pools. *Nat Rev Neurosci*. **6**, 57–69

22. Alabi, A. A., and Tsien, R. W. (2012) Synaptic Vesicle Pools and Dynamics. *Cold Spring Harbor Perspectives in Biology*. **4**, a013680–a013680

23. Rettig, J., and Neher, E. (2002) Emerging roles of presynaptic proteins in Ca++-triggered exocytosis. *Science*. **298**, 781–785

24. Huganir, R. L., and Nicoll, R. A. (2013) AMPARs and Synaptic Plasticity: The Last 25 Years. *Neuron*. **80**, 704–717

25. Nicoll, R. A. (2017) A Brief History of Long-Term Potentiation. *Neuron*. **93**, 281–290

26. Citri, A., and Malenka, R. C. (2007) Synaptic Plasticity: Multiple Forms, Functions, and Mechanisms. *Neuropsychopharmacology*. **33**, 18–41

27. Regehr, W. G. (2012) Short-term presynaptic plasticity. *Cold Spring Harbor*

Perspectives in Biology. **4**, a005702

28. Bliss, T. V., and Gardner-Medwin, A. R. (1973) Long-lasting potentiation of synaptic transmission in the dentate area of the unanaestetized rabbit following stimulation of the perforant path. *The Journal of Physiology*. **232**, 357–374

29. Malenka, R. C., and Bear, M. F. (2004) LTP and LTD: an embarrassment of riches. *Neuron*. **44**, 5–21

30. Lynch, G. S., Dunwiddie, T., and Gribkoff, V. (1977) Heterosynaptic depression: a postsynaptic correlate of long-term potentiation. *Nature*. **266**, 737–739

31. Feldman, D. (2012) The Spike-Timing Dependence of Plasticity. *Neuron*. **75**, 556–571

32. Davis, G. W. (2013) Homeostatic signaling and the stabilization of neural function. *Neuron*. **80**, 718–728

33. Turrigiano, G. (2012) Homeostatic Synaptic Plasticity: Local and Global Mechanisms for Stabilizing Neuronal Function. *Cold Spring Harbor Perspectives in Biology*. **4**, a005736–a005736

34. O'Leary, T., Williams, A. H., Franci, A., and Marder, E. (2014) Cell Types, Network Homeostasis, and Pathological Compensation from a Biologically Plausible Ion Channel Expression Model. *Neuron*. **82**, 809–821

35. Turrigiano, G. G., Leslie, K. R., Desai, N. S., Rutherford, L. C., and Nelson, S. B. (1998) Activity-dependent scaling of quantal amplitude in neocortical neurons. *Nature*. **391**, 892–896

36. Pozo, K., and Goda, Y. (2010) Unraveling Mechanisms of Homeostatic Synaptic Plasticity. *Neuron*. **66**, 337–351

37. Turrigiano, G. G. (2017) The dialectic of Hebb and homeostasis. *Philosophical Transactions of the Royal Society B: Biological Sciences*. **372**, 20160258–7

38. Zenke, F., and Gerstner, W. (2017) Hebbian plasticity requires compensatory processes on multiple timescales. *Philosophical Transactions of the Royal Society B: Biological Sciences*. **372**, 20160259–17

39. Yee, A. X., Hsu, Y.-T., and Chen, L. (2017) A metaplasticity view of the interaction between homeostatic and Hebbian plasticity. *Philosophical Transactions of the Royal Society B: Biological Sciences*. **372**, 20160155–9

40. Amtul, Z., and Atta-ur-Rahman (2015) Neural plasticity and memory: molecular mechanism. *Reviews in the Neurosciences*. **26**, 206–16

41. Fernandes, D., and Carvalho, A. L. (2016) Mechanisms of homeostatic plasticity in the excitatory synapse. *J Neurochem*. **139**, 973–996

42. Castillo, P. E., Schoch, S., Schmitz, F., Südhof, T. C., and Malenka, R. C. (2002) RIM1alpha is required for presynaptic long-term potentiation. *Nature*. **415**, 327–330

43. Davis, G. W., and Müller, M. (2015) Homeostatic control of presynaptic neurotransmitter release. *Annu. Rev. Physiol.* **77**, 251–270

44. Cohen, J. E., Lee, P. R., Chen, S., Li, W., and Fields, R. D. (2011) MicroRNA regulation of homeostatic synaptic plasticity. *Proceedings of the National Academy of Sciences*. **108**, 11650–11655

45. Chater, T. E., and Goda, Y. (2014) The role of AMPA receptors in postsynaptic mechanisms of synaptic plasticity. *Front. Cell. Neurosci.* **8**, 401

46. Turrigiano, G. G. (2008) The Self-Tuning Neuron: Synaptic Scaling of Excitatory Synapses. *CELL*. **135**, 422–435

47. Whitt, J. L., Petrus, E., and Lee, H.-K. (2014) Experience-dependent homeostatic synaptic plasticity in neocortex. *Neuropharmacology*. **78**, 45–54

48. Nishiyama, J., and Yasuda, R. (2015) Biochemical Computation for Spine Structural Plasticity. *Neuron*. **87**, 63–75

49. Lu, W., Man, H., Ju, W., Trimble, W. S., MacDonald, J. F., and Wang, Y. T. (2001) Activation of synaptic NMDA receptors induces membrane insertion of new AMPA receptors and LTP in cultured hippocampal neurons. *Neuron*. **29**, 243–254

50. Bliss, T. V. P., and Collingridge, G. L. (2013) Expression of NMDA receptor-dependent LTP in the hippocampus: bridging the divide. *Mol Brain*. **6**, 5

51. Jakawich, S. K., Nasser, H. B., Strong, M. J., McCartney, A. J., Perez, A. S., Rakesh, N., Carruthers, C. J. L., and Sutton, M. A. (2010) Local Presynaptic Activity GatesHomeostatic Changes in Presynaptic Function Driven by Dendritic BDNF Synthesis. *Neuron*. **68**, 1143–1158

52. Henry, F. E., McCartney, A. J., Neely, R., Perez, A. S., Carruthers, C. J. L., Stuenkel, E. L., Inoki, K., and Sutton, M. A. (2012) Retrograde Changes in

Presynaptic Function Driven by Dendritic mTORC1. *Journal of Neuroscience*. **32**, 17128–17142

53. Henry, F. E., Wang, X., Serrano, D., Perez, A. S., Carruthers, C. J. L., Stuenkel, E. L., and Sutton, M. A. (2018) A unique homeostatic signaling pathway links synaptic inactivity to postsynaptic mTORC1. *J. Neurosci.* 10.1523/JNEUROSCI.1843-17.2017

54. Jakawich, S. K., Neely, R. M., Djakovic, S. N., Patrick, G. N., and Sutton, M. A. (2010) An essential postsynaptic role for the ubiquitin proteasome system in slow homeostatic synaptic plasticity in cultured hippocampal neurons. *NSC*. **171**, 1016–1031

55. Scheschonka, A., Tang, Z., and Betz, H. (2007) Sumoylation in neurons: nuclear and synaptic roles? *Trends Neurosci.* **30**, 85–91

56. Loriol, C., Khayachi, A., Poupon, G., Gwizdek, C., and Martin, S. (2013) Activity-dependent regulation of the sumoylation machinery in rat hippocampal neurons. *Biol. Cell*. **105**, 30–45

57. Krumova, P., and Weishaupt, J. H. (2013) Sumoylation in neurodegenerative diseases. *Cell. Mol. Life Sci.* **70**, 2123–2138

58. Schorova, L., and Martin, S. (2016) Sumoylation in Synaptic Function and Dysfunction. *Front. Synaptic Neurosci.* **8**, 272

59. Scudder, S. L., and Patrick, G. N. (2015) Synaptic structure and function are altered by the neddylation inhibitor MLN4924. *Mol. Cell. Neurosci.* 10.1016/j.mcn.2015.02.010

60. Vogl, A. M., Brockmann, M. M., Giusti, S. A., Maccarrone, G., Vercelli, C. A., Bauder, C. A., Richter, J. S., Roselli, F., Hafner, A.-S., Dedic, N., Wotjak, C. T., Vogt-Weisenhorn, D. M., Choquet, D., Turck, C. W., Stein, V., Deussing, J. M., and Refojo, D. (2015) Neddylation inhibition impairs spine development, destabilizes synapses and deteriorates cognition. *Nature Publishing Group*. **18**, 239–251

61. Rock, K. L., Gramm, C., Rothstein, L., Clark, K., Stein, R., Dick, L., Hwang, D., and Goldberg, A. L. (1994) Inhibitors of the proteasome block the degradation of most cell proteins and the generation of peptides presented on MHC class I molecules. *CELL*. **78**, 761–771

62. Cohen-Kaplan, V., Livneh, I., Avni, N., Cohen-Rosenzweig, C., and Ciechanover, A. (2016) The ubiquitin-proteasome system and autophagy:

Coordinated and independent activities. *International Journal of Biochemistry and Cell Biology*. **79**, 403–418

63. Ciechanover, A., and Kwon, Y. T. (2015) Degradation of misfolded proteins in neurodegenerative diseases: therapeutic targets and strategies. **47**, e147–16

64. Cha-Molstad, H., Sung, K. S., Hwang, J., Kim, K. A., Yu, J. E., Yoo, Y. D., Jang, J. M., Han, D. H., Molstad, M., Kim, J. G., Lee, Y. J., Zakrzewska, A., Kim, S.-H., Kim, S. T., Kim, S. Y., Lee, H. G., Soung, N. K., Ahn, J. S., Ciechanover, A., Kim, B. Y., and Kwon, Y. T. (2015) Amino-terminal arginylation targets endoplasmic reticulum chaperone BiP for autophagy through p62 binding. *Nat. Cell Biol.* **17**, 917–929

65. Rabinovitz, M., and Fisher, J. M. (1964) Characteristics of the Inhibition of Hemoglobin Synthesis in Rabbit Reticulocytes by Threo-Alpha-Amino-Beta-Chlorobutyric Acid. *Biochim. Biophys. Acta*. **91**, 313–322

66. Etlinger, J. D., and Goldberg, A. L. (1977) A soluble ATP-dependent proteolytic system responsible for the degradation of abnormal proteins in reticulocytes. *Proc. Natl. Acad. Sci. U.S.A.* **74**, 54–58

67. Varshavsky, A. (2017) The Ubiquitin System, Autophagy, and Regulated Protein Degradation. *Annu. Rev. Biochem.* **86**, 123–128

68. Ciehanover, A., Hod, Y., and Hershko, A. (1978) A heat-stable polypeptide component of an ATP-dependent proteolytic system from reticulocytes. *Biochemical and Biophysical Research Communications*. **81**, 1100–1105

69. Ciechanover, A., Heller, H., Elias, S., Haas, A. L., and Hershko, A. (1980) ATP-dependent conjugation of reticulocyte proteins with the polypeptide required for protein degradation. *Proc. Natl. Acad. Sci. U.S.A.* **77**, 1365–1368

70. Hershko, A., Ciechanover, A., Heller, H., Haas, A. L., and Rose, I. A. (1980) Proposed role of ATP in protein breakdown: conjugation of protein with multiple chains of the polypeptide of ATP-dependent proteolysis. *Proc. Natl. Acad. Sci. U.S.A.* **77**, 1783–1786

71. Aaron Ciechanover (2009) Tracing the history of the ubiquitin proteolytic system: The pioneering article. *Biochemical and Biophysical Research Communications*. **387**, 1–10

72. Kwon, Y. T., and Ciechanover, A. (2017) The Ubiquitin Code in the Ubiquitin-Proteasome System and Autophagy. *Trends in Biochemical Sciences*. **42**, 873–886

73. Dikic, I. (2017) Proteasomal and Autophagic Degradation Systems. *Annu. Rev. Biochem.* **86**, 193–224

74. Swatek, K. N., and Komander, D. (2016) Ubiquitin modifications. *Nature Publishing Group*. **26**, 399–422

75. Clague, M. J., Heride, C., and Urbé, S. (2015) The demographics of the ubiquitin system. *Trends in Cell Biology*. **25**, 417–426

76. Kleiger, G., and Mayor, T. (2014) Perilous journey: a tour of the ubiquitin–proteasome system. *Trends in Cell Biology*. **24**, 352–359

77. Hegde, A. N. (2017) Proteolysis, synaptic plasticity and memory. *Neurobiol Learn Mem*. **138**, 98–110

78. Lip, P. Z. Y., Demasi, M., and Bonatto, D. (2017) The role of the ubiquitin proteasome system in the memory process. *Neurochemistry International*. **102**, 57–65

79. Alvarez-Castelao, B., and Schuman, E. M. (2015) The Regulation of Synaptic Protein Turnover. *Journal of Biological Chemistry*. **290**, 28623–28630

80. Tsai, N.-P. (2014) Ubiquitin proteasome system-mediated degradation of synaptic proteins: An update from the postsynaptic side. *BBA - Molecular Cell Research*. **1843**, 2838–2842

81. Yamada, T., Yang, Y., and Bonni, A. (2013) Spatial organization of ubiquitin ligase pathways orchestrates neuronal connectivity. *Trends Neurosci.* **36**, 218–226

82. Tai, H.-C., and Schuman, E. M. (2008) Ubiquitin, the proteasome and protein degradation in neuronal function and dysfunction. *Nat Rev Neurosci*. **9**, 826–838

83. Kevei, É., Pokrzywa, W., and Hoppe, T. (2017) Repair or destruction-an intimate liaison between ubiquitin ligases and molecular chaperones in proteostasis. *FEBS Letters*. **591**, 2616–2635

84. Hegde, A. N. (2010) The ubiquitin-proteasome pathway and synaptic plasticity. *Learning & Memory*. **17**, 314–327

85. McDowell, G. S., and Philpott, A. (2013) Non-canonical ubiquitylation: Mechanisms and consequences. *International Journal of Biochemistry and Cell Biology*. **45**, 1833–1842

86. Lin, A., Hou, Q., Jarzylo, L., Amato, S., Gilbert, J., Shang, F., and Man, H.-Y. (2011) Nedd4-mediated AMPA receptor ubiquitination regulates receptor turnover and trafficking. *J Neurochem*. **119**, 27–39

87. Budenholzer, L., Cheng, C. L., Li, Y., and Hochstrasser, M. (2017) Proteasome Structure and Assembly. *Journal of Molecular Biology*. 10.1016/j.jmb.2017.05.027

88. Cheng, Y. (2009) Toward an atomic model of the 26S proteasome. *Current Opinion in Structural Biology*. **19**, 203–208

89. Collins, G. A., and Goldberg, A. L. (2017) The Logic of the 26S Proteasome. *CELL*. **169**, 792–806

90. Leggett, D. S., Hanna, J., Borodovsky, A., Crosas, B., Schmidt, M., Baker, R. T., Walz, T., Ploegh, H., and Finley, D. (2002) Multiple associated proteins regulate proteasome structure and function. *Molecular Cell*. **10**, 495–507

91. Peth, A., Besche, H. C., and Goldberg, A. L. (2009) Ubiquitinated Proteins Activate the Proteasome by Binding to Usp14/Ubp6, which Causes 20S Gate Opening. *Molecular Cell*. **36**, 794–804

92. Marques, A. J., Palanimurugan, R., Matias, A. C., Ramos, P. C., and Dohmen, R. J. (2009) Catalytic Mechanism and Assembly of the Proteasome. *Chem. Rev.* **109**, 1509–1536

93. Guo, X., Huang, X., and Chen, M. J. (2017) Reversible phosphorylation of the 26S proteasome. *Protein & Cell*. **8**, 255–272

94. Ciechanover, A. (2015) The unravelling of the ubiquitin system. *Nature Publishing Group*. **16**, 322–324

95. Li, W., Bengtson, M. H., Ulbrich, A., Matsuda, A., Reddy, V. A., Orth, A., Chanda, S. K., Batalov, S., and Joazeiro, C. A. P. (2008) Genome-wide and functional annotation of human E3 ubiquitin ligases identifies MULAN, a mitochondrial E3 that regulates the organelle's dynamics and signaling. *PLoS ONE*. **3**, e1487

96. Koegl, M., Hoppe, T., Schlenker, S., Ulrich, H. D., Mayer, T. U., and Jentsch, S. (1999) A novel ubiquitination factor, E4, is involved in multiubiquitin chain assembly. *CELL*. **96**, 635–644

97. Hatakeyama, S., Yada, M., Matsumoto, M., Ishida, N., and Nakayama, K.-I. (2001) U Box Proteins as a New Family of Ubiquitin-Protein Ligases. *J. Biol.*

Chem. **276**, 33111–33120

98. Hatakeyama, S., and Nakayama, K.-I. I. (2003) U-box proteins as a new family of ubiquitin ligases. *Biochemical and Biophysical Research Communications*. **302**, 635–645

99. Huibregtse, J. M., Scheffner, M., Beaudenon, S., and Howley, P. M. (1995) A family of proteins structurally and functionally related to the E6-AP ubiquitin-protein ligase. *Proc. Natl. Acad. Sci. U.S.A.* **92**, 5249

100. Kishino, T., Lalande, M., and Wagstaff, J. (1997) UBE3A/E6-AP mutations cause Angelman syndrome. *Nat Genet*. **15**, 70–73

101. Matsuura, T., Sutcliffe, J. S., Fang, P., Galjaard, R. J., Jiang, Y. H., Benton, C. S., Rommens, J. M., and Beaudet, A. L. (1997) De novo truncating mutations in E6-AP ubiquitin-protein ligase gene (UBE3A) in Angelman syndrome. *Nat Genet*. **15**, 74–77

102. Jiang, Y. H., Armstrong, D., Albrecht, U., Atkins, C. M., Noebels, J. L., Eichele, G., Sweatt, J. D., and Beaudet, A. L. (1998) Mutation of the Angelman ubiquitin ligase in mice causes increased cytoplasmic p53 and deficits of contextual learning and long-term potentiation. *Neuron*. **21**, 799–811

103. Greer, P. L., Hanayama, R., Bloodgood, B. L., Mardinly, A. R., Lipton, D. M., Flavell, S. W., Kim, T.-K., Griffith, E. C., Waldon, Z., Maehr, R., Ploegh, H. L., Chowdhury, S., Worley, P. F., Steen, J., and Greenberg, M. E. (2010) The Angelman Syndrome protein Ube3A regulates synapse development by ubiquitinating arc. *CELL*. **140**, 704–716

104. Colledge, M., Snyder, E. M., Crozier, R. A., Soderling, J. A., Jin, Y., Langeberg, L. K., Lu, H., Bear, M. F., and Scott, J. D. (2003) Ubiquitination regulates PSD-95 degradation and AMPA receptor surface expression. *Neuron*. **40**, 595–607

105. Yang, Y., Kim, A. H., Yamada, T., Wu, B., Bilimoria, P. M., Ikeuchi, Y., la Iglesia, de, N., Shen, J., and Bonni, A. (2009) A Cdc20-APC ubiquitin signaling pathway regulates presynaptic differentiation. *Science*. **326**, 575–578

106. van Roessel, P., Elliott, D. A., Robinson, I. M., Prokop, A., and Brand, A. H. (2004) Independent regulation of synaptic size and activity by the anaphase-promoting complex. *CELL*. **119**, 707–718

107. Kim, A. H., Puram, S. V., Bilimoria, P. M., Ikeuchi, Y., Keough, S., Wong, M., Rowitch, D., and Bonni, A. (2009) A centrosomal Cdc20-APC pathway controls dendrite morphogenesis in postmitotic neurons. *CELL*. **136**, 322–336

108. Yao, I., Takagi, H., Ageta, H., Kahyo, T., Sato, S., Hatanaka, K., Fukuda, Y., Chiba, T., Morone, N., Yuasa, S., Inokuchi, K., Ohtsuka, T., MacGregor, G. R., Tanaka, K., and Setou, M. (2007) SCRAPPER-Dependent Ubiquitination of Active Zone Protein RIM1 Regulates Synaptic Vesicle Release. *CELL*. **130**, 943–957

109. Chin, L. S., Vavalle, J. P., and Li, L. (2002) Staring, a Novel E3 Ubiquitin-Protein Ligase That Targets Syntaxin 1 for Degradation. *Journal of Biological Chemistry*. **277**, 35071–35079

110. Willeumier, K., Pulst, S. M., and Schweizer, F. E. (2006) Proteasome Inhibition Triggers Activity-Dependent Increase in the Size of the Recycling Vesicle Pool in Cultured Hippocampal Neurons. *Journal of Neuroscience*. **26**, 11333–11341

111. Rinetti, G. V., and Schweizer, F. E. (2010) Ubiquitination acutely regulates presynaptic neurotransmitter release in mammalian neurons. *Journal of Neuroscience*. **30**, 3157–3166

112. Speese, S. D., Trotta, N., Rodesch, C. K., Aravamudan, B., and Broadie, K. (2003) The ubiquitin proteasome system acutely regulates presynaptic protein turnover and synaptic efficacy. *Curr. Biol.* **13**, 899–910

113. Lin, A. W., and Man, H.-Y. (2013) Ubiquitination of neurotransmitter receptors and postsynaptic scaffolding proteins. *Neural Plast.* **2013**, 432057–10

114. Widagdo, J., Guntupalli, S., Jang, S. E., and Anggono, V. (2017) Regulation of AMPA Receptor Trafficking by Protein Ubiquitination. *Front Mol Neurosci*. **10**, 461–10

115. Patrick, G. N., Bingol, B., Weld, H. A., and Schuman, E. M. (2003) Ubiquitin-Mediated Proteasome Activity Is Required for Agonist-Induced Endocytosis of GluRs. *Current Biology*. **13**, 2073–2081

116. Lahaie, N., Kralikova, M., Prézeau, L., Blahos, J., and Bouvier, M. (2016) Post-endocytotic Deubiquitination and Degradation of the Metabotropic γ-Aminobutyric Acid Receptor by the Ubiquitin-specific Protease 14. *Journal of Biological Chemistry*. **291**, 7156–7170

117. Büttner, C., Sadtler, S., Leyendecker, A., Laube, B., Griffon, N., Betz, H., and Schmalzing, G. (2001) Ubiquitination Precedes Internalization and Proteolytic Cleavage of Plasma Membrane-bound Glycine Receptors. *J. Biol. Chem.* **276**, 42978–42985

118. Bays, N. W., Gardner, R. G., Seelig, L. P., Joazeiro, C. A., and Hampton, R. Y. (2001) Hrd1p/Der3p is a membrane-anchored ubiquitin ligase required for ER-associated degradation. *Nat. Cell Biol.* **3**, 24–29

119. Schoebel, S., Mi, W., Stein, A., Ovchinnikov, S., Pavlovicz, R., DiMaio, F., Baker, D., Chambers, M. G., Su, H., Li, D., Rapoport, T. A., and Liao, M. (2017) Cryo-EM structure of the protein-conducting ERAD channel Hrd1 in complex with Hrd3. *Nature Publishing Group*. **548**, 352–355

120. Baldridge, R. D., and Rapoport, T. A. (2016) Autoubiquitination of the Hrd1 Ligase Triggers Protein Retrotranslocation in ERAD. *CELL*. **166**, 394–407

121. Vashistha, N., Neal, S. E., Singh, A., Carroll, S. M., and Hampton, R. Y. (2016) Direct and essential function for Hrd3 in ER-associated degradation. *Proceedings of the National Academy of Sciences*. **113**, 5934–5939

122. Schulz, J., Avci, D., Queisser, M. A., Gutschmidt, A., Dreher, L.-S., Fenech, E. J., Volkmar, N., Hayashi, Y., Hoppe, T., and Christianson, J. C. (2017) Conserved cytoplasmic domains promote Hrd1 ubiquitin ligase complex formation for ER-associated degradation (ERAD). *Journal of Cell Science*. **130**, 3322–3335

123. Hosokawa, N., and Wada, I. (2016) Association of the SEL1L protein transmembrane domain with HRD1 ubiquitin ligase regulates ERAD-L. *FEBS J.* **283**, 157–172

124. Gauss, R., Jarosch, E., Sommer, T., and Hirsch, C. (2006) A complex of Yos9p and the HRD ligase integrates endoplasmic reticulum quality control into the degradation machinery. *Nat. Cell Biol.* **8**, 849–854

125. Bernasconi, R., Pertel, T., Luban, J., and Molinari, M. (2008) A dual task for the Xbp1-responsive OS-9 variants in the mammalian endoplasmic reticulum: inhibiting secretion of misfolded protein conformers and enhancing their disposal. *J. Biol. Chem.* **283**, 16446–16454

126. Wang, Y., Fu, X., Gaiser, S., Köttgen, M., Kramer-Zucker, A., Walz, G., and Wegierski, T. (2007) OS-9 Regulates the Transit and Polyubiquitination of TRPV4 in the Endoplasmic Reticulum. *J. Biol. Chem.* **282**, 36561–36570

127. Christianson, J. C., Shaler, T. A., Tyler, R. E., and Kopito, R. R. (2008) OS-9 and GRP94 deliver mutant alpha1-antitrypsin to the Hrd1-SEL1L ubiquitin ligase complex for ERAD. *Nat. Cell Biol.* **10**, 272–282

128. Hwang, J., Walczak, C. P., Shaler, T. A., Olzmann, J. A., Zhang, L., Elias, J. E.,

and Kopito, R. R. (2017) Characterization of protein complexes of the endoplasmic reticulum-associated degradation E3 ubiquitin ligase Hrd1. *Journal of Biological Chemistry*. **292**, 9104–9116

129. Harada, K., Kato, M., and Nakamura, N. (2016) USP19-Mediated Deubiquitination Facilitates the Stabilization of HRD1 Ubiquitin Ligase. *IJMS*. **17**, 1829–9

130. Shmueli, A., Tsai, Y. C., Yang, M., Braun, M. A., and Weissman, A. M. (2009) Targeting of gp78 for ubiquitin-mediated proteasomal degradation by Hrd1: cross-talk between E3s in the endoplasmic reticulum. *Biochemical and Biophysical Research Communications*. **390**, 758–762

131. Lee, K. A., Hammerle, L. P., Andrews, P. S., Stokes, M. P., Mustelin, T., Silva, J. C., Black, R. A., and Doedens, J. R. (2011) Ubiquitin Ligase Substrate Identification through Quantitative Proteomics at Both the Protein and Peptide Levels. *J. Biol. Chem.* **286**, 41530–41538

132. Yamasaki, S., Yagishita, N., Sasaki, T., Nakazawa, M., Kato, Y., Yamadera, T., Bae, E., Toriyama, S., Ikeda, R., Zhang, L., Fujitani, K., Yoo, E., Tsuchimochi, K., Ohta, T., Araya, N., Fujita, H., Aratani, S., Eguchi, K., Komiya, S., Maruyama, I., Higashi, N., Sato, M., Senoo, H., Ochi, T., Yokoyama, S., Amano, T., Kim, J., Gay, S., Fukamizu, A., Nishioka, K., Tanaka, K., and Nakajima, T. (2007) Cytoplasmic destruction of p53 by the endoplasmic reticulum-resident ubiquitin ligase 'Synoviolin'. *The EMBO Journal*. **26**, 113–122

133. Yamasaki, S., Yagishita, N., Nishioka, K., and Nakajima, T. (2007) The roles of synoviolin in crosstalk between endoplasmic reticulum stress-induced apoptosis and p53 pathway. *Cell Cycle*. **6**, 1319–1323

134. Mao, J., Xia, Q., Liu, C., Ying, Z., Wang, H., and Wang, G. (2017) A critical role of Hrd1 in the regulation of optineurin degradation and aggresome formation. *Hum. Mol. Genet.* **26**, 1877–1889

135. Ying, H., and Yue, B. Y. J. T. (2012) Cellular and molecular biology of optineurin. *Int Rev Cell Mol Biol*. **294**, 223–258

136. Hamdan, N., Kritsiligkou, P., and Grant, C. M. (2017) ER stress causes widespread protein aggregation and prion formation. *The Journal of Cell Biology*. **216**, 2295–2304

137. Kawada, K., Iekumo, T., Saito, R., Kaneko, M., Mimori, S., Nomura, Y., and Okuma, Y. (2014) Aberrant neuronal differentiation and inhibition of dendrite outgrowth resulting from endoplasmic reticulum stress. *J. Neurosci. Res.* **92**,

1122–1133

138. Omura, T., Kaneko, M., Okuma, Y., Orba, Y., Nagashima, K., Takahashi, R., Fujitani, N., Matsumura, S., Hata, A., Kubota, K., Murahashi, K., Uehara, T., and Nomura, Y. (2006) A ubiquitin ligase HRD1 promotes the degradation of Pael receptor, a substrate of Parkin. *J Neurochem*. **99**, 1456–1469

139. Shen, Y. X., Sun, A. M., Fang, S., Feng, L. J., Li, Q., Hou, H. L., Liu, C., Wang, H. P., Shen, J. L., Luo, J., and Zhou, J. N. (2012) Hrd1 Facilitates Tau Degradation and Promotes Neuron Survival. *Curr. Mol. Med.* **12**, 138–152

140. Yang, H., Zhong, X., Ballar, P., Luo, S., Shen, Y., Rubinsztein, D. C., Monteiro, M. J., and Fang, S. (2007) Ubiquitin ligase Hrd1 enhances the degradation and suppresses the toxicity of polyglutamine-expanded huntingtin. *Experimental Cell Research*. **313**, 538–550

141. Sutton, M. A., and Schuman, E. M. (2006) Dendritic Protein Synthesis, Synaptic Plasticity, and Memory. *CELL*. **127**, 49–58

142. Pfeiffer, B. E., and Huber, K. M. (2006) Current Advances in Local Protein Synthesis and Synaptic Plasticity. *Journal of Neuroscience*. **26**, 7147–7150

143. Jarome, T. J., and Helmstetter, F. J. (2014) Protein degradation and protein synthesis in long-term memory formation. *Front Mol Neurosci*. **7**, 61

144. Ma, X. M., and Blenis, J. (2009) Molecular mechanisms of mTOR-mediated translational control. *Nat Rev Mol Cell Bio*. **10**, 307–318

145. Kelleher, R. J., III, Govindarajan, A., and Tonegawa, S. (2004) Translational Regulatory Mechanisms in Persistent Forms of Synaptic Plasticity. *Neuron*. **44**, 59–73

146. Costa-Mattioli, M., Sossin, W. S., Klann, E., and Sonenberg, N. (2009) Translational Control of Long-Lasting Synaptic Plasticity and Memory. *Neuron*. **61**, 10–26

147. Penney, J., Tsurudome, K., Liao, E. H., Elazzouzi, F., Livingstone, M., Gonzalez, M., Sonenberg, N., and Haghighi, A. P. (2012) TOR is required for the retrograde regulation of synaptic homeostasis at the Drosophila neuromuscular junction. *Neuron*. **74**, 166–178

148. Ebert, D. H., and Greenberg, M. E. (2013) Activity-dependent neuronal signalling and autism spectrum disorder. *Nature*. **493**, 327–337

149. Buffington, S. A., Huang, W., and Costa-Mattioli, M. (2014) Translational Control in Synaptic Plasticity and Cognitive Dysfunction. *Annu. Rev. Neurosci.* **37**, 17–38

150. Nelson, S. B., and Valakh, V. (2015) Excitatory/Inhibitory Balance and Circuit Homeostasis in Autism Spectrum Disorders. *Neuron*. **87**, 684–698

151. Davis, L. K., Meyer, K. J., Rudd, D. S., Librant, A. L., Epping, E. A., Sheffield, V. C., and Wassink, T. H. (2009) Novel copy number variants in children with autism and additional developmental anomalies. *J Neurodev Disord*. **1**, 292–301

152. Kumar, R., Corbett, M. A., Smith, N. J. C., Jolly, L. A., Tan, C., Keating, D. J., Duffield, M. D., Utsumi, T., Moriya, K., Smith, K. R., Hoischen, A., Abbott, K., Harbord, M. G., Compton, A. G., Woenig, J. A., Arts, P., Kwint, M., Wieskamp, N., Gijsen, S., Veltman, J. A., Bahlo, M., Gleeson, J. G., Haan, E., and Gecz, J. (2014) Homozygous mutation of STXBP5L explains an autosomal recessive infantile-onset neurodegenerative disorder. *Hum. Mol. Genet.* **24**, 2000–2010

153. Batten, S. R., Matveeva, E. A., Whiteheart, S. W., Vanaman, T. C., Gerhardt, G. A., and Slevin, J. T. (2017) Linking kindling to increased glutamate release in the dentate gyrus of the hippocampus through the STXBP5/tomosyn-1 gene. *Brain Behav*. **7**, e00795–11

154. Ashery, U., Bielopolski, N., Barak, B., and Yizhar, O. (2009) Friends and foes in synaptic transmission: the role of tomosyn in vesicle priming. *Trends Neurosci.* **32**, 275–282

155. Gracheva, E. O., Burdina, A. O., Holgado, A. M., Berthelot-Grosjean, M., Ackley, B. D., Hadwiger, G., Nonet, M. L., Weimer, R. M., and Richmond, J. E. (2006) Tomosyn Inhibits Synaptic Vesicle Priming in Caenorhabditis elegans. *PLoS Biol.* **4**, e261–12

156. McEwen, J. M., Madison, J. M., Dybbs, M., and Kaplan, J. M. (2006) Antagonistic regulation of synaptic vesicle priming by Tomosyn and UNC-13. *Neuron*. **51**, 303–315

157. Sakisaka, T., Yamamoto, Y., Mochida, S., Nakamura, M., Nishikawa, K., Ishizaki, H., Okamoto-Tanaka, M., Miyoshi, J., Fujiyoshi, Y., Manabe, T., and Takai, Y. (2008) Dual inhibition of SNARE complex formation by tomosyn ensures controlled neurotransmitter release. *The Journal of Cell Biology*. **183**, 323–337

158. Cazares, V. A., Njus, M. M., Manly, A., Saldate, J. J., Subramani, A., Ben-Simon, Y., Sutton, M. A., Ashery, U., and Stuenkel, E. L. (2016) Dynamic

Partitioning of Synaptic Vesicle Pools by the SNARE-Binding Protein Tomosyn. *Journal of Neuroscience*. **36**, 11208–11222

159. Hatsuzawa, K., Lang, T., Fasshauer, D., Bruns, D., and Jahn, R. (2003) The R-SNARE motif of tomosyn forms SNARE core complexes with syntaxin 1 and SNAP-25 and down-regulates exocytosis. *J. Biol. Chem.* **278**, 31159–31166

160. Pobbati, A. V., Razeto, A., Böddener, M., Becker, S., and Fasshauer, D. (2004) Structural basis for the inhibitory role of tomosyn in exocytosis. *J. Biol. Chem.* **279**, 47192–47200

161. Fujita, Y., Shirataki, H., Sakisaka, T., Asakura, T., Ohya, T., Kotani, H., Yokoyama, S., Nishioka, H., Matsuura, Y., Mizoguchi, A., Scheller, R. H., and Takai, Y. (1998) Tomosyn: a syntaxin-1-binding protein that forms a novel complex in the neurotransmitter release process. *Neuron*. **20**, 905–915

162. Gladycheva, S. E., Lam, A. D., Liu, J., D'Andrea-Merrins, M., Yizhar, O., Lentz, S. I., Ashery, U., Ernst, S. A., and Stuenkel, E. L. (2007) Receptor-mediated regulation of tomosyn-syntaxin 1A interactions in bovine adrenal chromaffin cells. *J. Biol. Chem.* **282**, 22887–22899

163. Yizhar, O., Lipstein, N., Gladycheva, S. E., Matti, U., Ernst, S. A., Rettig, J., Stuenkel, E. L., and Ashery, U. (2007) Multiple functional domains are involved in tomosyn regulation of exocytosis. *J Neurochem*. **103**, 604–616

164. Yamamoto, Y., Mochida, S., Kurooka, T., and Sakisaka, T. (2009) Reciprocal intramolecular interactions of tomosyn control its inhibitory activity on SNARE complex formation. *J. Biol. Chem.* **284**, 12480–12490

165. Burdina, A. O., Klosterman, S. M., Shtessel, L., Ahmed, S., and Richmond, J. E. (2011) In Vivo Analysis of Conserved C. elegans Tomosyn Domains. *PLoS ONE*. **6**, e26185–8

166. Williams, A. L., Bielopolski, N., Meroz, D., Lam, A. D., Passmore, D. R., Ben-Tal, N., Ernst, S. A., Ashery, U., and Stuenkel, E. L. (2011) Structural and functional analysis of tomosyn identifies domains important in exocytotic regulation. *Journal of Biological Chemistry*. **286**, 14542–14553

167. Chen, K., Richlitzki, A., Featherstone, D. E., Schwärzel, M., and Richmond, J. E. (2011) Tomosyn-dependent regulation of synaptic transmission is required for a late phase of associative odor memory. *Proceedings of the National Academy of Sciences*. **108**, 18482–18487

168. Barak, B., Okun, E., Ben-Simon, Y., Lavi, A., Shapira, R., Madar, R., Wang, Y.,

Norman, E., Sheinin, A., Pita, M. A., Yizhar, O., Mughal, M. R., Stuenkel, E., van Praag, H., Mattson, M. P., and Ashery, U. (2013) Neuron-specific expression of tomosyn1 in the mouse hippocampal dentate gyrus impairs spatial learning and memory. *Neuromolecular Med.* **15**, 351–363

169. Neveu, D., and Zucker, R. S. (1996) Postsynaptic levels of [Ca2+] needed to trigger LTD and LTP. *Neuron*. **16**, 619–629

CHAPTER II

The ubiquitin-proteasome system functionally links neuronal Tomosyn-1 to dendritic morphology

2.1 Abstract

Altering the expression of Tomosyn-1 (Tomo-1), a soluble, R-SNARE domain-containing protein, significantly affects behavior in mice, Drosophila, and *Caenorhabditis elegans*. Yet, the mechanisms modulating Tomo-1 expression and its regulatory activity remain poorly defined. We found that Tomo-1 expression levels influence postsynaptic spine density. Tomo-1 overexpression increased dendritic spine density, while Tomo-1 knockdown (KD) decreased spine density. These findings identified a novel action of Tomo-1 on dendritic spines, which is unique because it occurs independently of Tomo-1's C-terminal R-SNARE domain. We also demonstrated that the ubiquitin-proteasome system (UPS), which is known to influence synaptic strength, dynamically regulates Tomo-1 protein levels. Immunoprecipitated and affinity-purified Tomo-1 from cultured rat hippocampal neurons was ubiquitinated, and the levels of ubiquitinated Tomo-1 dramatically increased upon pharmacological proteasome blockade. Moreover, Tomo-1 ubiquitination appeared to be mediated through an interaction with the E3 ubiquitin ligase HRD1, as immunoprecipitation of Tomo-1 from neurons co-precipitated HRD1, and this interaction increases upon proteasome inhibition. Furthermore, *in vitro*

reactions indicated direct, HRD1 concentration-dependent Tomo-1 ubiquitination. We also noted that the UPS regulates both Tomo-1 expression and functional output, as HRD1 KD in hippocampal neurons increased Tomo-1 protein level and dendritic spine density. Notably, the effect of HRD1 KD on spine density was mitigated by additional KD of Tomo-1, indicating a direct HRD1/Tomo-1 effector relationship. In summary, our results indicate that the UPS is likely to participate in tuning synaptic efficacy and spine dynamics by precise regulation of neuronal Tomo-1 levels.

2.2 Introduction

Synaptic structure and activity within the central nervous system are continually modified as the result of ongoing cognitive, affective, motor, and environmental experiences. Manifestations of this plasticity, while diverse in mechanism, are largely composed of dynamic changes in the molecular regulation of synaptic efficacy, intrinsic electrical properties, and/or cell morphology. While activity-dependent regulation of the synaptic proteome via *de novo* translation has long been recognized (1, 2), it was not until the 1990s that the role of the ubiquitin-proteasome system (UPS) began to be appreciated in targeted degradation of proteins participating in synaptic plasticity (3).

Accumulating evidence has now established a key role for the UPS in regulating the development and efficacy of synapses (4-6). Acting within both pre- and post-synaptic compartments, the UPS has been reported to control a number of specific actions, including: synapse maturation and maintenance, silencing presynaptic activity, and inhibiting the assembly of SNARE core complexes (7-10). The UPS also

determines the AMPA receptor content and functional state of the postsynaptic density (PSD) (11, 12), degrading neurotransmitter receptors and scaffolding proteins, in response to neural activity directing proteasomes to dendritic spines (13, 14). Moreover, extensive evidence implicates the UPS in regulating spine dynamics (15) and trans-synaptic plasticity (16). Differential targeting of positive and negative regulators of synaptic plasticity by the UPS is therefore proposed to contribute to the physiological dynamic range of neurotransmitter release and reception, and hence, the efficacy of information transfer at synapses.

Tomosyn-1 (Tomo-1) is a soluble, SNARE-family protein, primarily known as a potent negative regulator of vesicle fusion (17) that strongly reduces evoked exocytosis of neurotransmitter-containing vesicles (18-20) and plasticity induction within the brain (21-23). Though soluble, Tomo-1 also associates with secretory vesicles and plasma membranes in neuroendocrine cells (24, 25) and neurons (26-28). Tomo-1 has been observed to regulate neurite outgrowth and increase branching complexity in developing cultured rat hippocampal neurons and chemically-differentiated NG108 cells (29). Moreover, our recent study demonstrated an importance of Tomo-1 in modulating distribution of presynaptic vesicles among functionally defined vesicle pools, separating actively recycling vesicles from non-fusogenic resting vesicles (30).

Highly conserved orthologs of Tomo-1 are found in *S. cerevisiae* (Sro7p/77p), *C. elegans* (TOM-1), and *D. melanogaster* (Lgl), where they appear to exhibit strong similarities in structural properties (31-35) and mechanistic actions (36-38). TOM-1 has been reported to participate in trans-synaptic plasticity via the neurexin-neuroligin

pathway in *C. elegans* (39). Tomo-1 is also critical for some forms of plasticity and memory, including hippocampal-dependent learning and memory in mice (22), and associative odor memory in *D. melanogaster* (21). These reports suggest the activity and functional impacts of Tomo-1 may be dynamically modifiable as a result of neural activity.

Tomo-1 is subject to multiple forms of post-translational modification in neurons, including phosphorylation by PKA (36) and CDK5 (30), and SUMOylation (40) by PIASγ (41). While PKA phosphorylation at serine-724 and SUMOylation at lysine-730 both reduce the inhibitory actions of Tomo-1, they do so by different means, as only PKA phosphorylation reduces Tomo-1 interaction with the R-SNARE syntaxin-1a. By comparison, CDK5 phosphorylation of Tomo-1 has been reported to increase its inhibitory properties on membrane trafficking (30). Sro7p/77p also functionally regulate membrane vesicle trafficking with their activity subject to regulation by Rab-GTPases (Sec4) and a type V myosin (Myo2) (31). Like Tomo-1, the related Tomo-2 protein is also expressed within cytoplasm of neurons, including those within the hippocampus in mice (42). Interestingly, expression of Tomo-2 in HEK293T or the insulin-secreting INS1 cell lines revealed it was a target of UPS-mediated degradation (43). However, the role of the UPS in regulating Tomo-1 level within neurons remains unknown.

Characterizing processes determining Tomo-1 protein level and functional state is important based on Tomo-1's key role in modulating vesicle release probability and trans-synaptic tuning in neurons. The purpose of the current study was to examine UPS-mediated regulation of Tomo-1 in hippocampal neurons and the impact of this

regulation on synaptic structure. In addition, SNARE-domain containing proteins, including Tomo-1, and the UPS have been linked to the proteinopathy and protein aggregation associated with neurological and neurodegenerative diseases; including Autism Spectrum Disorders (ASD) (44-46), Alzheimer's Disease (AD) (47, 48) and Parkinson's Disease (PD) (49, 50). Specifically, Tomo-1 gene variation in humans have been correlated with ASD (51).

2.3 Results

Tomo-1 Expression Level Alters Dendritic Spine Density

As Tomo-1 is reported to alter membrane trafficking and vesicle fusion, we initially examined if Tomo-1 alters the density or morphology of dendritic spines in synaptically mature cultures of rat hippocampal neurons (17-24 DIV). Neurons were transfected with a soluble mCherry fluorophore (mCH), and co-transfected with one of the following expression constructs: 1) N-terminal tagged eGFP-m-Tomo-1 (Tomo-1), 2) eGFP-m-Tomo-1 containing a C-terminal R-SNARE motif deletion (ΔCT), 3) cytosolic eGFP, as a control for the overexpression of vectors containing eGFP (GFP), 4) shRNA targeting m-Tomo-1 for knockdown (KD), and 5) the same shRNA vector with a scrambled nucleotide sequence replacing the Tomo-1 target sequence (SCR). In addition, we examined a condition in which shRNA KD of rat Tomo-1 was rescued with co-transfection of shRNA-resistant human N-terminal tagged mCH-Tomo-1. Effectiveness of the Tomo-1 KD and rescue was confirmed by both immunocytochemistry (ICC, Fig. 2.1A-B, D) and Western blot (WB, Fig. 2.1C-D). ICCs

were quantified in transfected, shRNA-expressing neurons, relative to neighboring non-transfected control neurons. High-resolution confocal imaging of neurons transfected with GFP-Tomo-1 also demonstrated localization within the cytosol to dendrites and spines (Fig. 2.2A). For spine analysis co-expression of mCH and either GFP-Tomo-1, or shRNA constructs also encoding GFP, was confirmed by imaging of both mCH and GFP spectral lines. WBs of lysates from virally-infected neuronal cultures demonstrated that our expression constructs successfully KD, overexpress, and rescue Tomo-1 in neurons (Fig. 2.1C-D). To restrict fluorescence analysis to processes arising from individual neurons, we transfected cultures under conditions generating low transfection efficiency (≈ 2-5 cells per coverslip). To assess alterations in dendritic spine density and morphology, transfected neurons were subjected to laser-scanning confocal microscopy (LSCM) of mCH fluorescence intensity over a series of Z-planes. Acquired Z-stacks were subsequently compiled to render 3-dimensional reconstructed dendrites from which spine density and morphology was quantified by following a single dendritic arbor projecting from each neuronal cell body. Representative images of dendrite segments for each condition tested are shown in Fig. 2.2B.

Importantly, our results demonstrate that exogenous Tomo-1 expression specifically and significantly increased average spine density. In contrast, shRNA-mediated KD decreased dendritic spine density, an effect overcome by Tomo-1 rescue, relative to respective controls (Fig. 2.2C). This identifies a novel postsynaptic function for Tomo-1, as the sparse transfection makes an indirect presynaptic effect unlikely. Notably, this effect occurred independently of Tomo-1's C-terminal R-SNARE domain.

That is, the effects on spine density of Tomo-1 lacking its R-SNARE domain (ΔCT) were not significantly different from those overexpressing wild-type Tomo-1. Expression of the scrambled shRNA control sequence (SCR) had no significant effect on spine density relative to GFP control. Although Tomo-1 overexpression and knockdown was found to affect spine density, no significant effects were found on total spine length (Fig. 2.2D), spine head maximum diameter (Fig. 2.2E), or spine head volume (Fig. 2.2F). However, the rescue of Tomo-1 expression did indicate increases in maximum spine head diameter and volume (Fig. 2.2E-F, purple). Moreover, as shown in Fig. 2.2G-H, cumulative frequency distributions of dendrite spine count versus distance from neuronal soma confirmed statistically significant differences between Tomo-1, ΔCT, and KD relative to respective controls. Notably, the cumulative distributions were generally linear for each condition, indicating a uniform distribution of spine number over the measured distance of the dendrite. These results are the first to indicate Tomo-1 protein has the capacity to regulate the genesis or stability of dendritic spines, and potentially, the integrative synaptic drive of hippocampal neurons in culture.

Endogenous Tomo-1 Colocalizes with PSD95 in Dendritic Spines

Next, we examined by ICC if endogenous Tomo-1 is colocalized with the postsynaptic density protein PSD95, which may implicate its presence locally within spines of hippocampal neurons. Antigen specificity of the antibodies was confirmed by ICC of transfected HEK293T cells selectively overexpressing Tomo-1, Tomo-2, or empty vector control (Fig. 2.3A). Antibody specificity was further determined by WB of

transfected HEK293T cell lysates (Fig. 2.3B). As shown in Fig. 2.3C, ICC demonstrated that Tomo-1, while expressed throughout neurons, exhibits intense punctate immunofluorescence signals within neuronal processes. While several prior reports have noted that Tomo-1 colocalizes with presynaptic markers, our results reveal Tomo-1 is also often found localized at postsynaptic sites, as indicated by colocalization of individual Tomo-1 and PSD95 immunofluorescent puncta (Fig. 2.3C, white arrowheads; Fig. 2.3D, top). Indeed, line profiles of immunofluorescence along straightened dendrites show sites with highly correlated enrichment of Tomo-1 and PSD95 (Fig. 2.3D, bottom). Furthermore, pixel-by-pixel analysis of intensity profiles between the spectral channels further supports the validity of the observed colocalization between Tomo-1 and PSD95 (Fig. 2.3E, Pearson's overlap coefficient; r=0.885, r^2=0.783, Manders' correlation coefficients; M1=0.759 (fraction of PSD95 overlapping Tomo-1), M2=0.889 (fraction of Tomo-1 overlapping PSD95)).

Proteasomal Regulation of Tomo-1 Determines its Abundance

As Tomo-1 expression level correlated with changes in dendritic spine density we next evaluated if the UPS may dynamically regulate neuronal Tomo-1 levels. First, we tested the effects of inhibiting the proteolytic activity of the 26S proteasome complex via bath application of MG132 (MG; 50μM, 4H) or Lactacystin (Lac; 10μM, 4H) vs. DMSO vehicle control. Proteasome blockade via either drug significantly increased neuronal Tomo-1 protein levels, as shown by WB analysis of whole-cell lysate (Input) samples (Fig. 2.4A, G). Proteasome inhibition demonstrated no significant effect on total β-actin

level. Depletion immunoprecipitation (IP) of Tomo-1 from lysate samples following proteasome blockade largely reproduced effects found on WB Input samples (Fig. 2.4B, H). Specificity of the anti-Tomo-1 antibody used for IP was verified, as no immunoreactivity was apparent in WB of rabbit IgG control or Tomo-2 IPs (Fig. 2.4C-D).

Tomo-1 Interacts with the E3 Ubiquitin Ligase HRD1 in a Proteasome Activity-dependent Fashion

HRD1 is an E3 ubiquitin ligase integral in the endoplasmic reticulum (ER) membrane (52). It is known to inhibit apoptosis following buildup of misfolded proteins and ER stress (53) and it is critical for ER-associated degradation (ERAD) (54). HRD1 protein is expressed in neurons, but not glia, of the hippocampus, dentate gyrus, and cerebral cortex (55), all of which also exhibit Tomo-1 protein expression (42, 56). Notably, HRD1 has previously been identified as an interacting partner of Tomo-2 in a proteomics screen of Tomo-2 IP from the INS1 pancreatic β-cell line, and was further reported to regulate Tomo-2 level when co-expressed in HEK293FT cells (43). Therefore, we next investigated if Tomo-1 interacts with HRD1 in hippocampal neurons, and if this is an E3-mediated mechanism by which Tomo-1 is specifically ubiquitinated and targeted for degradation. To test this, Tomo-1 was immunoprecipitated from neuronal lysates and the IP sample was tested for HRD1 co-precipitation. As shown in Fig. 2.4B, Tomo-1 IP resulted in co-precipitation of HRD1. As control, IP with anti-rabbit IgG, resulted in no Tomo-1 or HRD1 immunoreactivity (Fig. 2.4C). To date, most known Tomo-1 protein interactions have been reported to occur via its R-SNARE domain,

which is homologous to the R-SNARE of VAMP2. However, as shown in Fig. 2.4E, IP of VAMP2 from neuronal cultures failed to co-IP HRD1, indicating that the Tomo-1 SNARE motif is unlikely a domain essential for interaction between Tomo-1 and HRD1. Though the UPS inhibitors MG or Lac increased Tomo-1 level in neuronal cultures, no significant increase in the level of HRD1 occurred following these treatments (Fig. 2.4F, I). Importantly however, proteasome blockade increased the extent to which HRD1 co-precipitated with endogenous Tomo-1 (Fig. 2.4B, J). These results indicate that perturbation of proteasome activity-dependent regulation not only affects Tomo-1 protein level, but may also alter the extent of which Tomo-1 interacts with HRD1.

HRD1 is Present in Neuronal Processes and Synapses

As mammalian HRD1 is localized to the ER membrane we next examined by ICC if HRD1 is present within neuronal processes, such as dendrites, where it may possess the ability to ubiquitinate and spatially regulate postsynaptic Tomo-1. Indeed, the ER has been reported to extend from somatic areas, where it is heavily enriched, into dendritic shafts and spines of neurons (57). Furthermore, localized ER stress responses have been detected in dendrites of cultured mouse hippocampal neurons (58). As shown in Fig. 2.5A, ICC of HRD1 in neuronal cultures demonstrated extensive HRD1 immunofluorescence within somata, as expected, but notably also within neuronal processes (Fig. 2.5A-B). A fluorescence intensity alignment profile of HRD1 and PSD95 along straightened dendrites demonstrated localization within processes (Fig. 2.5B, bottom). However, the diffuse dendritic distribution of HRD1 suggested it was not

specifically located at sites of PSD95 fluorescent puncta (Fig. 2.5C, Pearson's overlap coefficient; r=0.437, r^2=0.191, Manders' correlation coefficients; M1=0.724 (fraction of PSD95 overlapping HRD1), M2=0.517 (fraction of HRD1 overlapping PSD95)).

The finding of an ER-localized E3 ligase within dendrites of primary hippocampal neurons suggests that HRD1 regulation of Tomo-1 may occur beyond the somatic compartment. As such, we next investigated if interaction between endogenous Tomo-1 and HRD1 proteins occur in neurons, including processes, using a proximity-ligation assay (PLA) in fixed cultures. Interestingly, PLA fluorescent puncta indicated that Tomo-1 and HRD1 interact within the somata and non-somatic regions (Fig. 2.5D, and inset). Specificity of this PLA interaction was demonstrated by the absence of a PLA signal when an interaction between Tomo-1 and the cytosolic exocytic regulatory protein Munc18 was tested. Furthermore, fluorescent puncta were not apparent in antibody omission control PLA reactions (data not shown).

Tomo-1 Protein is Ubiquitinated Prior to Proteasomal Degradation

To determine if Tomo-1 is subject to HRD1-mediated ubiquitination within neurons, we next infected neuronal cultures with an N-terminal tagged YFP-Tomo-1 fusion protein, which efficiently precipitated with an anti-GFP nanobody (Fig. 2.6A). Importantly, IP samples from the YFP-Tomo-1 expressing neurons demonstrated ubiquitinated YFP-Tomo-1 conjugates (Fig. 2.6B). Conjugated-ubiquitin immunoreactivity was not apparent in IP samples of the Tomo-1 knockdown condition, in which cytosolic GFP was co-expressed. Furthermore, with GFP expression (Fig.

2.6C, top) no ubiquitin immunoreactivity was observed at 26kD, the molecular mass of GFP-family proteins, following GFP IP (Fig. 2.6C, bottom). This finding indicated that Tomo-1, and not the YFP (a GFP point mutant) fluoroprotein, was ubiquitinated.

We next examined if ubiquitination of the exogenously expressed YFP-Tomo-1 was altered by pharmacological proteasome blockade. As shown in Fig. 2.6D-F, the expression level of YFP-Tomo-1 was increased by approximately 1.5-fold vs. DMSO vehicle control after a 4-hour treatment with either MG or Lac. To mitigate deubiquitination in these experiments the broad-spectrum deubiquitinating enzyme (DUB) inhibitor PR-619 was co-applied with proteasome inhibitors. Fig. 2.6E, G shows that the increase in Tomo-1 level following proteasome blockade was accompanied by a significant increase in Tomo-1 ubiquitination, and, notably, the co-IP of HRD1 with YFP-Tomo-1 also increased upon MG treatment. Importantly, the fraction of Tomo-1 that was ubiquitinated following proteasome blockade significantly increased relative to total Tomo-1 IP level.

HRD1 Ubiquitinates Tomo-1 to Regulate its Level

To determine if HRD1 is capable of directly ubiquitinating Tomo-1, we utilized an *in vitro* ubiquitination assay. For this assay, we expressed and affinity-purified Tomo-1 protein from HEK293T cells, and used commercially available purified HRD1 and its various upstream cofactors (ubiquitin, UBE1, UBE2D2, and ATP). As shown in Fig. 2.6H, Tomo-1 is ubiquitinated in a concentration-dependent fashion by HRD1. Moreover, significant ubiquitination above background did not occur in control

conditions lacking HRD1, Tomo-1, or ATP, or when testing the empty vector control expressed and purified in the same manner as Tomo-1. Replacement of either the upstream E2 ubiquitin-conjugating enzyme (with UBE2G2), or the HRD1 itself (by another E3 enzyme of the same RING-type class: CHIP/STUB1) failed to induce Tomo-1 ubiquitination (data not shown).

HRD1 Degrades Tomo-1 to Increase Dendritic Spine Density

We next investigated if HRD1 ubiquitination and proteasomal targeting of Tomo-1 may modify the density of dendritic spines. To address this question, we tested shRNA constructs for HRD1 KD, and examined their effect on endogenous Tomo-1 protein level in hippocampal neuronal cultures. Two lentivirus-driven shRNAs targeting non-overlapping regions of HRD1 mRNA were tested. The shHRD1 constructs resulted in significant (39% and 47%) decreases in HRD1 protein level relative to a scrambled shRNA control, as determined by WB analysis of whole cell lysate samples (Fig. 2.7A). The incomplete KD of HRD1 within these neuronal lysates was likely the result of an only 56% transduction efficiency in cultured neurons (Fig. 2.7B). This suggests that the level of HRD1 within infected neurons may be lower than 50% of control. Viral infection was highly specific to neurons, as evidenced by neuronal-specific nuclei labeling with anti-NeuN. Our incomplete knockdown of HRD1 is of similar extent to previously reported RNAi-based knockdown of HRD1 in differentiated neurons (59). However, utilizing ICC fluorescence imaging to assess HRD1 KD efficiency, we observed that HRD1 fluorescence intensity levels in cells infected with a 50:50 mixture of both HRD1

shRNAs decrease approximately 72.2% as compared with SCR controls (Fig. 2.7C-D). Notably, the decrease found via WB analysis of HRD1 protein level following 52.5% knockdown resulted in a significant increase in Tomo-1 protein level by an average of 140.6% of control (Fig. 2.7E-F).

We next investigated the effects of HRD1 KD on dendritic spines, to determine if the effects of Tomo-1 on spine density are dependent upon regulation by HRD1. We performed confocal imaging and 3D reconstruction and analysis of dendritic spines as in Fig. 2.2. First, neuronal cultures were transfected with a soluble mCH fluorophore and co-transfected with either; shRNAs targeting HRD1 (HRD1 KD), or the scrambled shRNA vector. Each shRNA construct co-expresses a soluble GFP reporter fluorophore. Representative images for each condition are shown in Fig 2.8A. HRD1 KD was found to significantly increase average spine density, from 3.9 to 5.8 spines per ten micrometers, relative to the SCR control (Fig. 2.8B). This effect parallels that observed following Tomo-1 overexpression, suggesting that HRD1 may tune spine density via Tomo-1 ubiquitination and targeting for degradation. Effects of HRD1 KD exhibited a statistically significant on average spine length, but no effect was found on head diameter or volume (Fig. 2.8C-E). Cumulative spine frequency in the HRD1 KD was similar to the change observed for Tomo-1 overexpression (significant increase vs. respective controls) (Fig. 2.8F). We next tested if the alteration in spine density or cumulative spine frequency following HRD1 KD is related to specific actions of HRD1 on Tomo-1. This was assessed by simultaneous shRNA-mediated knockdown of Tomo-1 and HRD1. Importantly, the effect of HRD1 KD to increase average spine density was

nearly completely blocked in the double KD condition (2KD, Fig. 2.8B, F). The 2KD condition also exhibited a significant increase in averaged spine head diameter, with an accompanying trend on spine head volume but not spine length (Fig. 2.8C-E). These data suggest that the actions of HRD1 on spine density occur directly on or within the Tomo-1 signaling pathway, which itself alters spine density.

2.4 Discussion

In the present study, we identify Tomo-1, a soluble R-SNARE motif-containing protein, as a novel positive regulator of the density of dendritic spines in cultured hippocampal neurons. Tomo-1 overexpression specifically increased dendritic spine density without influencing average spine length, maximum head diameter, or head volume. Conversely, Tomo-1 knockdown decreased dendritic spine density. Notably, we have also determined that Tomo-1 is an interacting partner of and a specific target substrate for ubiquitination by the E3 ligase HRD1, which subsequently promotes Tomo-1 degradation by the 26S proteasome. Ablation of HRD1 activity via targeted knockdown increased global Tomo-1 protein levels in cultured neurons. Furthermore, HRD1 knockdown increased dendritic spine density. This effect was blocked following simultaneous knockdown of HRD1 and Tomo-1, strongly suggesting a signaling pathway involving both proteins in determining spine density. Thus, our data show that HRD1-mediated regulation of Tomo-1 is a newly identified component in neuronal regulation of spine density by the UPS and, therefore, potentially on synaptic dynamics of hippocampal neurons.

Neurons are highly polarized cells, with complex regulatory mechanisms that control cell excitability, synaptic plasticity, and information transfer within the brain. Tomo-1 has conserved orthologs (60) across a diversity of organisms and systems, demonstrating their important function in membrane trafficking and intercellular signaling. In addition, Tomo-1 exhibits a low level of genic intolerance relative to that expected by neutral variation found in genes (RVIS -0.4 (27%) (61), suggesting that genetic variants of Tomo-1 may confer an increased risk of disease. Functionally, Tomo-1 has inhibitory actions on secretion within the brain (17), superior cervical ganglion neurons (36), bovine adrenal chromaffin cells (62), pancreatic ß-cells (25) and in PC12 (40, 63) and CHO (64) cell lines. The most commonly reported mechanism of Tomo-1 action has been its role in inhibiting the priming and concomitant fusion of the readily-releasable pool (RRP) of vesicles in neurons (19, 30, 65) and neuroendocrine cells (66). In addition to Tomo-1 actions on the RRP, Tomo-1 has recently been shown to control the proportional reallocation of neurotransmitter-containing vesicles between functionally identified presynaptic vesicle pools (30).

The current study identifies a completely novel postsynaptic effect of Tomo-1 – the regulation of dendritic spine density in cultured hippocampal neurons. Interestingly, this action of Tomo-1 occurs independently of its C-terminal R-SNARE domain. The effects of Tomo-1 on dendritic spines may be analogous to known membrane trafficking and cytoskeletal regulation roles mediated by Tomo-1 orthologs. For example, two yeast Tomo-1 proteins, Sro7p/77p, together with Sec4 and Myo2 (18, 67-69), modulate

exocytosis by associating with cytoskeletal components and regulating SNARE function on the plasma membrane (31, 37).

The key importance of Tomo-1 in orchestrating vesicle priming and exocytotic secretion of chemical messengers raises an imperative need to identify and characterize the signaling pathways which control it. However, identification of transcriptional, translational, and degradative mechanisms mediating the expression level of Tomo-1 and, potentially, the dynamic range of its activity in neurons, is lacking. The present study has uncovered a novel form of Tomo-1 protein regulation in central neurons via the ubiquitin-proteasome system. We have identified HRD1, an ER-resident RING-type E3 ubiquitin ligase, as a novel upstream regulator which specifically targets Tomo-1 for degradation. Indeed, PLA imaging data indicated that while endogenous Tomo-1 and HRD1 are abundant in the cell soma, they also generally appear to be overlapping within neuronal dendrites. Further, HRD1 was co-IPd with Tomo-1 from neuronal lysate, and *in vitro* reactions using purified HRD1 and Tomo-1 proteins demonstrated concentration-dependent Tomo-1 ubiquitination by HRD1. The potential for similar actions occurring *in vivo* is supported by our results demonstrating that pharmacological proteasome blockade, via bath application of MG132 or Lactacystin, increased neuronal Tomo-1 protein level. Moreover, this action occurred on a shorter timescale than the half-life of most synaptic proteins (70), suggesting that ubiquitination may be used to selectively target Tomo-1 for rapid proteasomal degradation. However, future consideration is warranted for the concurrent examination of Tomo-1 biosynthetic

activity, as production rates may be linked to reduced UPS-mediated degradation or actions of proteasome blockers.

A proteomics screen of pull-down samples of Tomo-2 from the insulin-secreting INS1 ß-cell line also identified HRD1 as one of the highest confidence Tomo-2 interacting partners, in addition to HRD1 adaptor proteins (43). It is currently unknown at which lysine residues Tomo-1 is ubiquitinated by HRD1, nor to what extent ubiquitination alters the half-life of Tomo-1. Nonetheless, HRD1's well-established function in ubiquitinating target substrates for proteasomal degradation during ER-associated degradation (ERAD) can now be expanded to include actions within dendrites and on synaptic proteins. In addition, as Tomo-1 and HRD1 colocalize to dendrites where they likely interact, the potential exists for localized regulation of Tomo-1 protein level within, or near, postsynaptic sites. A rapid, potentially local, degradation of Tomo-1 may occur in a similar fashion to dephosphorylation-induced, UPS-mediated degradation of fragile X mental retardation protein (FMRP) in the dendrites and synapses of cultured rat neurons (71).

Specific E3 ubiquitin ligases are known to influence synaptic physiology and plasticity in both non-proteolytic (72) and proteolytic-dependent manners (73). Some of these have been shown to be dependent upon postsynaptic activity (11, 74, 75). Spine morphogenesis and number (76), as well as spine maintenance (77), including specific AMPA receptor subunit levels and membrane integration (78), are tightly controlled by the UPS. Within the microenvironment of the synapse, targeted protein degradation involving many specific E3 ubiquitin ligases, confers substrate specificity in

ubiquitination. Indeed, numerous neuronal E3s have been identified that functionally regulate specific levels of postsynaptic proteins. These include γ-actin (79), GKAP, and Shank (80), which are regulated by TRIM3, PSD95 by Mdm2 (13) upon facilitation by CDK5 (81), AMPARs by RNF167 (82) and Nedd4-2 (94), and the postsynaptic cytoskeletal protein and immediate early gene Arc by both UBE3A (83) and RNF216/TRIAD3 (84). Targeted ubiquitination of presynaptic proteins is also prominent. For example, the active zone (AZ) protein RIM1, which scaffolds the multi-protein modules which regulate priming and release of NT-containing vesicles, is acted upon by the E3 ligase SCRAPPER and results in rapid alteration in presynaptic release (85). Furthermore, the AZ proteins Bassoon and Piccolo, which are subject to regulation by the E3 ligase Siah1, were shown to be crucial in the ubiquitination and maintenance of numerous presynaptic proteins (8).

Prior reports have identified HRD1 as important in regulating neuronal cell biology. For example, upregulation of HRD1 following ER stress in differentiated neurons decreases neurite outgrowth and dendritic arborization (59). Furthermore, HRD1 has been shown to promote the degradation of other components of the synaptic proteome, including the Parkin-associated endothelin receptor-like receptor, PaeIR (55) and expanded polyglutamine variants of Huntingtin (86). Our results indicate that HRD1, which is well known to act on membrane delimited proteins, also regulates the cytosolic protein Tomo-1. While HRD1 targeting of soluble proteins has been rarely reported, it has been shown to facilitate proteasomal degradation and aggresome formation of Optineurin (87), a cytosolic protein involved in the maintenance of the Golgi complex,

membrane trafficking, and exocytosis. Interestingly, Optineurin, like the Tomo-1 orthologs Sro7p/77p, is reported to interact with myosin and Rab family proteins (31, 38, 88).

E3 ligase-mediated ubiquitination of substrate proteins is often sensitive to the state of the target protein's PTMs. Tomo-1 is regulated via multiple modifications, including phosphorylation at specific amino acid sites by PKA (36), Akt/PKB (64), and CDK5 (30) kinases, in addition to SUMOylation (40), which is mediated by the E3 PIAS (41). Furthermore, there is a growing body of evidence indicating facilitated co-regulation of protein substrates by phosphorylation, ubiquitination, and other PTMs. For example, CDK5, a kinase recently reported to phosphorylate Tomo-1 and exert a functional impact on the RRP, is downregulated following the S-nitrosylation of its upstream activator p35. This causes p35 ubiquitination by the E3 PJA2 and degradation (89). While the physiological signal driving HRD1-mediated ubiquitination of Tomo-1 is unknown, it may result from up- or down-regulated PTM of Tomo-1, or indirectly following the PTM of kinases and other upstream Tomo-1 regulators. Such integrative mechanisms may serve to balance the rate and targets of degradation and also provide the possibility for diversity in subcellular localization and activity-dependence.

Ubiquitination and proteasomal degradation of synaptic proteins does not necessarily indicate an impact on plasticity. It is currently unknown if the relationship between Tomo-1 and HRD1 is regulated following neuronal activity, for example, in a homeostatic fashion. TOM-1, a Tomo-1 ortholog in *C. elegans* was, however, reported to increase presynaptically in response to neurexin/neuroligin-mediated retrograde

downregulation of presynaptic NT release (39). The molecular mechanism driving the change in TOM-1 protein level remains uncharacterized. Furthermore, we have previously shown that Tomo-1 contributes to CNQX-induced synaptic scaling in hippocampal neurons (30), a form of homeostatic plasticity occurring following synaptic inactivation via AMPAR blockade. Future investigations are required to address the physiological parameters regulating HRD1-mediated Tomo-1 ubiquitination and the resulting functional consequences.

2.5 Materials and Methods

Animals

All animal handling procedures are approved by and in full compliance with the regulations of the University Committee on Use and Care of Animals of the University of Michigan, in addition to the National Institutes of Health guidelines.

Antibodies

Affinity-purified Rb anti-Tomosyn-1 polyclonal antibody (catalog no. 183103), and affinity-purified Rb anti-Tomosyn-2 polyclonal antibody (catalog no. 183203), and the Ms anti-PSD95 monoclonal antibody (catalog no. 124011) were from Synaptic Systems (Göttingen, Germany). The Ms anti-β-actin monoclonal antibody (clone AC74, catalog no. A2228) was from Sigma-Aldrich (St. Louis, MO). The Rb anti-HRD1 polyclonal antibody (catalog no. 13473-1-AP) was from ProteinTech (Chicago, IL). The Ms anti-conjugated-ubiquitin monoclonal antibody (clone FK2, catalog no. BML-PW8810) was

from Enzo Life Sciences (Farmingdale, NY). The Ms anti-GFP antibody (clone C163, catalog no. 33-2600) was from ThermoFisher (Waltham, MA). For western blots, IRDye 800CW-conjugated goat anti-mouse IgG H+L (catalog no. 926-68021) and IRDye 680LT-conjugated goat anti-rabbit IgG H+L (catalog no. 926-32210) fluorescent secondary antibodies were from Li-Cor Biosciences (Lincoln, NE). For light microscopy immunocytochemistry Alexa Fluor 488-, 594-, and 647-conjugated species-specific anti-IgG secondary antibodies raised in goat (catalog nos. A11073, A11012, and A21236 respectively) were from Invitrogen (Waltham, MA). Affinity-purified Ms anti-NeuN (neuronal nuclei) monoclonal antibody (Clone A60, catalog. no. MAB377) was from Millipore (Billerica, MA).

Cell Culture and Transfections

All results were obtained from dissociated rat hippocampal neuronal cultures (17-28 DIV), unless otherwise noted. Hippocampal neuronal cultures were prepared as previously described, with minor adjustments (90). Briefly, hippocampal neurons from embryonic day 19-20 Sprague-Dawley rats of either sex (Charles River) were plated at 400-450 cells/mm^2 on either 18mm diameter, #1.5 thickness coverglass (Neuvitro, catalog no. GG-18) or on 14mm microwell glass- bottom 35mm culture dishes (MatTek, catalog no. P35G-0.170-14-C) and maintained in an incubator containing 95%/5% O_2/CO_2 and 100% humidity at 37°C in NBActiv4 medium (catalog no. Nb4, BrainBits, Springfield, IL) for up to 4 weeks *in vitro* prior to experimentation. Half of the neuronal culture medium was replaced every 3-4 days until experimentation.

Hippocampal cultures were co-transfected at 13-21 DIV for spine imaging at 17-25 DIV. Transfection was achieved using 200µL of NBActiv4, including 1µL Lipofectamine 2000 (Invitrogen, catalog no. 11668019) per dish and pCAG-mCherry (0.4µg/dish), in addition to one of the following constructs (1µg/dish): GFP-shTomo-1, GFP-shHRD1, GFP-shSCR, GFP-Tomo-1, GFP-Tomo-1 lacking the C-terminus. Transfection solutions were allowed to stand for 30 min. before being dripped onto the cell cultures. Cultures were incubated for 1 hour with the Lipofectamine/DNA mix, after which media was exchanged with fresh NBActiv4 media. Pyramidal neurons were then imaged 3-5 days post-transfection.

HEK293T cells (catalog no. CRL-3216, ATCC, Manassas, VA, ≤15 passages) were seeded in plastic T-75 tissue culture flasks at <75% confluence in an incubator containing 95%/5% O_2/CO_2 and 100% humidity at 37°C in DMEM (Gibco catalog no. 11960) containing: 10% FBS (Gibco catalog no. 10437-028), 1% glutamax (ThermoFisher, catalog no. 35050061), 1% penicillin-streptomycin (Sigma, catalog no. P4333), and 1% non-essential amino acids (Gibco, catalog no. 11140-050).

Cloning of Full-length Rat m-Tomo-1 Constructs into the Gateway Expression Vector

The coding sequence of rat m-Tomosyn-1 (NCB accession # NP_110470.1) was cloned into the NativePure Gateway destination vector pcDNA3.2/capTEV-CT/V5-DEST (Invitrogen, catalog no. BN3002) for expression in HEK293T cells and native affinity purification for use in the *in vitro* ubiquitination reactions.

Drugs

The following chemicals were used for this study, as noted: DMSO (Life Technologies, catalog no. D12345), MG132 (Cayman Chemicals, catalog no. 10012628), Lactacystin (Tocris, catalog no. 2267), PR-619 (Tocris, catalog no. 4482). Where noted, protease inhibitor cocktail minus EDTA (Roche, catalog no. 11580800) was added to lysis and/or IP buffers.

Image Acquisition, Analysis, and Quantification

Live cell imaging of neuronal spines was performed on a Nikon Eclipse Ti inverted microscope operating a Nikon A1 laser-scanning confocal system. Specimens were housed under incubation conditions throughout imaging in a gas-, temperature-, and humidity-controlled imaging chamber (Tokai Hit). Laser illumination was provided at 488nm (air-cooled, argon ion laser at 40 mW, Spectra-Physics) and 543nm (HeNe laser at 5 mW, Melles Griot). Fluorescence images were acquired with the NIS Elements AR imaging suite (Nikon, version 4.51.00) with pinhole size set to 57.5μm (2 A.U.) using a 60X oil-immersion objective (Plan Apo 60X Oil DIC N2) and 3X digital zoom. Images were captured at 1024x1024 pixels, with a 0.5 frames/second scan speed and 0.338μm Z-step size. Identical settings for laser intensity and background offset were maintained between all experimental conditions. An entire dendrite emanating from one somatic branch point per neuron was fully imaged and auto-compiled into a Z-stack. The Z-stacks were then re-constructed in 3D and analyzed offline using Imaris 7 software (Bitplane, version 7.7.2). Automated detection and analysis of spines was performed on

single dendrites from point of initiation at the soma through 150µm of dendrite shaft length.

ICC imaging was performed on an Olympus BX61WI upright laser-scanning confocal microscope using a 20X, 0.75NA air (Olympus America, catalog no. UAPO340) or 60X, 1.42NA oil-immersion objective (Olympus America, catalog no. PLAPON-60X) at 1024x1024 pixels image size and 10μs pixel dwell time. Identical settings for gain, laser intensity, background offset, and pinhole size were maintained between all experimental conditions. Fluorescence images were then analyzed offline with the FIJI imaging suite, including the JACoP plugin (91).

PLA experiments were imaged on an Olympus IX-81 inverted spinning-disc confocal microscope using an ApoN 60X, 1.49 NA oil-immersion objective (Olympus America, catalog no. APON 60XOTIRF) in wide-field (disc-out) configuration. Illumination was provided by a 300W xenon arc lamp (Sutter Instrument, LB-LS/30) coupled to an electronically-shuttered liquid light guide for controlled transmission of light to the microscope optics. Images were captured with an ImagEM EM-CCD camera (catalog no. C9100-13, Hamamatsu City, Shizuoka, Japan) with 16µm pixel-size using Metamorph image acquisition software (software version no. 7.7.1.0, Molecular Devices, Sunnyvale, CA). The following optical filter-sets were used for DAPI, mCherry and GFP fluorophores, respectively: excitation 405/25; 472/30; 416/25, and emission 450/30; 520/35; 464/23.

Immunocytochemistry and Proximity Ligation Assay

ICC was performed on cultured hippocampal neurons adhered to the center wells of glass-bottomed 35mm dishes pre-coated with poly-D-lysine (catalog no. P35GC-1.5-14-C, MatTek, Ashland MA) as listed above. Cells were fixed and stained according to published protocol (92). All antibody dilutions and rinses were in PBS + 3% BSA. Primary antibodies were added at indicated dilutions for one hour, followed by rinses (5x, 5 min. each) and addition of secondary antibodies for 45 minutes, followed by rinses as above, and stored in Vectashield with DAPI (catalog no. H-1200, Vector Labs, Burlingame, CA) at 4°C prior to imaging. PLA reactions were performed in the exact fashion as ICC procedures through primary antibody incubation. Next, anti-rabbit PLA^+ (catalog no. DUO92002) and anti-mouse PLA^- (catalog no. DUO92004) probes (Sigma-Aldrich) were added for 45 min. at 37°C, followed by rinses (3x, 5 min. each, in PBS containing 0.2% BSA, 0.1% Triton X-100). Next, ligation and amplification solutions (kit catalog no. DUO92007) were sequentially added for 30 and 100 min., respectively, with rinses as above between and prior to imaging.

Immunoprecipitation of Endogenous Tomosyn-1 and HRD1 from Hippocampal Neuronal Culture

Immunoprecipitation of endogenous protein from cultured hippocampal neurons was performed using either the Tomo-1-specific or HRD1 antibodies noted above by pre-binding 2µg antibody to 50µL protein A magnetic dynabead slurry (Pierce, catalog no. 88845) per 35mm dish in 100mM Na-phosphate buffer (pH 8.0) containing (mM): 75 Na_2HPO_4 and 25 NaH_2PO_4. Cultures were lysed and collected in non-denaturing lysis

buffer (pH 7.5) containing (mM): 50 NaCl, 25 Tris, 2 $MgCl_2$, 1 $CaCl_2$, 0.5% NP-40, and 2x recommended concentration of complete EDTA-free protease inhibitor cocktail. Samples were then equalized for total protein concentration (1-3µg/µL) and sample volume (100-300µL) prior to incubation with the conjugated beads for one hour at 4°C. The samples were then rinsed in lysis buffer and boiled in 1x SDS sample buffer for five minutes before being loaded for PAGE and western blotting.

In Vitro Ubiquitination Assay

The Gateway rat m-Tomosyn-1 construct noted above was used to express Tomo-1 in HEK293T to encourage proper post-translational modification and 3-dimensional protein structure prior to experimental procedures. Cells were seeded at 50% confluence from liquid nitrogen stocks in 10cm cell culture dishes for ≈ 16 hours and serum-starved in 10mL Opti-MEM (Gibco catalog no. 31985) for one hour prior to transfection. Transfection occurred using 25µg plasmid DNA and 25µL Lipofectamine 2000 (Invitrogen, catalog no. 1166809) in 10mL Opti-MEM, per dish, for five hours under standard incubator conditions before standard HEK cell medium replacement. 48-72 hours following transfection the cells were lysed under non-denaturing conditions in lysis buffer containing (mM): 100 Tris, 100 KCl, 0.2 EDTA, 1.5 $MgCl_2$, 0.01 pepstatin-A (Sigma, catalog no. P5318) and protease inhibitor cocktail minus EDTA (Roche) at 2x recommended concentration. Lysates were then subjected to 3 freeze-thaw cycles using liquid nitrogen and centrifuged at 3,000xG for 10 minutes for de-nucleation. NP-40 was added to the lysate supernatants to a final concentration of 1% v/v. Lysates were

then incubated with streptavidin-agarose beads (Invitrogen, catalog no. S951) for three hours at 4°C to purify the biotinylated epitope-tagged m-Tomo-1 fusion construct. Final purity and protein concentration were quantified using a serial dilution vs. BSA standard on a coomassie-stained SDS-PAGE gel.

For use in ubiquitin reactions, 2µg purified Tomosyn-1 bound to the streptavidin-agarose beads was suspended in assay buffer containing the following (mM): 100 Tris, 10 $MgCl_2$, and 0.2 DTT (Invitrogen, catalog no. 15508-013) and subjected to the following reaction conditions at 37°C for 45 minutes with mixing (E3Lite Ubiquitin Ligase Kit, catalog no. UC101, LifeSensors, Malvern, PA): 20µg/mL wild-type human ubiquitin (catalog no. SI201), 10nM UBE1 (catalog no. UB101), 100nM UBE2D2 (catalog no. UB207H), 16-250nM HRD1 (catalog no. UB307), 200µM ATP (catalog no. A50-09-200, SignalChem, Richmond, BC, Canada). Negative control experiments were run exactly as described above, with substitution of the E2 UBE2D2 with UBE2G2 (catalog no. UB227) or the E3 HRD1 with CHIP/STUB1 (catalog no. UB309).

RNA Interference and Lentiviral Construct Generation for Targeting HRD1 and Tomo-1

Lentiviral vectors encoding a short hairpin RNAi (shRNA) for targeted knockdown of rat HRD1 were created in the pGFP-C-shLenti and pRFP-CB-shLenti expression vectors (Origene, Rockville, MD, catalog nos. TL704173 and TR30032) which independently encode (via U6 promoter) the following shRNA sequences, respectively: TGGTTGGCTGAAGACCGTGTGGACTTTAT, TTGTCAGCCACGCTTATCACAGCATCCTG. Non-targeted scrambled shRNA

sequences (shSCR): CAGGAACGCATAGACGCATGA, in the same lentiviral vectors were used for control experiments. Targeted knockdown of all Tomo-1 isoforms was accomplished using the same vector with the following custom shRNA sequence inserted: ACTGCTTCAGCCAGTGATTGTGTCTCCAA.

All shRNA constructs were packaged and produced at the University of Michigan Vector Core (Ann Arbor, MI). Briefly, HEK293T cells were Lipofectamine-transfected with vectors encoding REV, MDL, pvSVG, and each lentiviral plasmid-containing expression construct. At 42 hours post-transfection, the virion-containing medium was collected, filtered through a 0.45µm filter to remove cell debris, and ultra-centrifuged at 42,152xG at 4°C for 2H. The supernatant was then discarded and the viral pellet gently resuspended in 10mL NBActiv4 neuronal culture medium (to ≈ $1x10^7$ MOI/mL). 500µL aliquots were quickly frozen and stored at -80°C. Neuronal cultures were treated with a 1:5 (HRD1 knockdown) or 1:10 (Tomo-1 knockdown) dilution of virus at 10-18 DIV and allowed to express for 4-7 days before experimentation.

Western blotting

SDS-PAGE gels were wet-transferred onto nitrocellulose membranes at 10V for 1.2 hours and blocked in non-mammalian Odyssey blocking buffer (Li-Cor Biosciences, Lincoln, NE, catalog no. 927-40000). Blocking, primary antibody, and secondary antibody incubations were all performed for 1 hour at room temperature and were rinsed 3x for 5 minutes each in PBS + 0.1% Tween-20 (PBS-T) between incubations. All primary antibodies were used at a 1:1,000 dilution in PBS-T for western blotting, except

for the following: anti-β-actin (AC74) 1:8,000, anti-GFP (C163) 1:8,000, and anti-ubiquitin (FK2) 1:250. All secondary antibodies were used at a 1:15,000 dilution in PBS-T. Western blot images were collected with an Odyssey CLx Infrared Imaging System (Li-Cor model no. 9120) at 84μm resolution in high quality mode and within the linear range of exposure. Fluorescence density was quantified with the open-source ImageJ software including the FIJI imaging suite (93) and the gel analyzer plugin.

YFP-Tomo-1 Protein Expression and Purification

Mouse m-Tomosyn-1 (NCB accession # NP_001074813.2) cloned into the pLenti-hSyn-eYFP backbone (22) was provided by Dr. Uri Ashery (Tel Aviv University) and used for efficient transduction and expression in cultured hippocampal neurons, as well as for immunoprecipitation following *in vivo* ubiquitination experiments. Immunoprecipitation of YFP-Tomosyn proteins was performed using GFP-Trap magnetic beads (catalog no. gtma20, ChromoTek, Planegg, Germany). Cells were lysed in buffer containing: 150mM NaCl, 50mM Tris, 1% NP-40, 10μM PR-619, and 2x recommended concentration of protease inhibitor cocktail. Lysates were centrifuged at 10,000xG and supernatants assayed using the Bradford method for total protein quantification. Total protein and volume equalizations were performed on all samples prior to incubation with the anti-GFP beads for 90 minutes at 4°C to purify the YFP-Tomosyn fusion construct. The samples were then rinsed in lysis buffer and boiled in 1.5X LDS sample buffer + reducing agent (Invitrogen, catalog nos. B0007, B0009) for 10 minutes before being loaded for PAGE and western blotting.

Statistical Analyses

All statistical analyses were performed with Prism 6 (version 6.0f, Graphpad Software, La Jolla, CA). Where indicated two-tailed t-tests or analysis of variance (ANOVA) were used for comparisons of population means. Post-hoc t-tests were used for multiple comparisons between specific groups. Cumulative frequency distributions were compared using a Kolmogorov-Smirnov test. Sample means throughout are presented ± SEM, with significance thresholds set to # $p < 0.1$; * $p < 0.05$; ** $p < 0.01$ for all tests.

Use of Biological Replicates

Each experiment performed in the current study used unique and independent samples (n = culture dishes for protein level biochemistry; reactions for *in vitro* ubiquitination assays; single dendrites of individual neurons for spine analysis; neurons for ICC imaging) including paired controls where noted. Significant results were determined from at least three independent neuronal preparations.

2.6 Acknowledgements

This work was supported by NIH grants; F31 NS087883 (JJS), RO1 NS053978, and RO1 NS097498 (ELS). We thank Drs. Michael Sutton, Alan Attie, and Uri Ashery for valuable research discussion. We also thank Dr. Christina Whiteus for helpful

comments on the manuscript. This research made use of the following University of Michigan core facilities; Vector, DNA Sequencing, Microscopy and Image Analysis.

Figure 2.1: Knockdown, overexpression, and rescue of Tomo-1 protein in hippocampal neurons.

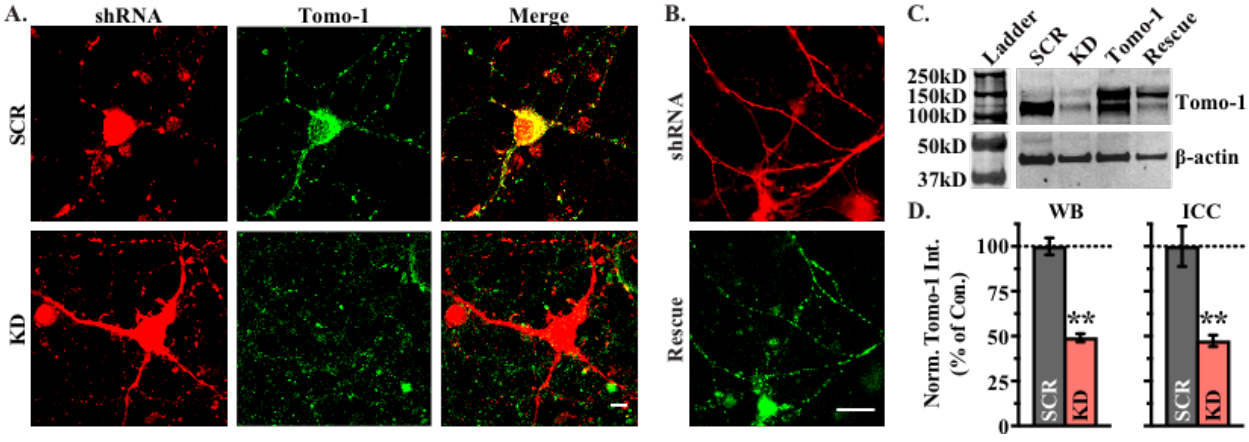

Figure 2.1: Knockdown, overexpression, and rescue of Tomo-1 protein in hippocampal neurons.

A, Representative LSCM fluorescence micrographs of shRNA expression reporter (tRFP, red), Tomo-1 expression (anti-Tomo-1, green), and merged overlays in neurons following expression of the scrambled shRNA control (SCR) or an shRNA targeting Tomo-1 for KD. Scale = 10µm. *B*, Fluorescence micrographs of a neuron expressing Tomo-1 shRNA (red) + shRNA-resistant mCH-Tomo-1 (green, Rescue). *C*, Comparison of Tomo-1 expression by WB (20µg/lane) following lentiviral-infection with; scrambled shRNA vector control (SCR), shRNA targeting Tomo-1 + GFP (KD), GFP-Tomo-1 fusion protein (Tomo-1), or an shRNA-resistant mCH-Tomo-1 (Rescue). *D*, Lentiviral infection with an shRNA targeting Tomo-1 for knockdown (red) decreases Tomo-1 intensity to 49.1 ± 2.3% (via WB, n = 4) and 47.4 ± 3.1% (via ICC, n =8) of scrambled shRNA control vector (grey). All data presented as population mean ± SEM, with n# defined as individual neurons or independent culture dishes. Statistical significance (**, $p < 0.01$), where indicated, was determined vs. SCR vector control using was determined using two-tailed t-tests.

Figure 2.2: Effect of Tomo-1 protein abundance on dendritic spine density.

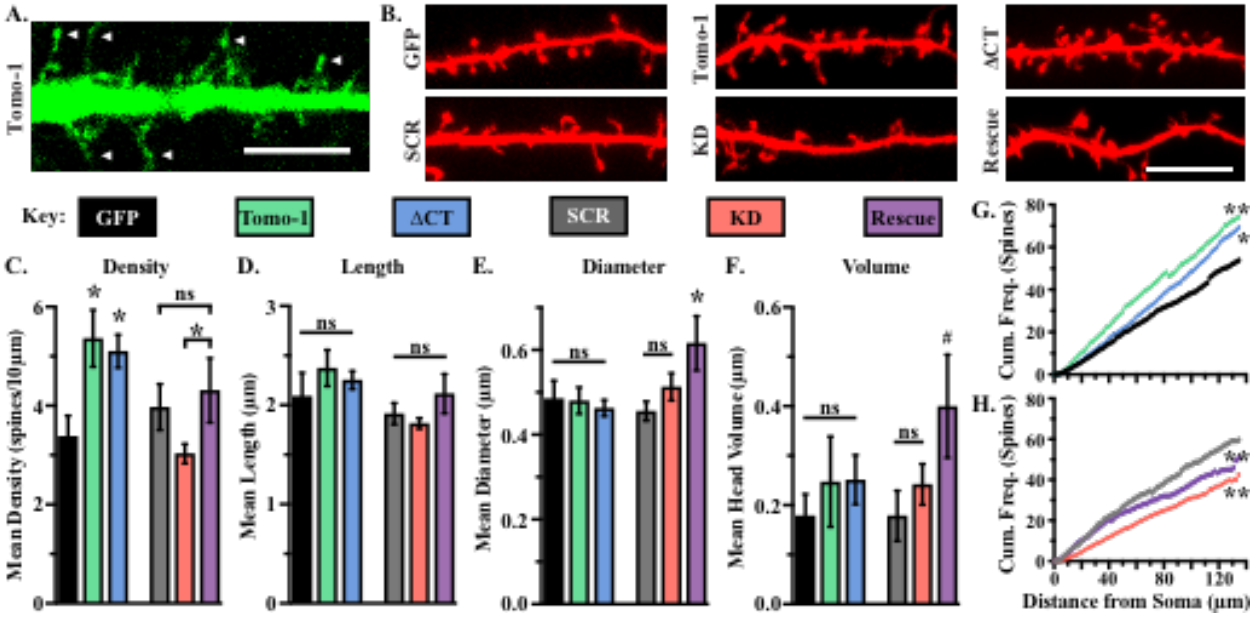

Figure 2.2: Effect of Tomo-1 protein abundance on dendritic spine density.

A, GFP-Tomo-1 expression within a fixed dendrite indicates Tomo-1 OE localizes to dendritic spines (white arrowheads), scale bar = 10µm. *B*, Representative fluorescence micrographs of dendrites in transfected neurons expressing cytosolic mCH (red) and one of the following; GFP control (GFP, n = 9), GFP-Tomo-1 (Tomo-1, n = 8), GFP-Tomo-1 ΔCT, (n = 13), scrambled shRNA control (SCR, n = 7), Tomo-1 shRNA (KD, n = 14), or Tomo-1 shRNA + shRNA-resistant mCH-Tomo-1 (Rescue, n = 7), scale bar = 10μm. *C-F*, Averaged spine density (*C*), spine length (*D*), maximum spine head diameter (*E*), and spine head volume (*F*) for each indicated condition. *G-H*, Comparison of cumulative frequency distributions of spine density in neurons in each condition. All data presented as population mean ± SEM, with n# defined as individual dendrites or neurons from independent culture dishes. Statistical significance (#, $p<0.1$; *, $p < 0.05$; **, $p < 0.01$), where indicated, was determined vs. GFP or SCR vector controls using one-way ANOVAs with multiple comparisons of the mean or Kolmogorov-Smirnov tests of cumulative frequency distributions.

Figure 2.3: Tomo-1 localizes within postsynaptic compartments and is sensitive to shRNA-mediated knockdown.

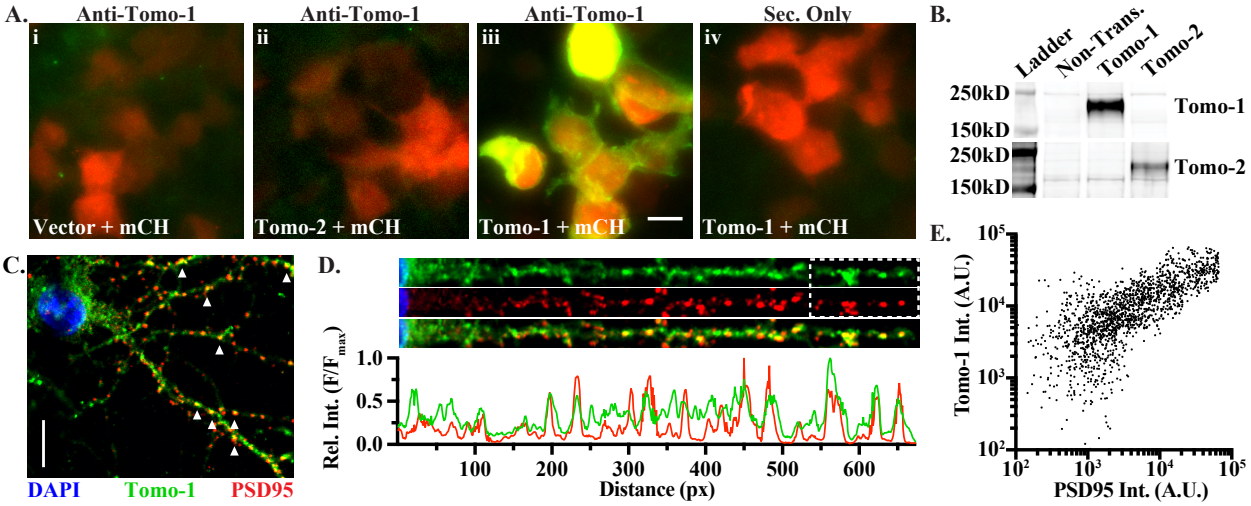

Figure 2.3: Tomo-1 localizes within postsynaptic compartments and is sensitive to shRNA-mediated knockdown.

A, ICC of Tomo-1 (green) in HEK293T cells following expression of mCH (red) with; (i) empty vector, (ii) Tomo-2, (iii) Tomo-1, or (iv) Tomo-1 (secondary antibody only), scale bar = 10µm. *B*, Anti-Tomo-1 WB of lysates from non-transfected HEK293T cells versus cells transfected with Tomo-1 or Tomo-2. *C*, Representative ICC image of hippocampal neuron displaying merged fluorescence of endogenous Tomo-1 (green), PSD95 (red), and nuclei (blue, DAPI), scale bar = 10µm. *D*, Representative intensity line scans of Tomo-1 (green) and PSD95 (red) fluorescence of an individual straightened dendrite indicate coincident immunofluorescence (lower plot). Merged Tomo-1+PSD95 fluorescence (lower micrograph). *E*, Cytofluorogram of Tomo-1 and PSD95 intensities from the dashed box region in part D (Pearson's overlap coefficient; r=0.885, r^2=0.783, Manders' correlation coefficients; M1=0.759; representing fraction of PSD95 overlapping Tomo-1, M2=0.889; representing fraction of Tomo-1 overlapping PSD95).

Figure 2.4: Effect of proteasome blockade on neuronal Tomo-1 protein and its interaction with the E3 ligase HRD1.

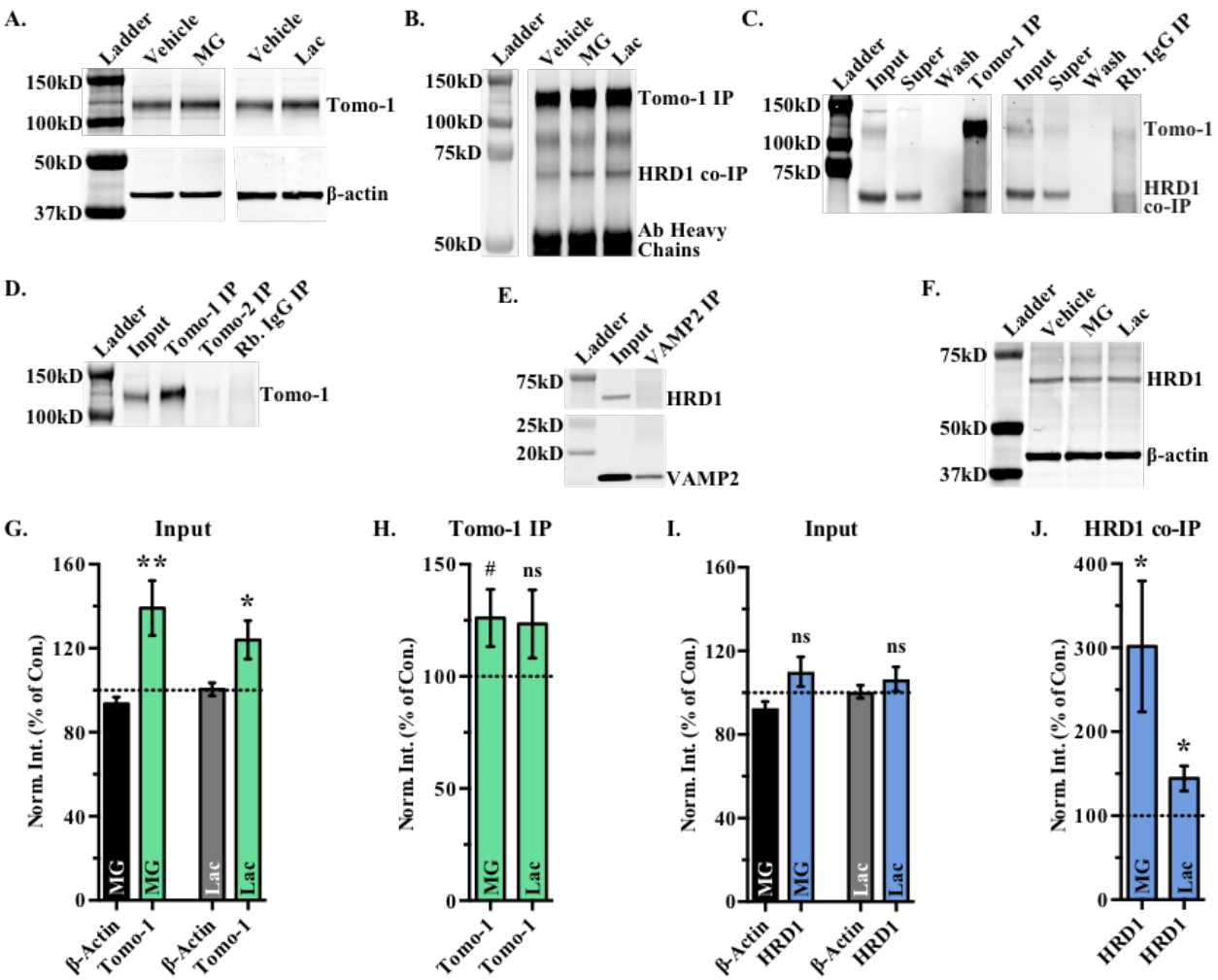

Figure 2.4: Effect of proteasome blockade on neuronal Tomo-1 protein and its interaction with the E3 ligase HRD1.

A, WBs of neuronal cultures treated with proteasome inhibitors MG132 (MG, 50µM, 4H) or Lactacystin (Lac, 10µM, 4H) vs. DMSO vehicle control on endogenous Tomo-1 protein levels. *B*, WB of proteasome treatments, as in part A, on Tomo-1 IP and HRD1 co-IP levels. *C*, IP of Tomo-1 co-IPs HRD1, however IgG control IP does not co-IP HRD1. Tomo-1 was immunodepleted from lysates (Input), with little immunoreactive Tomo-1 in post-IP supernatant (Super). *D*, The Tomo-1 antibody is selective for precipitating Tomo-1 protein from lysates as Tomo-1 IP (15 DIV, 20µg/sample), but not rabbit IgG control (Rb. IgG) or Tomo-2, showed Tomo-1 immunoreactivity. *E*, IP of VAMP2 does not result in co-IP of HRD1. *F*, Treatment of cultures with the proteasome inhibitors, as in part A, resulted in no significant change in endogenous HRD1 in lysate. Data are normalized against ß-actin protein levels (MG; n=7, Lac; n=7). *G*, Quantification of Tomo-1 inputs from part A (normalized to ß-actin protein levels, MG; n=28, Lac; n=21). *H*, Quantification of Tomo-1 IPs from part B. Averages are presented as percent change vs. vehicle-treated controls (dotted line, MG; n=7, Lac; n=7)). *I-J,* Quantification of HRD1 from lysate inputs (I) and HRD1 co-IP with Tomo-1 (J), (MG; n=6, Lac; n=7). All data presented as population mean ± SEM, with n# defined as independent neuronal culture dishes. Statistical significance (#, $p < 0.1$; *, $p < 0.05$; **, $p < 0.01$), where indicated, was determined using two-tailed t-tests.

Figure 2.5: The E3 ligase HRD1 is present throughout neuronal processes and interacts with Tomo-1.

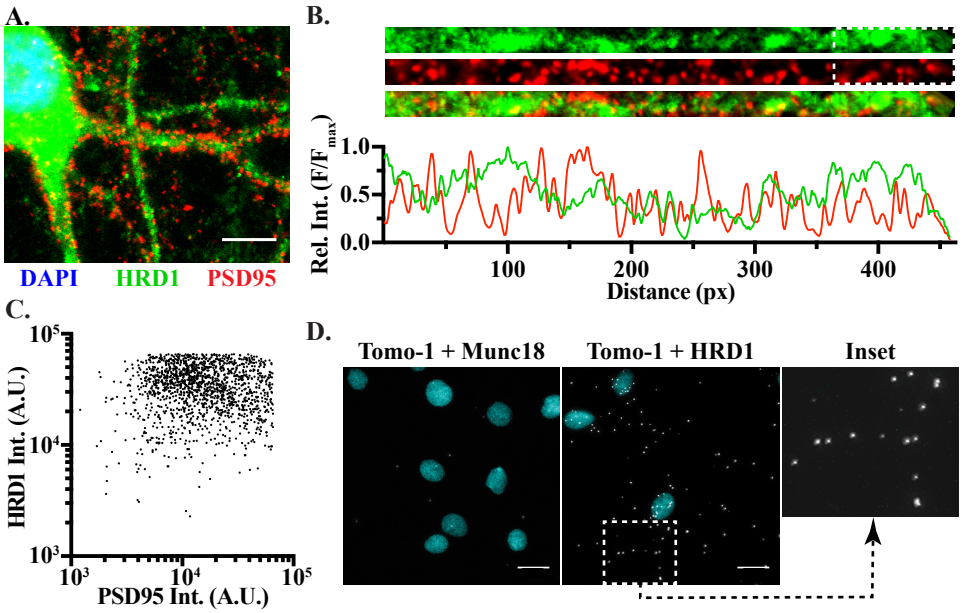

Figure 2.5: The E3 ligase HRD1 is present throughout neuronal processes and interacts with Tomo-1.

A, Representative ICC image showing merged immunoreactive fluorescence of endogenous HRD1 (green), PSD95 (red), and nuclei (DAPI, blue) in cultured neurons, scale bar = 10µm. Note presence of HRD1 in dendrites. *B*, Representative fluorescence intensity line scans of HRD1 (green) and PSD95 (red) of an individual straightened dendrite indicate coincident immunofluorescence (lower plot). Merged Tomo-1+PSD95 fluorescence is also shown (lower micrograph). *C*, Cytofluorogram analysis of fluorescence intensity relationship between HRD1 and PSD95 from dashed box region on dendrite highlighted in part B (Pearson's overlap coefficient; r=0.437, r^2=0.191, Manders' correlation coefficients; M1=0.724; representing fraction of PSD95 overlapping HRD1, M2=0.517; fraction of HRD1 overlapping PSD95), indicates a lack of specific colocalization. *D*, Representative Tomo-1 and HRD1 interaction assessed via proximity ligation analysis (PLA) demonstrates substantive numbers of fluorescent puncta in somatic regions and along neuronal processes (12 DIV), scale bar = 10µm. Inset expands outlined region. PLA testing for interaction between Tomo-1 and the synaptic protein Munc18 (top) resulted in low levels of fluorescent puncta similar to secondary antibody treatment alone (not shown).

Figure 2.6: Tomo-1 in hippocampal neurons is subject to *in situ* ubiquitination and is ubiquitinated *in vitro* by HRD1.

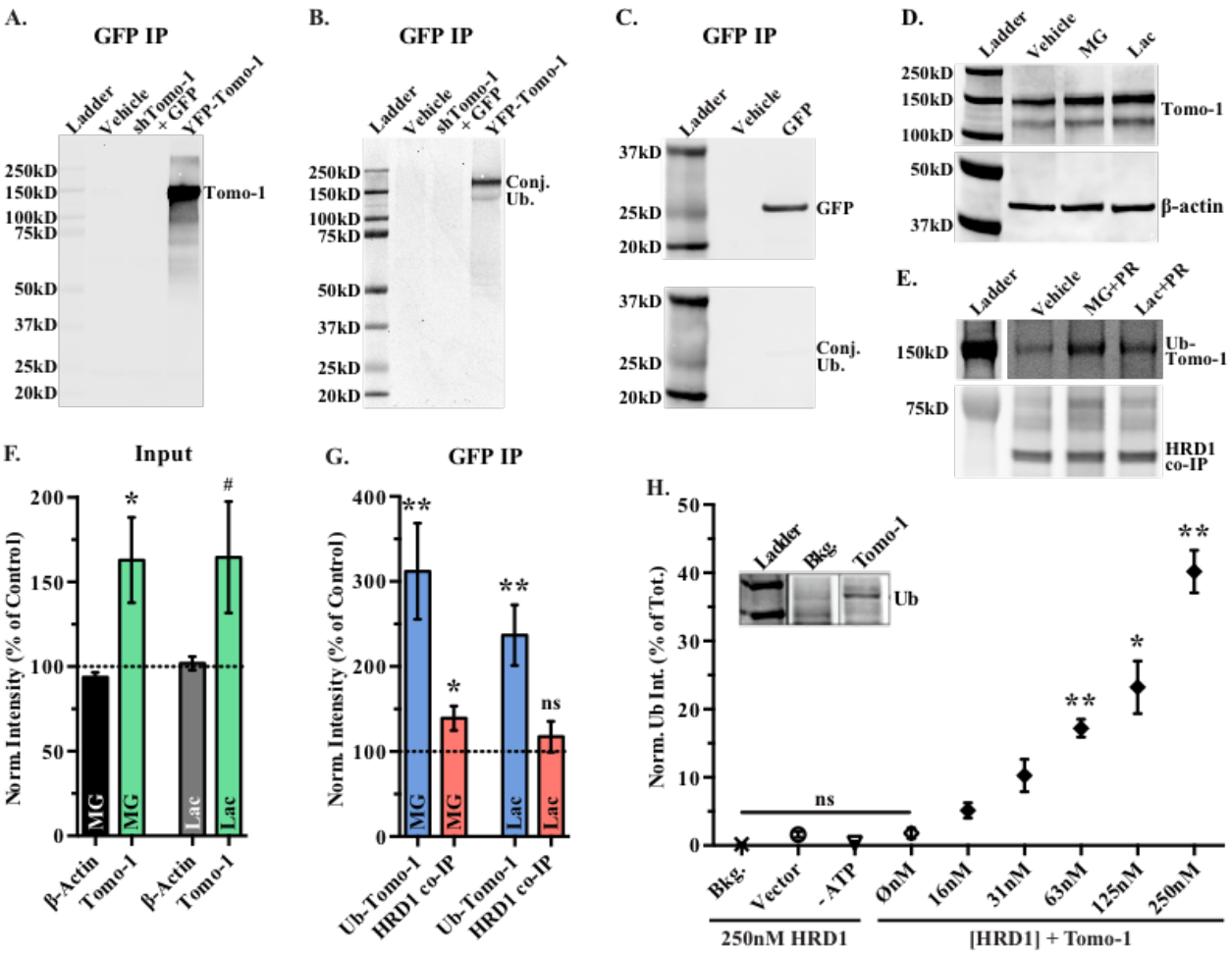

Figure 2.6: Tomo-1 in hippocampal neurons is subject to *in situ* ubiquitination and is ubiquitinated *in vitro* by HRD1.

A-*B*, WB of YFP-Tomo-1 IPs from lentivirus-infected neurons were probed for immunoreactivity against Tomo-1 (A) and conjugated-ubiquitin (B). Neuronal infection with a lentivirus expressing shTomo-1 and free GFP demonstrated no anti-conjugated-ubiquitin reactivity at 26 kD (B). *C*, WB of GFP (top) and conjugated ubiquitin (bottom) following GFP IP from infected neurons. *D*, WB for endogenous Tomo-1 and expressed YFP-Tomo-1 from lysates of neurons following treatment with the proteasome inhibitors MG (50µM, 4H) or Lac (10µM, 4H). *E*, WB of Tomo-1 IP probed for conjugated ubiquitin (top) and for HRD1 (bottom) following treatment with proteasome inhibitors + 10*µ*M PR-619 (PR). *F*, Averaged YFP-Tomo-1 and ß-actin levels from part D (MG n=18, Lac n=13). *G*, Averaged ubiquitinated Tomo-1 level and HRD1 co-IP levels from part E (MG, n=10; Lac, n=8). Above data (F-G) presented as population mean ± SEM, with n# defined as independent neuronal culture dishes. Averages are expressed as percent change relative to paired, vehicle-treated experimental controls (dotted line). Statistical significance (#, $p < 0.1$, *, $p < 0.05$, **, $p < 0.01$) was determined using two-tailed t-tests. *H*, Concentration-dependent *in vitro* ubiquitination of purified Tomo-1 by HRD1. Inset displays anti-ubiquitin WB of representative reaction product. Data are expressed relative to background and negative controls with significance (*, $p < 0.05$; **, $p < 0.01$, n=3) determined via multiple comparisons ANOVA.

Figure 2.7: Knockdown of HRD1 protein and functional relationship with Tomo-1.

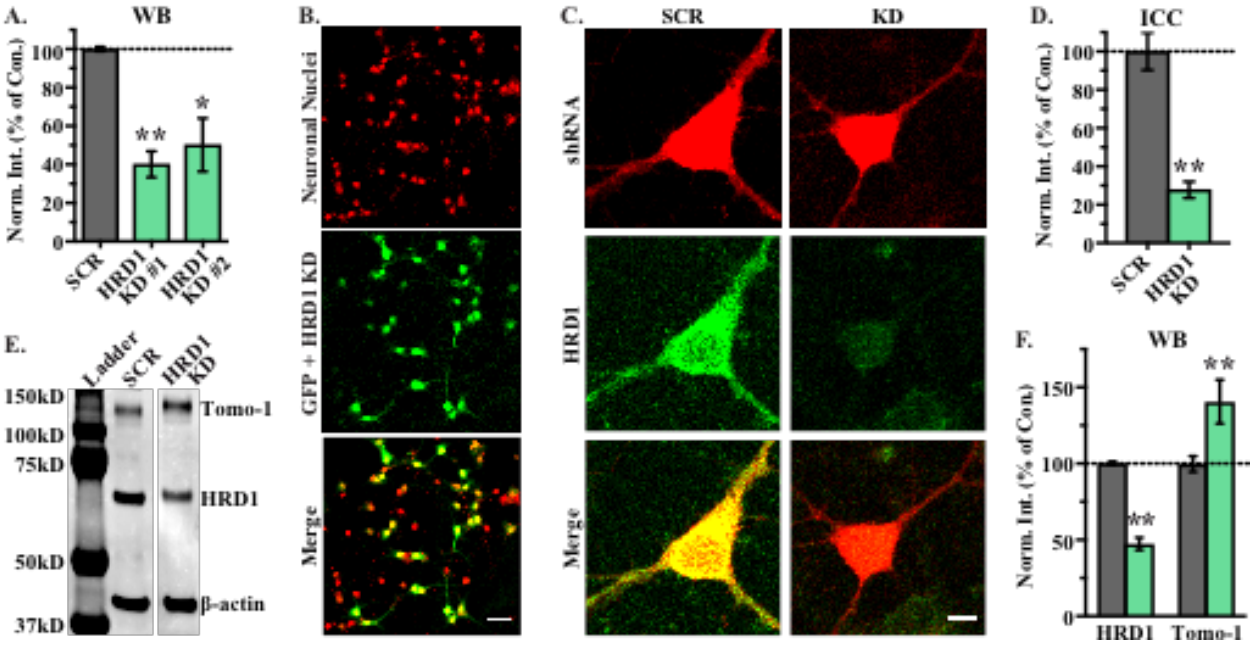

Figure 2.7: Knockdown of HRD1 protein and functional relationship with Tomo-1.

A, Histograms of shRNA-mediated decreases in HRD1 from virally-transduced cultures with two different shRNA KD sequences targeting HRD1 (mean ± SEM, multiple comparisons ANOVA, *, $p < 0.05$, **, $p < 0.01$, n=3). *B*, Representative images of shHRD1-infected neuronal cultures. Transduction efficiency was quantified by counting shHRD1-expressing neurons (GFP-positive, middle) versus the total number of neurons present (anti-NeuN, top). Transduction efficiency averaged 56%, with < 8% non-neuronal infection (n=1,972 neurons, 20 FOVs, 4 dishes), scale bar = 50µm. *C*, Representative LSCM fluorescence micrographs of shRNA expression reporter (tRFP, red), HRD1 expression (anti-HRD1, green), and merged overlays in neurons following expression of the scrambled shRNA control (SCR) or an shRNA targeting HRD1 for KD, as in part B. Scale bar = 10µm. *D*, Histograms of shRNA-mediated decrease in HRD1 level following ICC of cultures infected with a 1:1 ratio of both HRD1 shRNA KD vectors. Values (mean ± SEM, n=9) are normalized to anti-HRD1 ICC signal in scrambled shRNA (SCR) infected neurons. *E*, WB comparison of neuronal HRD1 expression between lentiviral-infected SCR and HRD1 shRNA KD. *F*, Histogram comparing HRD1 and Tomo-1 expression levels in neuronal cultures treated with a mix of the HRD1 KD shRNAs (green) or SCR control (grey). All data presented as population mean ± SEM, with n# defined as individual neurons or independent culture dishes (HRD1 n=17, Tomo-1 n=14). Statistical significance (*, $p < 0.05$; **, $p < 0.01$), where indicated, was determined vs. SCR vector control using two-tailed or multiple t-tests.

Figure 2.8: Effect of HRD1 protein abundance on dendritic spine density.

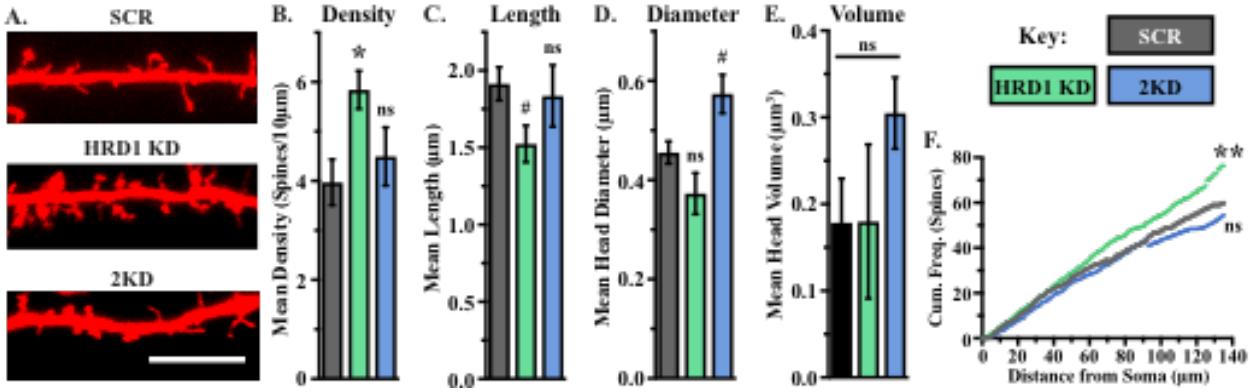

Figure 2.8: Effect of HRD1 protein abundance on dendritic spine density.

A, Representative LSCM fluorescence micrographs of dendrites emanating from cultured hippocampal neurons transfected with and expressing cytosolic mCH (red) and HRD1 shRNA (HRD1 KD), or Tomo-1 shRNA + HRD1 shRNA (2KD), scale bar = 10μm. *B-E*, Comparison of averaged spine density (*B*), spine length (*C*), spine head maximum diameter (*D*), and spine head volume (*E*) of individual neurons (14-28 DIV) for the following conditions; HRD1 KD (green, n = 7), SCR control (SCR, grey, n = 7), or shRNAs targeting both HRD1 and Tomo-1 (2KD, blue, n = 8). *F*, Cumulative frequency distributions of spine density from above conditions. All data presented as population mean ± SEM, with n# defined as individual dendrites or neurons from independent culture dishes. Statistical significance (#, $p<0.1$; *, $p < 0.05$; **, $p < 0.01$), where indicated, was determined vs. SCR vector control using one-way ANOVAs with multiple comparisons of the mean or Kolmogorov-Smirnov tests of cumulative frequency distributions.

2.7 Bibliography

1. Rosenberg, T., Gal-Ben-Ari, S., Dieterich, D. C., Kreutz, M. R., Ziv, N. E., Gundelfinger, E. D., and Rosenblum, K. (2014) The roles of protein expression in synaptic plasticity and memory consolidation. *Front Mol Neurosci*. **7**, 1–14

2. Sutton, M. A., and Schuman, E. M. (2006) Dendritic Protein Synthesis, Synaptic Plasticity, and Memory. *CELL*. **127**, 49–58

3. Hegde, A. N., Goldberg, A. L., and Schwartz, J. H. (1993) Regulatory subunits of cAMP-dependent protein kinases are degraded after conjugation to ubiquitin: a molecular mechanism underlying long-term synaptic plasticity. *Proc. Natl. Acad. Sci. U.S.A.* **90**, 7436–7440

4. Hegde, A. N. (2017) Proteolysis, synaptic plasticity and memory. *Neurobiol Learn Mem*. **138**, 98–110

5. Alvarez-Castelao, B., and Schuman, E. M. (2015) The Regulation of Synaptic Protein Turnover. *Journal of Biological Chemistry*. **290**, 28623–28630

6. Pak, D. T. S., and Sheng, M. (2003) Targeted protein degradation and synapse remodeling by an inducible protein kinase. *Science*. **302**, 1368–1373

7. Patrick, G. N. (2006) Synapse formation and plasticity: recent insights from the perspective of the ubiquitin proteasome system. *Current Opinion in Neurobiology*. **16**, 90–94

8. Waites, C. L., Leal-Ortiz, S. A., Okerlund, N., Dalke, H., Fejtova, A., Altrock, W. D., Gundelfinger, E. D., and Garner, C. C. (2013) Bassoon and Piccolo maintain synapse integrity by regulating protein ubiquitination and degradation. *The EMBO Journal*. **32**, 954–969

9. Jiang, X., Litkowski, P. E., Taylor, A. A., Lin, Y., Snider, B. J., and Moulder, K. L. (2010) A role for the ubiquitin-proteasome system in activity-dependent presynaptic silencing. *Journal of Neuroscience*. **30**, 1798–1809

10. Zhang, Q., Li, Y., Zhang, L., Yang, N., Meng, J., Zuo, P., Zhang, Y., Chen, J., Wang, L., Gao, X., and Zhu, D. (2013) E3 ubiquitin ligase RNF13 involves spatial learning and assembly of the SNARE complex. *Cell. Mol. Life Sci.* **70**, 153–165

11. Ehlers, M. D. (2003) Activity level controls postsynaptic composition and signaling via the ubiquitin-proteasome system. *Nat. Neurosci.* **6**, 231–242

12. Schwarz, L. A., and Patrick, G. N. (2012) Ubiquitin-dependent endocytosis,

trafficking and turnover of neuronal membrane proteins. *Mol. Cell. Neurosci.* **49**, 387–393

13. Colledge, M., Snyder, E. M., Crozier, R. A., Soderling, J. A., Jin, Y., Langeberg, L. K., Lu, H., Bear, M. F., and Scott, J. D. (2003) Ubiquitination regulates PSD-95 degradation and AMPA receptor surface expression. *Neuron*. **40**, 595–607

14. Bingol, B., and Schuman, E. M. (2006) Activity-dependent dynamics and sequestration of proteasomes in dendritic spines. *Nature*. **441**, 1144–1148

15. Hamilton, A. M., Oh, W. C., Vega-Ramirez, H., Stein, I. S., Hell, J. W., Patrick, G. N., and Zito, K. (2012) Activity-dependent growth of new dendritic spines is regulated by the proteasome. *Neuron*. **74**, 1023–1030

16. Huang, J., Ikeuchi, Y., Malumbres, M., and Bonni, A. (2015) A Cdh1-APC/FMRP Ubiquitin Signaling Link Drives mGluR-Dependent Synaptic Plasticity in the Mammalian Brain. *Neuron*. **86**, 726–739

17. Ashery, U., Bielopolski, N., Barak, B., and Yizhar, O. (2009) Friends and foes in synaptic transmission: the role of tomosyn in vesicle priming. *Trends Neurosci.* **32**, 275–282

18. Lehman, K., Rossi, G., Adamo, J. E., and Brennwald, P. (1999) Yeast homologues of tomosyn and lethal giant larvae function in exocytosis and are associated with the plasma membrane SNARE, Sec9. *The Journal of Cell Biology*. **146**, 125–140

19. Sakisaka, T., Yamamoto, Y., Mochida, S., Nakamura, M., Nishikawa, K., Ishizaki, H., Okamoto-Tanaka, M., Miyoshi, J., Fujiyoshi, Y., Manabe, T., and Takai, Y. (2008) Dual inhibition of SNARE complex formation by tomosyn ensures controlled neurotransmitter release. *The Journal of Cell Biology*. **183**, 323–337

20. Bielopolski, N., Lam, A. D., Bar-On, D., Sauer, M., Stuenkel, E. L., and Ashery, U. (2014) Differential Interaction of Tomosyn with Syntaxin and SNAP25 Depends on Domains in the WD40-Propeller Core and Determines Its Inhibitory Activity. *Journal of Biological Chemistry*. **289**, 17087–17099

21. Chen, K., Richlitzki, A., Featherstone, D. E., Schwärzel, M., and Richmond, J. E. (2011) Tomosyn-dependent regulation of synaptic transmission is required for a late phase of associative odor memory. *Proceedings of the National Academy of Sciences*. **108**, 18482–18487

22. Barak, B., Okun, E., Ben-Simon, Y., Lavi, A., Shapira, R., Madar, R., Wang, Y., Norman, E., Sheinin, A., Pita, M. A., Yizhar, O., Mughal, M. R., Stuenkel, E., van

Praag, H., Mattson, M. P., and Ashery, U. (2013) Neuron-specific expression of tomosyn1 in the mouse hippocampal dentate gyrus impairs spatial learning and memory. *Neuromolecular Med.* **15**, 351–363

23. Ben-Simon, Y., Rodenas-Ruano, A., Alviña, K., Lam, A. D., Stuenkel, E. L., Castillo, P. E., and Ashery, U. (2015) A Combined Optogenetic-Knockdown Strategy Reveals a Major Role of Tomosyn in Mossy Fiber Synaptic Plasticity. *CELREP*. **12**, 396–404

24. Cheviet, S., Bezzi, P., Ivarsson, R., Renström, E., Viertl, D., Kasas, S., Catsicas, S., and Regazzi, R. (2006) Tomosyn-1 is involved in a post-docking event required for pancreatic beta-cell exocytosis. *Journal of Cell Science*. **119**, 2912–2920

25. Zhang, W., Lilja, L., Mandic, S. A., Gromada, J., Smidt, K., Janson, J., Takai, Y., Bark, C., Berggren, P.-O., and Meister, B. (2006) Tomosyn is expressed in beta-cells and negatively regulates insulin exocytosis. *Diabetes*. **55**, 574–581

26. Fujita, Y., Shirataki, H., Sakisaka, T., Asakura, T., Ohya, T., Kotani, H., Yokoyama, S., Nishioka, H., Matsuura, Y., Mizoguchi, A., Scheller, R. H., and Takai, Y. (1998) Tomosyn: a syntaxin-1-binding protein that forms a novel complex in the neurotransmitter release process. *Neuron*. **20**, 905–915

27. McEwen, J. M., Madison, J. M., Dybbs, M., and Kaplan, J. M. (2006) Antagonistic regulation of synaptic vesicle priming by Tomosyn and UNC-13. *Neuron*. **51**, 303–315

28. Takamori, S., Holt, M., Stenius, K., Lemke, E. A., Grønborg, M., Riedel, D., Urlaub, H., Schenck, S., Brügger, B., Ringler, P., Müller, S. A., Rammner, B., Gräter, F., Hub, J. S., De Groot, B. L., Mieskes, G., Moriyama, Y., Klingauf, J., Grubmüller, H., Heuser, J., Wieland, F., and Jahn, R. (2006) Molecular Anatomy of a Trafficking Organelle. *CELL*. **127**, 831–846

29. Sakisaka, T., Baba, T., Tanaka, S., Izumi, G., Yasumi, M., and Takai, Y. (2004) Regulation of SNAREs by tomosyn and ROCK: implication in extension and retraction of neurites. *The Journal of Cell Biology*. **166**, 17–25

30. Cazares, V. A., Njus, M. M., Manly, A., Saldate, J. J., Subramani, A., Ben-Simon, Y., Sutton, M. A., Ashery, U., and Stuenkel, E. L. (2016) Dynamic Partitioning of Synaptic Vesicle Pools by the SNARE-Binding Protein Tomosyn. *Journal of Neuroscience*. **36**, 11208–11222

31. Watson, K., Rossi, G., Temple, B., and Brennwald, P. (2015) Structural basis for recognition of the Sec4 Rab GTPase by its effector, the Lgl/tomosyn homologue,

Sro7. *Molecular Biology of the Cell*. **26**, 3289–3300

32. Burdina, A. O., Klosterman, S. M., Shtessel, L., Ahmed, S., and Richmond, J. E. (2011) In Vivo Analysis of Conserved C. elegans Tomosyn Domains. *PLoS ONE*. **6**, e26185–8

33. Pobbati, A. V., Razeto, A., Böddener, M., Becker, S., and Fasshauer, D. (2004) Structural basis for the inhibitory role of tomosyn in exocytosis. *J. Biol. Chem.* **279**, 47192–47200

34. Yizhar, O., Lipstein, N., Gladycheva, S. E., Matti, U., Ernst, S. A., Rettig, J., Stuenkel, E. L., and Ashery, U. (2007) Multiple functional domains are involved in tomosyn regulation of exocytosis. *J Neurochem*. **103**, 604–616

35. Yamamoto, Y., Mochida, S., Miyazaki, N., Kawai, K., Fujikura, K., Kurooka, T., Iwasaki, K., and Sakisaka, T. (2010) Tomosyn inhibits synaptotagmin-1-mediated step of Ca2+-dependent neurotransmitter release through its N-terminal WD40 repeats. *Journal of Biological Chemistry*. **285**, 40943–40955

36. Baba, T., Sakisaka, T., Mochida, S., and Takai, Y. (2005) PKA-catalyzed phosphorylation of tomosyn and its implication in Ca2+-dependent exocytosis of neurotransmitter. *The Journal of Cell Biology*. **170**, 1113–1125

37. Hattendorf, D. A., Andreeva, A., Gangar, A., Brennwald, P. J., and Weis, W. I. (2007) Structure of the yeast polarity protein Sro7 reveals a SNARE regulatory mechanism. *Nature*. **446**, 567–571

38. Rossi, G., Watson, K., Demonch, M., Temple, B., and Brennwald, P. (2014) In vitro Reconstitution of Rab-dependent Vesicle Clustering by the Yeast Lethal Giant Larvae/Tomosyn Homolog, Sro7. *Journal of Biological Chemistry*. 10.1074/jbc.M114.595892

39. Hu, Z., Hom, S., Kudze, T., Tong, X.-J., Choi, S., Aramuni, G., Zhang, W., and Kaplan, J. M. (2012) Neurexin and neuroligin mediate retrograde synaptic inhibition in C. elegans. *Science*. **337**, 980–984

40. Williams, A. L., Bielopolski, N., Meroz, D., Lam, A. D., Passmore, D. R., Ben-Tal, N., Ernst, S. A., Ashery, U., and Stuenkel, E. L. (2011) Structural and functional analysis of tomosyn identifies domains important in exocytotic regulation. *Journal of Biological Chemistry*. **286**, 14542–14553

41. Geerts, C. J., Jacobsen, L., van de Bospoort, R., Verhage, M., and Groffen, A. J. A. (2014) Tomosyn Interacts with the SUMO E3 Ligase PIASγ. *PLoS ONE*. **9**, e91697–8

42. Barak, B., Williams, A., Bielopolski, N., Gottfried, I., Okun, E., Brown, M. A., Matti, U., Rettig, J., Stuenkel, E. L., and Ashery, U. (2010) Tomosyn expression pattern in the mouse hippocampus suggests both presynaptic and postsynaptic functions. *Front Neuroanat*. **4**, 149

43. Bhatnagar, S., Soni, M. S., Wrighton, L. S., Hebert, A. S., Zhou, A. S., Paul, P. K., Gregg, T., Rabaglia, M. E., Keller, M. P., Coon, J. J., and Attie, A. D. (2014) Phosphorylation and degradation of tomosyn-2 de-represses insulin secretion. *Journal of Biological Chemistry*. **289**, 25276–25286

44. Davis, L. K., Meyer, K. J., Rudd, D. S., Librant, A. L., Epping, E. A., Sheffield, V. C., and Wassink, T. H. (2009) Novel copy number variants in children with autism and additional developmental anomalies. *J Neurodev Disord*. **1**, 292–301

45. Bolte, E. R. (2003) The role of cellular secretion in autism spectrum disorders: a unifying hypothesis. *Med. Hypotheses*. **60**, 119–122

46. Lehman, N. L. (2009) The ubiquitin proteasome system in neuropathology. *Acta Neuropathol.* **118**, 329–347

47. Sharma, M., Burré, J., and Südhof, T. C. (2012) Proteasome inhibition alleviates SNARE-dependent neurodegeneration. *Sci Transl Med*. **4**, 147ra113

48. Hegde, A. N., Haynes, K. A., Bach, S. V., and Beckelman, B. C. (2014) Local ubiquitin-proteasome-mediated proteolysis and long-term synaptic plasticity. *Front Mol Neurosci*. **7**, 96

49. Shin, J.-H., Ko, H. S., Kang, H., Lee, Y., Lee, Y.-I., Pletinkova, O., Troconso, J. C., Dawson, V. L., and Dawson, T. M. (2011) PARIS (ZNF746) repression of PGC-1α contributes to neurodegeneration in Parkinson's disease. *CELL*. **144**, 689–702

50. Garcia-Reitböck, P., Anichtchik, O., Bellucci, A., Iovino, M., Ballini, C., Fineberg, E., Ghetti, B., Corte, Della, L., Spano, P., Tofaris, G. K., Goedert, M., and Spillantini, M. G. (2010) SNARE protein redistribution and synaptic failure in a transgenic mouse model of Parkinson's disease. *Brain*. **133**, 2032–2044

51. Lin, Y.-C., Frei, J. A., Kilander, M. B. C., Shen, W., and Blatt, G. J. (2016) A Subset of Autism-Associated Genes Regulate the Structural Stability of Neurons. *Front. Cell. Neurosci.* **10**, 805–35

52. Nadav, E., Shmueli, A., Barr, H., Gonen, H., Ciechanover, A., and Reiss, Y. (2003) A novel mammalian endoplasmic reticulum ubiquitin ligase homologous to

the yeast Hrd1. *Biochemical and Biophysical Research Communications*. **303**, 91–97

53. Kaneko, M., Ishiguro, M., Niinuma, Y., Uesugi, M., and Nomura, Y. (2002) Human HRD1 protects against ER stress-induced apoptosis through ER-associated degradation. *FEBS Letters*. **532**, 147–152

54. Gauss, R., Jarosch, E., Sommer, T., and Hirsch, C. (2006) A complex of Yos9p and the HRD ligase integrates endoplasmic reticulum quality control into the degradation machinery. *Nat. Cell Biol.* **8**, 849–854

55. Omura, T., Kaneko, M., Tabei, N., Okuma, Y., and Nomura, Y. (2008) Immunohistochemical localization of a ubiquitin ligase HRD1 in murine brain. *J. Neurosci. Res.* **86**, 1577–1587

56. Groffen, A. J. A., Jacobsen, L., Schut, D., and Verhage, M. (2005) Two distinct genes drive expression of seven tomosyn isoforms in the mammalian brain, sharing a conserved structure with a unique variable domain. *J Neurochem*. **92**, 554–568

57. Ramírez, O. A., and Couve, A. (2011) The endoplasmic reticulum and protein trafficking in dendrites and axons. *Trends in Cell Biology*. **21**, 219–227

58. Murakami, T., Hino, S. I., Saito, A., and Imaizumi, K. (2007) Endoplasmic reticulum stress response in dendrites of cultured primary neurons. *Neuroscience*. **146**, 1–8

59. Kawada, K., Iekumo, T., Saito, R., Kaneko, M., Mimori, S., Nomura, Y., and Okuma, Y. (2014) Aberrant neuronal differentiation and inhibition of dendrite outgrowth resulting from endoplasmic reticulum stress. *J. Neurosci. Res.* **92**, 1122–1133

60. Kienle, N., Kloepper, T. H., and Fasshauer, D. (2009) Phylogeny of the SNARE vesicle fusion machinery yields insights into the conservation of the secretory pathway in fungi. *BMC Evol Biol*. **9**, 19–14

61. Petrovski, S., Wang, Q., Heinzen, E. L., Allen, A. S., and Goldstein, D. B. (2013) Genic intolerance to functional variation and the interpretation of personal genomes. *PLoS Genet*. **9**, e1003709

62. Gladycheva, S. E., Lam, A. D., Liu, J., D'Andrea-Merrins, M., Yizhar, O., Lentz, S. I., Ashery, U., Ernst, S. A., and Stuenkel, E. L. (2007) Receptor-mediated regulation of tomosyn-syntaxin 1A interactions in bovine adrenal chromaffin cells. *J. Biol. Chem.* **282**, 22887–22899

63. Hatsuzawa, K., Lang, T., Fasshauer, D., Bruns, D., and Jahn, R. (2003) The R-SNARE motif of tomosyn forms SNARE core complexes with syntaxin 1 and SNAP-25 and down-regulates exocytosis. *J. Biol. Chem.* **278**, 31159–31166

64. Nagano, K., Takeuchi, H., Gao, J., Mori, Y., Otani, T., Wang, D., and Hirata, M. (2015) Tomosyn is a novel Akt substrate mediating insulin-dependent GLUT4 exocytosis. *Int. J. Biochem. Cell Biol.* **62**, 62–71

65. Gracheva, E. O., Burdina, A. O., Holgado, A. M., Berthelot-Grosjean, M., Ackley, B. D., Hadwiger, G., Nonet, M. L., Weimer, R. M., and Richmond, J. E. (2006) Tomosyn Inhibits Synaptic Vesicle Priming in Caenorhabditis elegans. *PLoS Biol.* **4**, e261–12

66. Yizhar, O., Matti, U., Melamed, R., Hagalili, Y., Bruns, D., Rettig, J., and Ashery, U. (2004) Tomosyn inhibits priming of large dense-core vesicles in a calcium-dependent manner. *Proc. Natl. Acad. Sci. U.S.A.* **101**, 2578–2583

67. Kagami, M., Toh e, A., and Matsui, Y. (1998) Sro7p, a Saccharomyces cerevisiae counterpart of the tumor suppressor l(2)gl protein, is related to myosins in function. *Genetics*. **149**, 1717–1727

68. Gangar, A., Rossi, G., Andreeva, A., Hales, R., and Brennwald, P. (2005) Structurally Conserved Interaction of Lgl Family with SNAREs Is Critical to Their Cellular Function. *Current Biology*. **15**, 1136–1142

69. Rossi, G., and Brennwald, P. (2011) Yeast homologues of lethal giant larvae and type V myosin cooperate in the regulation of Rab-dependent vesicle clustering and polarized exocytosis. *Molecular Biology of the Cell*. **22**, 842–857

70. Cohen, L. D., Zuchman, R., Sorokina, O., Müller, A., Dieterich, D. C., Armstrong, J. D., Ziv, T., and Ziv, N. E. (2013) Metabolic Turnover of Synaptic Proteins: Kinetics, Interdependencies and Implications for Synaptic Maintenance. *PLoS ONE*. **8**, e63191–20

71. Nalavadi, V. C., Muddashetty, R. S., Gross, C., and Bassell, G. J. (2012) Dephosphorylation-induced ubiquitination and degradation of FMRP in dendrites: a role in immediate early mGluR-stimulated translation. *Journal of Neuroscience*. **32**, 2582–2587

72. Pavlopoulos, E., Trifilieff, P., Chevaleyre, V., Fioriti, L., Zairis, S., Pagano, A., Malleret, G., and Kandel, E. R. (2011) Neuralized1 Activates CPEB3: A Function for Nonproteolytic Ubiquitin in Synaptic Plasticity and Memory Storage. *CELL*. **147**, 1369–1383

73. Hamilton, A. M., and Zito, K. (2013) Breaking It Down: The Ubiquitin Proteasome System in Neuronal Morphogenesis. *Neural Plast.* **2013**, 1–10

74. Mabb, A. M., and Ehlers, M. D. (2010) Ubiquitination in Postsynaptic Function and Plasticity. *Annu. Rev. Cell Dev. Biol.* **26**, 179–210

75. Tsai, N.-P. (2014) Ubiquitin proteasome system-mediated degradation of synaptic proteins: An update from the postsynaptic side. *BBA - Molecular Cell Research*. **1843**, 2838–2842

76. Dindot, S. V., Antalffy, B. A., Bhattacharjee, M. B., and Beaudet, A. L. (2007) The Angelman syndrome ubiquitin ligase localizes to the synapse and nucleus, and maternal deficiency results in abnormal dendritic spine morphology. *Hum. Mol. Genet.* **17**, 111–118

77. Kim, H., Kunz, P. A., Mooney, R., Philpot, B. D., and Smith, S. L. (2016) Maternal Loss of Ube3a Impairs Experience-Driven Dendritic Spine Maintenance in the Developing Visual Cortex. *Journal of Neuroscience*. **36**, 4888–4894

78. Guntupalli, S., Jang, S. E., Zhu, T., Huganir, R. L., Widagdo, J., and Anggono, V. (2017) GluA1 subunit ubiquitination mediates amyloid-β-induced loss of surface α-amino-3-hydroxy-5-methyl-4-isoxazolepropionic acid (AMPA) receptors. *Journal of Biological Chemistry*. **292**, 8186–8194

79. Schreiber, J., Végh, M. J., Dawitz, J., Kroon, T., Loos, M., Labonté, D., Li, K. W., Van Nierop, P., Van Diepen, M. T., De Zeeuw, C. I., Kneussel, M., Meredith, R. M., Smit, A. B., and Van Kesteren, R. E. (2015) Ubiquitin ligase TRIM3 controls hippocampal plasticity and learning by regulating synaptic γ-actin levels. *The Journal of Cell Biology*. **211**, 569–586

80. Hung, A. Y., Sung, C. C., Brito, I. L., and Sheng, M. (2010) Degradation of Postsynaptic Scaffold GKAP and Regulation of Dendritic Spine Morphology by the TRIM3 Ubiquitin Ligase in Rat Hippocampal Neurons. *PLoS ONE*. **5**, e9842–11

81. Bianchetta, M. J., Lam, T. T., Jones, S. N., and Morabito, M. A. (2011) Cyclin-dependent kinase 5 regulates PSD-95 ubiquitination in neurons. *Journal of Neuroscience*. **31**, 12029–12035

82. Lussier, M. P., Herring, B. E., Nasu-Nishimura, Y., Neutzner, A., Karbowski, M., Youle, R. J., Nicoll, R. A., and Roche, K. W. (2012) Ubiquitin ligase RNF167 regulates AMPA receptor-mediated synaptic transmission. *Proceedings of the National Academy of Sciences*. **109**, 19426–19431

83. Greer, P. L., Hanayama, R., Bloodgood, B. L., Mardinly, A. R., Lipton, D. M., Flavell, S. W., Kim, T.-K., Griffith, E. C., Waldon, Z., Maehr, R., Ploegh, H. L., Chowdhury, S., Worley, P. F., Steen, J., and Greenberg, M. E. (2010) The Angelman Syndrome protein Ube3A regulates synapse development by ubiquitinating arc. *CELL*. **140**, 704–716

84. Mabb, A. M., Je, H. S., Wall, M. J., Robinson, C. G., Larsen, R. S., Qiang, Y., Corrêa, S. A. L., and Ehlers, M. D. (2014) Triad3A Regulates Synaptic Strength by Ubiquitination of Arc. *Neuron*. **82**, 1299–1316

85. Yao, I., Takagi, H., Ageta, H., Kahyo, T., Sato, S., Hatanaka, K., Fukuda, Y., Chiba, T., Morone, N., Yuasa, S., Inokuchi, K., Ohtsuka, T., MacGregor, G. R., Tanaka, K., and Setou, M. (2007) SCRAPPER-Dependent Ubiquitination of Active Zone Protein RIM1 Regulates Synaptic Vesicle Release. *CELL*. **130**, 943–957

86. Yang, H., Zhong, X., Ballar, P., Luo, S., Shen, Y., Rubinsztein, D. C., Monteiro, M. J., and Fang, S. (2007) Ubiquitin ligase Hrd1 enhances the degradation and suppresses the toxicity of polyglutamine-expanded huntingtin. *Experimental Cell Research*. **313**, 538–550

87. Mao, J., Xia, Q., Liu, C., Ying, Z., Wang, H., and Wang, G. (2017) A critical role of Hrd1 in the regulation of optineurin degradation and aggresome formation. *Hum. Mol. Genet.* **26**, 1877–1889

88. Ying, H., and Yue, B. Y. J. T. (2012) Cellular and molecular biology of optineurin. *Int Rev Cell Mol Biol*. **294**, 223–258

89. Zhang, P., Fu, W.-Y., Fu, A. K. Y., and Ip, N. Y. (2015) S-nitrosylation-dependent proteasomal degradation restrains Cdk5 activity to regulate hippocampal synaptic strength. *Nat Commun*. **6**, 1–11

90. Jakawich, S. K., Nasser, H. B., Strong, M. J., McCartney, A. J., Perez, A. S., Rakesh, N., Carruthers, C. J. L., and Sutton, M. A. (2010) Local Presynaptic Activity GatesHomeostatic Changes in Presynaptic Function Driven by Dendritic BDNF Synthesis. *Neuron*. **68**, 1143–1158

91. Bolte, S., and Cordelières, F. P. (2006) A guided tour into subcellular colocalization analysis in light microscopy. *Journal of Microscopy*. **224**, 213–232

92. Glynn, M. W., and McAllister, A. K. (2006) Immunocytochemistry and quantification of protein colocalization in cultured neurons. *Nat Protoc*. **1**, 1287–1296

93. Schindelin, J., Arganda-Carreras, I., Frise, E., Kaynig, V., Longair, M., Pietzsch, T., Preibisch, S., Rueden, C., Saalfeld, S., Schmid, B., Tinevez, J.-Y., White, D. J., Hartenstein, V., Eliceiri, K., Tomancak, P., and Cardona, A. (2012) Fiji: an open-source platform for biological-image analysis. *Nat Meth*. **9**, 676–682

94. Zhu, J., Lee, K. Y., Jewett, K. A., Man, H.-Y., Chung, H. J., and Tsai, N.-P. (2017) Epilepsy-associated gene Nedd4-2 mediates neuronal activity and seizure susceptibility through AMPA receptors. *PLoS Genet*. **13**, e1006634–24

CHAPTER III

Tomosyn-1 is ubiquitinated by HRD1 at multiple lysine residues

3.1 Abstract

Tomosyn-1 (Tomo-1), a soluble, R-SNARE domain-containing protein, elicits significant inhibitory effects in secretory cells, including on neurotransmitter-containing synaptic vesicle release in central neurons. It has recently been identified that Tomo-1 is subject to ubiquitination by the E3 ligase HRD1 in neurons, leading to its proteasomal degradation, and ultimately decreasing Tomo-1 levels to influence the density of postsynaptic dendritic spines in hippocampal neurons. However, the specific sites of Tomo-1 ubiquitination have yet to be identified. Here, via tandem mass spectroscopy, we found that mammalian m-Tomo-1 protein is specifically ubiquitinated at twelve independent lysine residues by HRD1 *in vitro*. A number of these newly identified Tomo-1 ubiquitination sites are at or near other known sites of post-translational modification, including phosphorylation and SUMOylation. Furthermore, our Tomo-1 isoform and homologue domain evaluation and antibody-based regional targeting of Tomo-1 from neuronal lysate has indicated four lysine residues which are highly likely to be ubiquitinated *in vivo*. Though generation and evaluation of a non-ubiquitinateable Tomo-1 mutant construct was inconclusive, our results have confirmed that Tomo-1 is indeed ubiquitinated by HRD1 and further informs the growing body of research indicating

Tomo-1 is a likely target for UPS-mediated degradation toward synaptic plasticity induction.

3.2 Introduction

The ubiquitination and degradation of synaptically active proteins has emerged as a vital cell biological mechanism by which neurons refine synaptic connections during development and modulate synaptic activity and plasticity in adult organisms (1). Protein degradation by the ubiquitin-proteasome system is completely dependent upon the post-translational attachment of ubiquitin molecules to target substrates. This action occurs via the concerted efforts of over 1,000 proteins in humans (2), ubiquitinating thousands of proteins at tens-of-thousands of individual sites (3, 4). Furthermore, refined biochemical methods, such as linkage-specific ubiquitin antibodies, in combination with technological advances in large-scale proteomic data acquisition and analysis capabilities have rapidly increased our recognition of the complexity and physiological importance of the UPS. Mass spectrometry (MS)-based methods, most commonly consisting of the tryptic digestion of ubiquitin within protein samples and the analysis of resulting di-glycine-containing peptides, have had a substantial impact on the study of ubiquitination (5). This approach facilitates the comprehensive annotation and quantification of specific protein ubiquitination sites from a wide variety of upstream sample generation techniques. Once a substrate protein has been identified, MS is one tool allowing for the targeted analysis of its ubiquitination and proteostasis characteristics.

In Chapter 2 of this dissertation the research identified that Tomo-1 proteostasis in neurons is at least partially controlled by the E3 ligase HRD1, including initial indications of a downstream functional effect on synaptic morphology (6). These results also confirmed, with *in vitro* assays utilizing purified components and *in vivo* assays from neuronal culture, that Tomo-1 is ubiquitinated and degraded. As such, the identification of Tomo-1 ubiquitination site(s) is of high priority.

The objectives of this series of experiments were three-fold; confirm Tomo-1 protein is ubiquitinated, identify which lysines of Tomo-1 are targeted and ubiquitinated by HRD1, and with this information generate a non-ubiquitinateable Tomo-1 mutant construct. Success in identifying the specific Tomo-1 residues subject to ubiquitination would promote future investigations to rigorously define downstream physiological effects on synaptic plasticity, including contributions of the observed dendritic spine density effects of Tomo-1 protein level. Furthermore, application of this mutant protein could allow for a non-ubiquitinateable Tomo-1 rescue expression paired with endogenous WT Tomo-1 KD. Here we review our investigations targeting identification of HRD1 ubiquitination sites of mammalian m-Tomosyn-1 protein.

3.3 Results

The initial discovery of Tomosyn resulted from a Syntaxin1a pull-down assay from the cytosol of rat cerebrum (7). It was later determined that Tomosyn is expressed by two genes, leading to Tomo-1 and Tomo-2 gene products (8). Tomo-1 and Tomo-2 are subsequently subject to alternative splicing, resulting in a total of seven protein

isoforms (see Fig. 3.1A). The three Tomo-1 isoforms (s-, m-, and b-Tomo-1, for small, medium, and big) maintain a high level of conserved structure, with sequence differences found exclusively within its hypervariable domain (9). Evidence suggests the s- and m-Tomo-1 variants are brain-specific and highly enriched in synaptic regions of neurons. Furthermore, there are several reported post-translational modifications of m-Tomo-1 within its hypervariable domain (see Fig. 3.1B), including protein kinase A (PKA) phosphorylation (10, 11) and SUMOylation (12) by PIAS (13). Notably, these post-translational modifications influence Tomo-1's interaction with partner proteins as well as its functional effects on the fusion of synaptic vesicles and neurotransmitter release. For example, PKA phosphorylation at serine-724 reduces Tomo-1's interaction with Syntaxin1, while PIAS-mediated SUMOylation at K730 did not appear to affect its Syntaxin1 interaction. However, Tomo-1 SUMOylation does apparently reduce its inhibitory actions (12). The conclusions from Chapter 2, that Tomo-1 is subject to ubiquitination by HRD1 for UPS-mediated degradation, led us to question if this could be another post-translational mechanism whereby Tomo-1 action is regulated in neurons.

Confirmation of Tomo-1 ubiquitination by HRD1 and identification of specific lysine residues

Testing the hypothesis that ubiquitination influences Tomo-1 function first required a more highly resolved examination of Tomo-1 ubiquitination than was reported via Western blots in Chapter 2. We implemented a tandem mass spectrometry strategy

for the confirmation and identification of specific ubiquitination sites of Tomo-1. During ubiquitination, a ubiquitin molecule is covalently conjugated to a specific amino acid of the target protein substrate, most commonly a lysine residue. Following m-Tomo-1 protein production and purification from HEK293T cells and *in vitro* ubiquitination by HRD1 we evaluated trypsin-digested Tomo-1 protein samples for positive identification of ubiquitinated lysine residues by mass-to-charge (M/z) shifts in recurring peptide fragments containing di-glycine motifs (see Fig. 3.1C for example M/z chromatogram). Positive hits were manually verified and compared with the Uniprot rat protein database and results yielded 12 unique ubiquitination sites of m-Tomo-1.

Modeling and probability-ranking Tomo-1 ubiquitination sites

The twelve identified ubiquitination sites are sequentially displayed in the schematic diagram of a linear Tomo-1 protein in Fig. 3.2A, four of which reside within the hypervariable domain. Notably, two of these ubiquitination sites are identical to or directly adjacent to sites of other known PTMS (SUMOylation at K730 and phosphorylation at S724, respectively). This may be of future consequence, as the interplay between PTMs is becoming widely recognized as a diverse mechanism for the biomolecular control of synaptic protein function. For example, the targeting of a site for ubiquitination and therefore likely inactivation or degradation, following a nearby phosphorylation event (14, 15). Relatedly, one study of exogenously expressed Tomo-2 protein showed that serine-to-alanine replacement of all 11 phosphorylatable residues inhibited its ubiquitination by HRD1, ultimately reducing its proteasomal degradation in

HEK293 cells (16). Given numerous potential SUMOylated and ubiquitinated lysine residues are proximal to phosphorylatable serine residues within and around the hypervariable domain of Tomo-1 and Tomo-2, both are likely candidates for regulation by phosphorylation events (13, 16).

Following the confirmation of Tomo-1 ubiquitination at specific, but numerous, lysine residues we next mapped their locations within the structure of Tomo-1 using 3D protein modelling software informed by the empirically determined structure of a Tomo-1 protein orthologue in another species. We then used this predicted structure to evaluate accessibility and solubility ratings of each site, in addition to the confidence intervals generated and frequency of occurrence of each site from the MS/MS results. These analyses led to four identified lysines judged to have the highest probability of being ubiquitinated within our samples. These four sites are labeled and displayed in-line with the 3D Tomo-1 ribbon structure model shown in Fig. 3.2B, two of which reside within its hypervariable domain.

Generation of 12xKR non-ubiquitinateable mutant Tomo-1

Following determination of a dozen Tomo-1 ubiquitination sites mediated by HRD1 we intended to validate their physiological significance by creating a ubiquitination-null mutant protein. This approach would allow using a KD and rescue or KI Tomo-1 null mutant approach for the targeted disruption of endogenous Tomo-1 turnover in neurons and subsequent examination of how Tomo-1 degradation influences its function and potential influence on neuronal physiology. To generate the construct

encoding a non-ubiquitinateable mutant Tomo-1 each identified lysine was replaced with an arginine. A lysine-to-arginine (K-R) site mutation is commonly employed to inhibit the covalent attachment of ubiquitin while maintaining the potentially important negatively charged amino acid residue at the site. We designed custom oligonucleotide primers to specifically target each site and introduce a point mutation (A-G) in the plasmid sequence and subsequently convert each lysine to an arginine during translation. To do so we utilized a commercially available cloning system to perform site-directed mutagenesis on the WT m-Tomo-1 contained within the tandem affinity-tagged construct used in Chapter 2, which was also the same construct used for *in vitro* assays and mass spectrometry. Performing iterative mutagenesis reactions allowed for the creation of plasmids encoding Tomo-1 with each lysine mutated to an arginine individually in conjunction with a single construct containing all 12 K-R mutations (12xKR Tomo-1).

Promiscuity in ubiquitination of the 12xKR Tomo-1

All constructs were fully sequenced and aligned to WT to ensure the intended nucleotide identities (fully WT, except for the single point mutations) and then expressed as previously described for WT Tomo-1 production. The 12xKR Tomo-1 protein was of high purity and maintained its apparent mass of ≈ 135kD, as indicated via SDS-PAGE followed by coomassie staining and displayed in Fig. 3.2C. However, the 12xKR Tomo-1 mutant only showed an approximate 50% decrease in ubiquitination (Fig 3.2D), following an *in vitro* ubiquitination assay described fully in Chapter 2. It is at present

unclear if HRD1 acts *in vitro* to promiscuously ubiquitinate Tomo-1 *in vitro*, perhaps due to the concentration of either protein, lack of regulatory HRD1 co-factors, or other assay parameters (e.g. temperature, time) and limitations. Alternatively, because target lysines were no longer present in the 12xKR assays, we cannot rule out opportunistic ubiquitination events catalyzed by HRD1, for example, the addition of ubiquitin molecules to the nearby non-mutated lysine residues still present in the 12xKR amino acid sequence.

Though attempted, anti-Tomo-1 IP from neuronal samples yielded too little Tomo-1 for identification of *in vivo* Ub sites via MS/MS and samples also contained non-specific co-IP levels of unrelated proteins. Notably, we have now generated lentiviral constructs expressing the WT and the 12xKR Tomo-1 proteins in a YFP-containing vector for follow-up testing and use in neurons, including repeating ubiquitination assays and resubmission for MS/MS analysis. Future work will now be better-equipped to minimize variation in sample yield and to generate samples *in vivo* in neuronal culture, where the full complement of HRD1 interacting partners and cell biological processes will presumably be unhindered. This would also allow for finer scale manipulations including increasing or decreasing neuronal activity via electrophysiological and pharmacological approaches. Once the 12xKR Tomo-1 has been fully evaluated it will be crucial to confirm the specificity of any findings using the constructs already generated and expressing Tomo-1 with the single K-R mutations for attribution of effects to specific lysine(s).

Antibody/antigenic sequence-based analysis of Tomo-1 ubiquitination sites

Though limited by protein yields and prevalence of ubiquitination in the series of experiments utilizing the 12xKR mutant, we attempted complementary methods of determining the specificity and implications of Tomo-1 ubiquitination *in vivo*. In conjunction with the homology modeling of 3D Tomo-1 protein structure and mapping of identified ubiquitination sites we made use of multiple specific antibody-based immunoprecipitation approaches to inform our interpretations of these results. Figure 3.3 displays an example Western blot of lysate and IP samples probed for Tomo-1 and HRD1 (Fig. 3.3A) and conjugated ubiquitin (Fig. 3.3B). For this set of experiments, we made use of the varying antigenic sequences of various commercially available anti-Tomosyn antibodies (for antigenic target sequences see Fig. 3.2A, bottom). Tomo-1 and Tomo-2 were each IPd from the same hippocampal neuronal culture lysate samples and subjected to SDS-PAGE. Upon protein denaturing in-gel followed by transfer to nitrocellulose the membranes were probed with a pan-Tomo (anti-Tomo1/2) antibody for detection. Two experimental conditions were tested in culture; a 4-hour treatment with the proteasome blocker MG132 and the cell-permeable, broad-spectrum DUB inhibitor PR-619 to non-specifically but heavily drive the buildup of ubiquitinated Tomo-1, and a DMSO vehicle control treatment for baseline comparison.

Strikingly, following the pharmacologically-driven and acute increase in the level of ubiquitinated Tomosyn in hippocampal neurons, the IP of each variant was drastically reduced. This effect was apparent as a lack of Tomosyn bands in the treated condition and the concurrent loss of conjugated ubiquitin banding at the apparent mass of

Tomosyn. It appears that the treated condition was indeed enriched in ubiquitinated proteins (see input sample lanes) but this Tomo-1 had a lack of affinity during subsequent antibody IP. The unbound fractions, though substantially diluted for the in-solution binding period following sample mass and volume equalization between conditions, each show what appear to be elevated Tomosyn levels vs. vehicle control unbound samples (Fig. 3.3A).

3.4 Discussion

Chapter 3 of this dissertation has identified multiple Tomo-1 sites specifically ubiquitinated by HRD1 *in vitro*, further justifying the necessity of evaluating post-translational modification of Tomo-1 in examination of its mechanistic implementation of inhibitory and morphological actions within the nervous system. Furthermore, this work has provided an additional tool for use in this evaluation, namely twelve individual (see Fig. 3.2A) and one total (12xKR) ubiquitination site mutant Tomo-1 constructs. Application of this mutant protein could allow for a non-ubiquitinateable 12xKR Tomo-1 rescue expression paired with endogenous WT Tomo-1 KD to aide in determination of the exact influence of Tomo-1 ubiquitination at these specific sites. In addition, while undertaking the research overviewed in Chapter 3 we have also inserted the full 12xKR Tomo-1 construct into the lentiviral YFP vector utilized in the Chapter 2 studies and began initial testing of its increased neuronal expression and greater yield during purification. Relatedly, its WT counterpart was also created and will facilitate repeating MS/MS evaluation of neuronal samples acquired *in vivo*.

The maintained 50% ubiquitination of 12xKR mutant Tomo-1 following *in vitro* assay may also be difficult to avoid *in vivo* without the inclusion of complementary techniques for compartment-specific study, such as fluorescence imaging or synaptic sample enrichment strategies, which would allow for further specification of where Tomo-1 is being regulated. A dual approach such as this would also lower the likelihood of any localized (e.g. pre- or post-synaptic, membrane-bound, phosphorylated) Tomo-1 effects from being occluded by the total cellular Tomo-1 content. It is currently presumed that the fraction of ubiquitinated Tomo-1 at any given time *in vivo* is far lower than the total, both due to potential rapid degradation of poly-ubiquitinated synaptic proteins (17, 18) and the proportion of synaptic vs. the total cellular Tomo-1 (see Chapter 2). Success in identifying the specific Tomo-1 residues subject to ubiquitination *in vivo* would promote future investigations to rigorously define downstream physiological effects on synaptic plasticity, including contributions of the observed dendritic spine density effects of Tomo-1 protein level outlined in Chapter 2.

The decrease in Tomo-1 IP following upregulated ubiquitination *in vivo* likely resulted from its antigenic sequence, which spans the entirety of the Tomo-1 hypervariable domain. This is informative because it appears that the treated condition, enriched in ubiquitinated proteins as evidenced by comparing input samples between the respective conditions, has a greatly-reduced affinity for the specific antibody used for IP. The implication underlying the loss of Tomosyn IP following ubiquitination is further evidence supporting the hypothesis that Tomo-1 is ubiquitinated within its hypervariable domain, where other PTMs are known to occur. Given a single ubiquitin is

≈ 7.8kD in size and poly-ubiquitination, typically of 4+ linked moieties, it is not unreasonable to hypothesize that a ≥ 31.2kD protein complex covalently attached to the target sequence of the Tomo-1 antibody disrupts their affinity for each other. Conversely, the WT and 12xKR Tomo-1 constructs tested *in vitro* and for MS/MS were purified from HEK293T lysate samples via their capacity for a streptavidin-biotin pull-down mechanism (see methods). The affinity tags of these constructs were fused to the C-terminus of the Tomo-1 protein in both cases, avoiding any potential disruption due to ubiquitination of their hypervariable regions. These data further support the utilization of the newly generated, affinity-tagged Tomo-1 WT and 12xKR lentiviral constructs *in vivo* in neurons for future experiments.

3.5 Materials and Methods

Animals

All animal handling procedures are approved by and in full compliance with the regulations of the University Committee on Use and Care of Animals of the University of Michigan, in addition to the National Institutes of Health guidelines.

Antibodies

Affinity-purified Rb anti-Tomosyn-1 polyclonal antibody (catalog no. 183103), affinity-purified Rb anti-Tomosyn-2 polyclonal antibody (catalog no. 183203), and affinity-purified Rb anti-Tomo-1/2 (pan-Tomo) antibody (catalog no. 183003) were from Synaptic Systems (Göttingen, Germany). The Ms anti-β-actin monoclonal antibody

(clone AC74, catalog no. A2228) was from Sigma-Aldrich (St. Louis, MO). The Rb anti-HRD1 polyclonal antibody (catalog no. 13473-1-AP) was from ProteinTech (Chicago, IL). The Ms anti-conjugated-ubiquitin monoclonal antibody (clone FK2, catalog no. BML-PW8810) was from Enzo Life Sciences (Farmingdale, NY). For western blots, IRDye 800CW-conjugated goat anti-mouse IgG H+L (catalog no. 926-68021) and IRDye 680LT-conjugated goat anti-rabbit IgG H+L (catalog no. 926-32210) fluorescent secondary antibodies were from Li-Cor Biosciences (Lincoln, NE).

Cell Culture and Transfections

Results from Chapter 3 were obtained from dissociated rat hippocampal neuronal cultures (prepared, treated, and lysed as described in Chapter 2) following *in vitro* culture for up to 5 weeks prior to experimentation, or HEK293T cells (prepared, transfected, and lysed as described in Chapter 2).

12xKR Tomo-1 mutant construct generation

All forward and reverse (anti-sense) primers for PCR-induced lysine-to-arginine mutations for the 12 indicated lysines of the rat m-tomosyn-1 coding sequence (NCB accession # NP_110470.1) were specifically designed using the free online tool offered by Agilent, which can be found at: https://www.genomics.agilent.com/primerDesignProgram.jsp. Primer sequences were then ordered from and generated by Integrated DNA Technologies (IDT) as custom oligonucleotide sequences. Primers were reconstituted according to manufacturer

specifications in molecular biology-grade water. Primers were then used in the QuikChange II XL (Agilent) protocol for the PCR reactions according to manufacturer specifications. Using the double-stranded DNA template of the Gateway rat m-Tomo-1 plasmid outlined in Chapter 2 methods. PCR products were Dpn1 digested to remove parental DNA and transformed into XL10-Gold E. coli according to protocol. Transformants were streaked onto antibiotic-selective LB-agar plates and grown according to protocol prior to DNA preps. Endo-free Maxi preps (Qiagen) were then completed to yield high-purity plasmid DNA samples, which were fully sequences at the University of Michigan DNA Sequencing Core and stored at -20C until use.

Drugs

The following chemicals were used in Chapter 3, as noted: DMSO (Life Technologies, catalog no. D12345), MG132 (Cayman Chemicals, catalog no. 10012628), PR-619 (Tocris, catalog no. 4482). Protease inhibitor cocktail minus EDTA (Roche, catalog no. 11580800) was added to the lysis and IP buffers at twice the manufacturer's recommended concentration.

Immunoprecipitation of Endogenous Tomosyn-1 and HRD1 from Hippocampal Neuronal Culture

Immunoprecipitation of endogenous protein from cultured hippocampal neurons was performed using either the Tomo-1-specific or Tomo-2-specific antibodies noted above by pre-binding 2µg antibody to 50µL protein A magnetic dynabead slurry (Pierce,

catalog no. 88845) per 35mm dish in 100mM Na-phosphate buffer (pH 8.0) containing (mM): 75 Na_2HPO_4 and 25 NaH_2PO_4. Cultures were lysed and collected in non-denaturing lysis buffer (pH 7.5) containing (mM): 50 NaCl, 25 Tris, 2 $MgCl_2$, 1 $CaCl_2$, 0.5% NP-40, and 2x recommended concentration of complete EDTA-free protease inhibitor cocktail. Samples were then equalized for total protein concentration (1-3µg/µL) and sample volume (100-300µL) prior to incubation with the conjugated beads for one hour at 4°C. The samples were then rinsed in lysis buffer and boiled in 1x SDS sample buffer for five minutes before being loaded for PAGE and western blotting.

In Vitro Ubiquitination Assay

The Gateway rat m-Tomosyn-1 construct noted above was used to express WT or 12xKR mutant Tomo-1 in HEK293T to encourage proper post-translational modification and 3-dimensional protein structure prior to experimental procedures. Cells were seeded at 50% confluence from liquid nitrogen stocks in 10cm cell culture dishes for ≈ 16 hours and serum-starved in 10mL Opti-MEM (Gibco catalog no. 31985) for one hour prior to transfection. Transfection occurred using 25µg plasmid DNA and 25µL Lipofectamine 2000 (Invitrogen, catalog no. 1166809) in 10mL Opti-MEM, per dish, for five hours under standard incubator conditions before standard HEK cell medium replacement. 48-72 hours following transfection the cells were lysed under non-denaturing conditions in lysis buffer containing (mM): 100 Tris, 100 KCl, 0.2 EDTA, 1.5 $MgCl_2$, 0.01 pepstatin-A (Sigma, catalog no. P5318) and protease inhibitor cocktail minus EDTA (Roche) at 2x recommended concentration. Lysates were then subjected

to 3 freeze-thaw cycles using liquid nitrogen and centrifuged at 3,000xG for 10 minutes for de-nucleation. NP-40 was added to the lysate supernatants to a final concentration of 1% v/v. Lysates were then incubated with streptavidin-agarose beads (Invitrogen, catalog no. S951) for three hours at 4°C to purify the biotinylated epitope-tagged m-Tomo-1 fusion construct. Final purity and protein concentration were quantified using a serial dilution vs. BSA standard on a SimplyBlue-stained SDS-PAGE gel.

For use in ubiquitin reactions, 2µg purified Tomo-1 bound to the streptavidin-agarose beads was suspended in assay buffer containing the following (mM): 100 Tris, 10 $MgCl_2$, and 0.2 DTT (Invitrogen, catalog no. 15508-013) and subjected to the following reaction conditions at 37°C for 45 minutes with mixing (E3Lite Ubiquitin Ligase Kit, catalog no. UC101, LifeSensors, Malvern, PA): 20µg/mL wild-type human ubiquitin (catalog no. SI201), 10nM UBE1 (catalog no. UB101), 100nM UBE2D2 (catalog no. UB207H), 250nM HRD1 (catalog no. UB307), 200µM ATP (catalog no. A50-09-200, SignalChem, Richmond, BC, Canada).

Mass Spectrometry

Mass spectrometry (MS) analysis of HEK293T lysate samples containing affinity-purified Tomo-1 protein was conducted by the University of Michigan Proteomics Resource Facility (PRF, Ann Arbor, MI). Samples were submitted after *in vitro* ubiquitination reaction samples were separated on poly-acrylamide gels and proteins were visualized in-gel with SimplyBlue SafeStain (Invitrogen, Cat. No. LC6060), according to the manufacturer's protocol. The PRF conducted in-gel digestion followed

by identification of ubiquitination sites via di-glycine indicators and site mapped. Trypsin digestion of excised SimplyBlue-stained protein bands beginning at the ≈ 135kDa Tomo-1 protein size and greater allowed peptides to be resolved on a nano-capillary reverse phase column and subjected to a high-resolution, linear ion-trap mass spectrometer (LTQ Orbitrap XL; Thermo Fisher Scientific). The full mass spectrometry scan was collected in Orbitrap (resolution 30,000 at 400 m/z), and data-dependent MS/MS spectra on the 12 most intense ions from each full MS scan were acquired. Proteins and peptides were identified by searching acquired data against the UniProt rat protein database, appended with decoy (reverse) sequences, using the X!Tandem/Trans-Proteomic Pipeline (TPP) software suite. All proteins identified with a ProteinProphet probability of >0.9 (FDR < 1%) were accepted. Spectral matches to ubiquitinated peptides were manually verified by the PRF.

Protein Domain Comparison and 3-Dimensional Protein Modeling

Tomo-1 and Tomo-2 splice isoforms were aligned from the following NCB accession numbers (in order s-, m-, b-Tomo-1, s-, m-, b-, xb-Tomo-2; NP_848036.1, NP_110470.1, NP_848035.1, NP_001108083.1, NP_001108085.1, NP_001108084.1, NP_766028.2). Tomo-1 3D structural modeling was generated from the FASTA CDS of rat m-Tomo-1 (NCB accession NP_110470.1) with I-TASSER (Iterative Threading ASSEmbly Refinement) via protocol (19).

Western blotting

SDS-PAGE gels were wet-transferred onto nitrocellulose membranes at 10V for 1.2 hours and blocked in non-mammalian Odyssey blocking buffer (Li-Cor Biosciences, Lincoln, NE, catalog no. 927-40000). Blocking, primary antibody, and secondary antibody incubations were all performed for 1 hour at room temperature and were rinsed 3x for 5 minutes each in PBS + 0.1% Tween-20 (PBS-T) between incubations. All primary antibodies were used at a 1:1,000 dilution in PBS-T for western blotting, except for the following: anti-β-actin (AC74) 1:8,000 and anti-ubiquitin (FK2) 1:250. All secondary antibodies were used at a 1:15,000 dilution in PBS-T. Western blot images were collected with an Odyssey CLx Infrared Imaging System (Li-Cor model no. 9120) at 84μm resolution in high quality mode and within the linear range of exposure. Fluorescence density was quantified with the open-source ImageJ software including the FIJI imaging suite (20) and the gel analyzer plugin.

3.6 Acknowledgements

This work was supported by NIH grants; F31 NS087883 (JJS), RO1 NS053978, and RO1 NS097498 (ELS). We thank Dr. Venkatesha Basrur and the University of Michigan Department of Pathology Proteomics Resource Facility, the Protein Folding Diseases Initiative, and the Vector and DNA Sequencing core facilities. We also thank the lab of Dr. Yang Zhang for assistance in utilization of the I-TASSER resource for protein structure and function prediction, and Dr. Samuel Slocum for helpful research discussion.

Figure 3.1: Tomosyn domains, splice isoforms, and post-translational modifications.

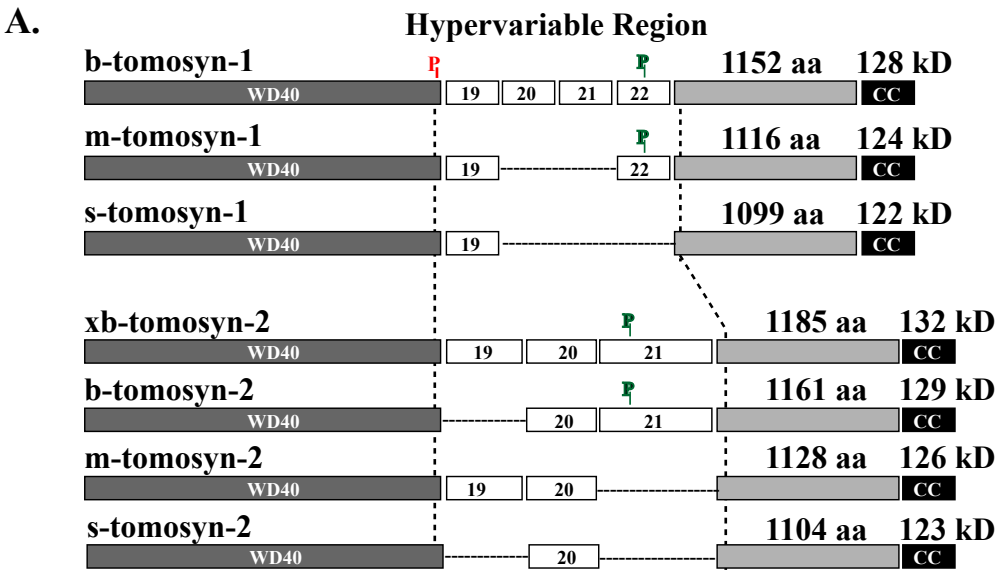

B. **Published Post-translational Modifications of m-Tomosyn-1**

PO_4:	S724	(by PKA)
SUMO2/3:	K730	(by PIAS)
Ubiquitin:	12 identified Ks	(by HRD1, others?)

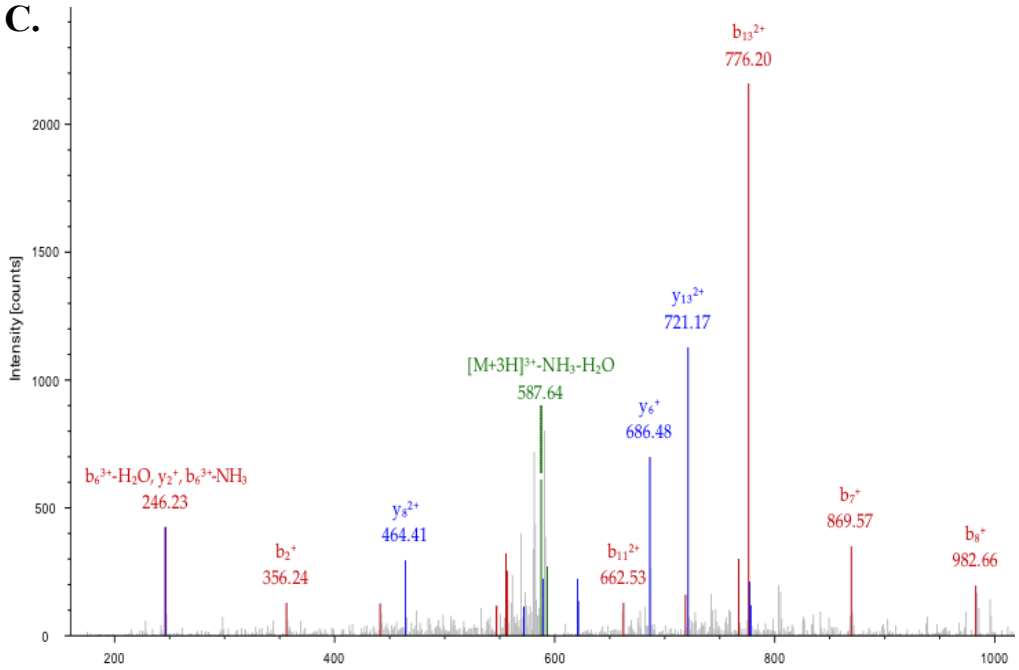

Figure 3.1: Tomosyn domains, splice isoforms, and post-translational modifications.

A, Aligned Tomo-1 and Tomo-2 protein splice isoforms indicating relative sizes, conserved domains, and known phosphorylation sites. *B*, Table outlining known PTMs of Tomo-1 and each corresponding upstream kinase, SUMO ligase, and ubiquitin ligase. *C*, Example chromatogram generated from tandem mass spectrometry analysis of affinity-purified Tomo-1 protein sample. Graph peaks indicate the charge shift of post-translationally modified protein fragments following enzymatic digestion.

Figure 3.2: Determination of Tomo-1 ubiquitination sites and lysine-arginine mutations.

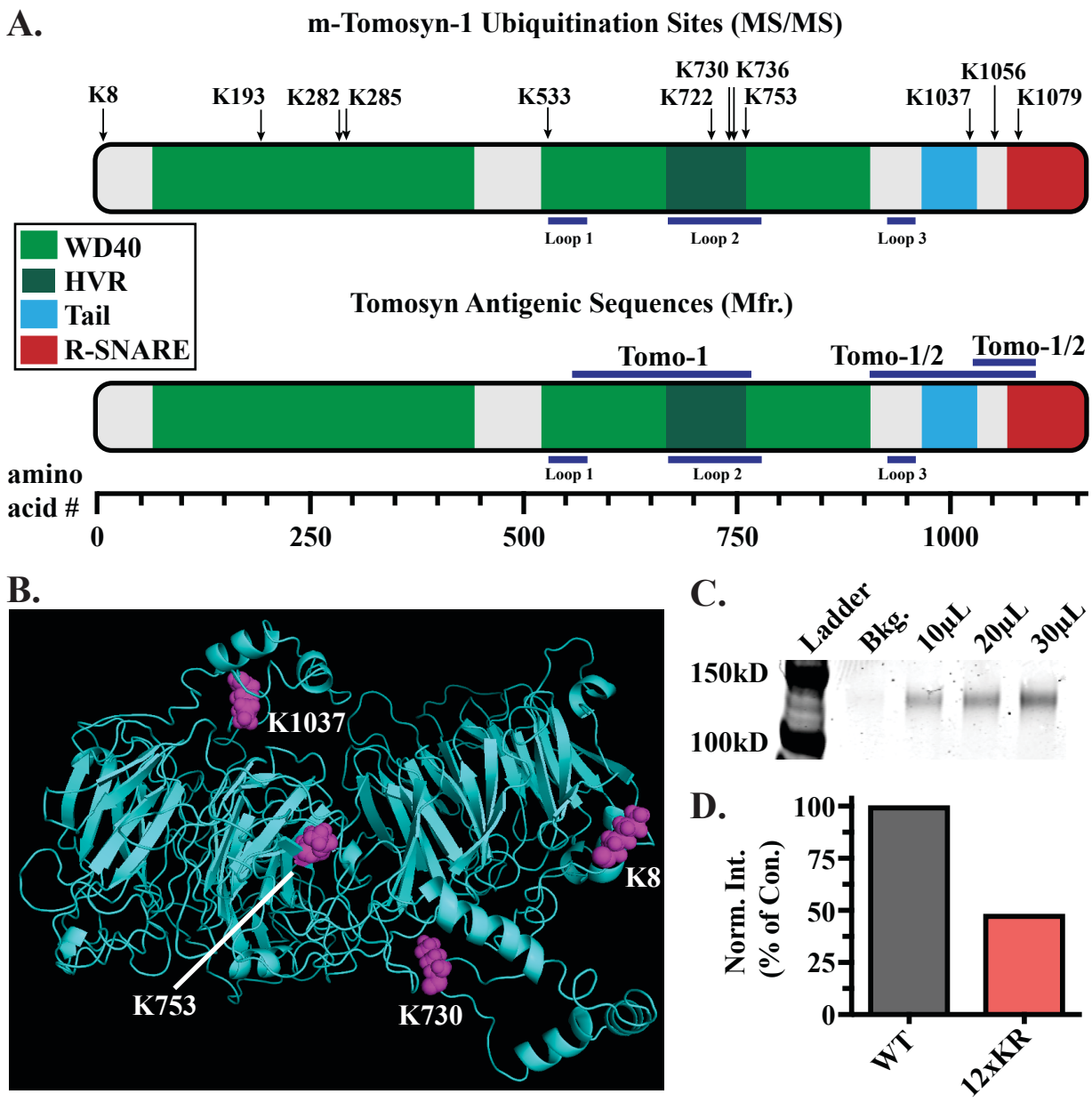

Figure 3.2: Determination of Tomo-1 ubiquitination sites and lysine-arginine mutations.

A, Linear map diagrams of Tomo-1, outlining its various protein domains, the 12 ubiquitination sites empirically determined by tandem mass spectrometry analysis, and the manufacturer-provided antigenic sequences of the anti-Tomosyn antibodies used in this study. *B*, I-TASSER (Iterative Threading ASSEmbly Refinement) program 3-dimensional ribbon structure model of rat m-Tomo-1 protein (cyan), including the four lysine residues rated as having the highest probability of being ubiquitinated (pink). The four highest probability ubiquitination sites were determined using confidence intervals calculated from the mass spectrometry data, frequency of occurrence, and accessibility ratings from the modeled 3-dimensional structure of m-Tomo-1. *C*, 12xKR Tomo-1 protein subjected to SDS-PAGE followed by coomassie staining indicating maintained WT apparent molecular mass and high purity yield. *D*, Histogram quantifying an *in vitro* ubiquitination assay on the 12xKR Tomo-1 mutant shows an approximate 50% decrease in ubiquitination when normalized to paired WT Tomo-1 control reaction.

Figure 3.3: Ubiquitination of Tomo-1 inhibits its antibody affinity.

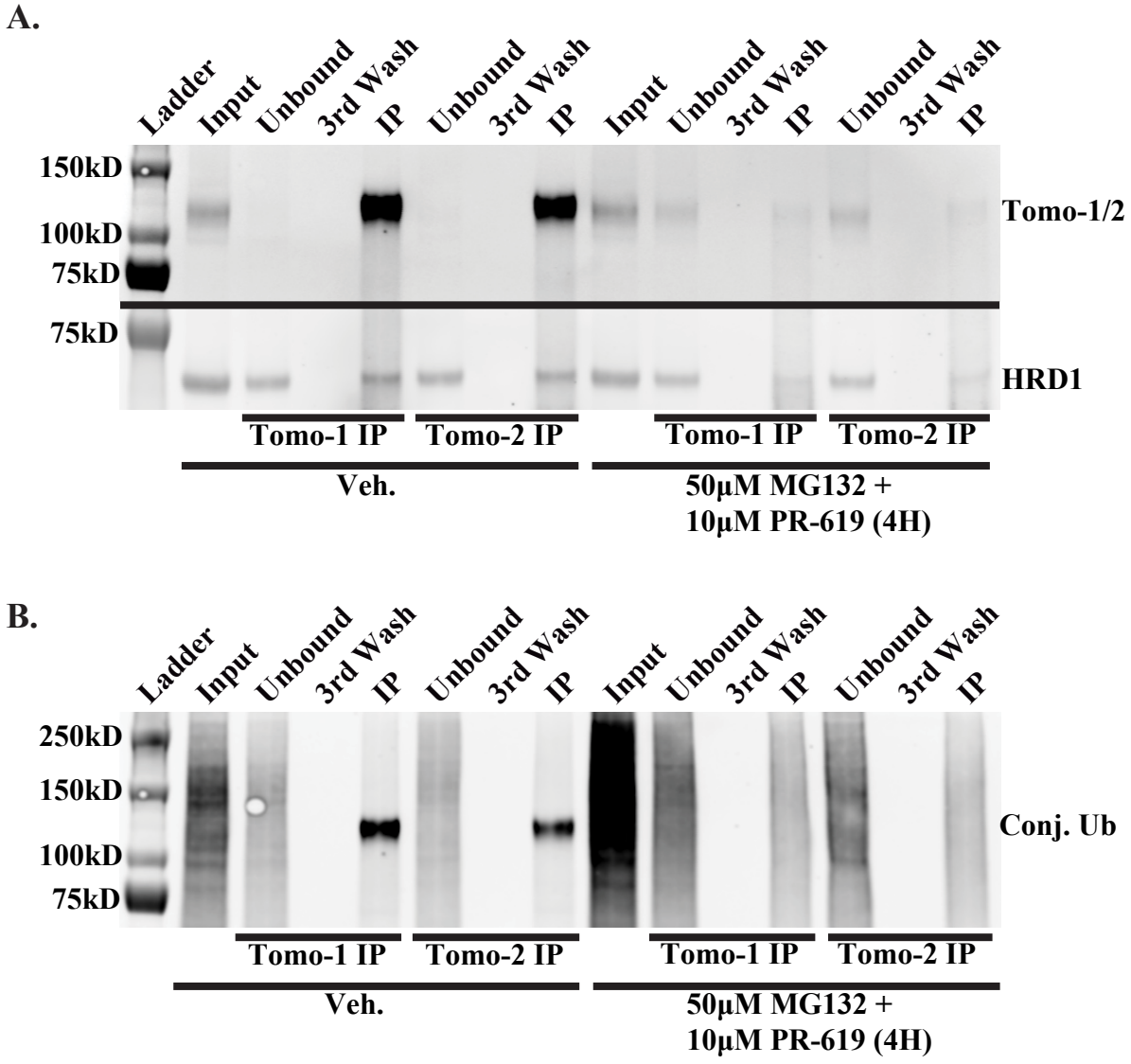

Figure 3.3: Ubiquitination of Tomo-1 inhibits its antibody affinity.

A-B, Example Western blot of lysate, unbound, 3rd wash, and Tomo-1 and Tomo-2 IP samples from hippocampal neuronal lysates following 4-hour DMSO vehicle or 50μM MG132 + 10μM PR-619 treatment. Blots were probed with pan-Tomo (Tomo-1/2) and HRD1 antibodies (part A) and a conjugated ubiquitin antibody (part B).

3.7 Bibliography

1. Hegde, A. N. (2017) Proteolysis, synaptic plasticity and memory. *Neurobiol Learn Mem*. **138**, 98–110

2. Clague, M. J., Heride, C., and Urbé, S. (2015) The demographics of the ubiquitin system. *Trends in Cell Biology*. **25**, 417–426

3. Peng, J., Schwartz, D., Elias, J. E., Thoreen, C. C., Cheng, D., Marsischky, G., Roelofs, J., Finley, D., and Gygi, S. P. (2003) A proteomics approach to understanding protein ubiquitination. *Nat Biotechnol*. **21**, 921–926

4. Kim, W., Bennett, E. J., Huttlin, E. L., Guo, A., Li, J., Possemato, A., Sowa, M. E., Rad, R., Rush, J., Comb, M. J., Harper, J. W., and Gygi, S. P. (2011) Systematic and Quantitative Assessment of the Ubiquitin-Modified Proteome. *Molecular Cell*. **44**, 325–340

5. Ordureau, A., Münch, C., and Harper, J. W. (2015) Quantifying Ubiquitin Signaling. *Molecular Cell*. **58**, 660–676

6. Saldate, J. J., Shiau, J., Cazares, V. A., and Stuenkel, E. L. (2017) The ubiquitin-proteasome system functionally links neuronal Tomosyn-1 to dendritic morphology. *Journal of Biological Chemistry*. 10.1074/jbc.M117.815514

7. Fujita, Y., Shirataki, H., Sakisaka, T., Asakura, T., Ohya, T., Kotani, H., Yokoyama, S., Nishioka, H., Matsuura, Y., Mizoguchi, A., Scheller, R. H., and Takai, Y. (1998) Tomosyn: a syntaxin-1-binding protein that forms a novel complex in the neurotransmitter release process. *Neuron*. **20**, 905–915

8. Groffen, A. J. A., Jacobsen, L., Schut, D., and Verhage, M. (2005) Two distinct genes drive expression of seven tomosyn isoforms in the mammalian brain, sharing a conserved structure with a unique variable domain. *J Neurochem*. **92**, 554–568

9. Yokoyama, S., Shirataki, H., Sakisaka, T., and Takai, Y. (1999) Three splicing variants of tomosyn and identification of their syntaxin-binding region. *Biochemical and Biophysical Research Communications*. **256**, 218–222

10. Baba, T., Sakisaka, T., Mochida, S., and Takai, Y. (2005) PKA-catalyzed phosphorylation of tomosyn and its implication in Ca2+-dependent exocytosis of neurotransmitter. *The Journal of Cell Biology*. **170**, 1113–1125

11. Cazares, V. A., Njus, M. M., Manly, A., Saldate, J. J., Subramani, A., Ben-Simon, Y., Sutton, M. A., Ashery, U., and Stuenkel, E. L. (2016) Dynamic Partitioning of

Synaptic Vesicle Pools by the SNARE-Binding Protein Tomosyn. *Journal of Neuroscience*. **36**, 11208–11222

12. Williams, A. L., Bielopolski, N., Meroz, D., Lam, A. D., Passmore, D. R., Ben-Tal, N., Ernst, S. A., Ashery, U., and Stuenkel, E. L. (2011) Structural and functional analysis of tomosyn identifies domains important in exocytotic regulation. *Journal of Biological Chemistry*. **286**, 14542–14553

13. Geerts, C. J., Jacobsen, L., van de Bospoort, R., Verhage, M., and Groffen, A. J. A. (2014) Tomosyn Interacts with the SUMO E3 Ligase PIASγ. *PLoS ONE*. **9**, e91697–8

14. Swatek, K. N., and Komander, D. (2016) Ubiquitin modifications. *Nature Publishing Group*. **26**, 399–422

15. Widagdo, J., Guntupalli, S., Jang, S. E., and Anggono, V. (2017) Regulation of AMPA Receptor Trafficking by Protein Ubiquitination. *Front Mol Neurosci*. **10**, 461–10

16. Bhatnagar, S., Soni, M. S., Wrighton, L. S., Hebert, A. S., Zhou, A. S., Paul, P. K., Gregg, T., Rabaglia, M. E., Keller, M. P., Coon, J. J., and Attie, A. D. (2014) Phosphorylation and degradation of tomosyn-2 de-represses insulin secretion. *Journal of Biological Chemistry*. **289**, 25276–25286

17. Cohen, L. D., Zuchman, R., Sorokina, O., Müller, A., Dieterich, D. C., Armstrong, J. D., Ziv, T., and Ziv, N. E. (2013) Metabolic Turnover of Synaptic Proteins: Kinetics, Interdependencies and Implications for Synaptic Maintenance. *PLoS ONE*. **8**, e63191–20

18. Cohen, L. D., and Ziv, N. E. (2017) Recent insights on principles of synaptic protein degradation. *F1000Res*. **6**, 675–12

19. Roy, A., Kucukural, A., and Zhang, Y. (2010) I-TASSER: a unified platform for automated protein structure and function prediction. *Nat Protoc*. **5**, 725–738

20. Schindelin, J., Arganda-Carreras, I., Frise, E., Kaynig, V., Longair, M., Pietzsch, T., Preibisch, S., Rueden, C., Saalfeld, S., Schmid, B., Tinevez, J.-Y., White, D. J., Hartenstein, V., Eliceiri, K., Tomancak, P., and Cardona, A. (2012) Fiji: an open-source platform for biological-image analysis. *Nat Meth*. **9**, 676–682

CHAPTER IV

Discussion: Targeted degradation: Pre- and post-synaptic effects on structural and functional plasticity

Collectively, the results acquired in completing this dissertation suggest that the SNARE protein Tomo-1 is a novel and specific target of UPS-mediated proteostatic regulation (see overview Fig. 4.1), and furthermore, that modulation of Tomo-1 protein level via this mechanism underlies the induction of structural and functional plasticity within the nervous system.

Our present characterization of the UPS-dependent regulation of Tomosyn furthers the field in that: it is the first reported identification of Tomo-1 ubiquitination and proteostasis regulation by the UPS, it identifies consequential functional effects of this regulation in live neurons, and it is the first report of morphological plasticity as a downstream effect of Tomo-1 regulation. Additionally, this is the first examination of an HRD1/Tomo-1 interaction, both biochemically and compartmentally, in neurons. Furthermore, this was the first examination of HRD1 in primary neurons, confirming it as a key regulator of both Tomo-1 proteostasis and Tomo-1's consequential effects on dendritic morphology. Additionally, the novel PLA results indicate a potential local regulation of Tomo-1 by HRD1 at relevant subcellular regions, perhaps at synapses. Relatedly, our *in vitro* ubiquitination assays of Tomo-1 are the first reported, as are the

twelve ubiquitination sites we identified via mass spectrometry. These sites provide an initial characterization of the biochemical mechanisms underlying Tomo-1 degradation, and thus provide the ability for more targeted examination. The Tomo-1 antibody affinity variation following proteasome and DUB inhibition in neurons, further informed by the isoform and 3D protein structure modeling, hint that some of these sites are likely ubiquitinated by HRD1 *in vivo*. Lastly, the *in vitro* assays yield an initial estimation for the concentration-dependence of Tomo-1 ubiquitination by HRD1. Previous characterization of HRD1 focused on fibroblasts (1, 2) and the related Neuro2a (3), COS-1 (4), and SHSY5Y (5, 6) cell lines. Although these studies made use of cells that are neuron-like in some respects, prior to the studies of this dissertation it was completely unknown how HRD1 acts within individual primary neurons to influence their physiology and morphology.

Work from many labs has suggested that neuronal activity induces retrograde messengers from postsynaptic neurons to influence their presynaptic counterparts and tune synaptic strength (7). For example, postsynaptic upregulation of mTORC1 activity (8, 9), and the closely associated signaling molecules BDNF (10) and phosphatidic acid (PA) (11), prompts the presynaptic facilitation initiated by decreased excitatory input, a homeostatic mechanism (12). Though much of the work on mTORC1 has focused on its modulation of the initiation of protein translation (13, 14), its upregulation of postsynaptic BDNF also acts as a retrograde signal to the presynaptic neuron and requires proteasomal activity to induce compensatory homeostatic plasticity (10, 15), LTP (16), and LTD (17). Thus, altering postsynaptic excitatory inputs is likely to drive activity-

dependent plasticity in presynaptic release through the initiation of a coordinated adaptation in the local translation and targeted degradation of synaptic regulatory proteins (18). It is of specific interest that this proposed mechanism of plasticity induction is not simply a rebalancing of opposing constitutive/steady-state mechanisms already in effect within individual pre- or post-synaptic neurons or terminals. It also requires coordinated physiological adaptations between distinct, but synaptically-coupled neurons. Our present findings further posit that this trans-synaptic mechanism implements a rebalancing of protein turnover rates via the upregulation of targeted degradation, that this is crucial for at least one type of morphological plasticity induction, and this may occur independently of or alongside known translational control mechanisms.

There is a growing body of evidence underscoring the importance of targeted synaptic protein degradation in neuronal physiology and plasticity (19-22). Much of this work focuses on the turnover and trafficking of neurotransmitter receptors (23-27) and scaffolding proteins (28, 29) of the postsynaptic compartment. However, presynaptic degradative mechanisms are becoming increasingly elucidated (30, 31). Notably, proteasomal degradation of the vesicle priming factor RIM by the E3 ligase SCRAPPER has been reported to mediate presynaptic activity and plasticity (32, 33). However, SCRAPPER-dependent RIM degradation primarily affects miniature and spontaneous, but not evoked, release (32, 34). Furthermore, as a critical vesicle priming factor, RIM levels are positively correlated with the probability of release. Therefore, if RIM were the primary presynaptic target of an mTORC1/BDNF-induced increase in proteasomal

degradation it would be expected to counter the observed upregulation of presynaptic activity following AMPAR inhibition-mediated homeostatic plasticity induction. Thus, BDNF-mediated increases in ubiquitination and proteasomal degradation, and the consequential increase in presynaptic output, strongly suggest that the target of degradation underlying homeostatic induction is a negative regulator of neurotransmitter release. The identity of the presynaptic inhibitor targeted by retrograde signaling from the postsynaptic neuron to facilitate homeostatic plasticity is yet to be identified. Our findings highlight Tomo-1 as a high-probability presynaptic inhibitory candidate for this presynaptic inhibitor.

Tomo-1 exhibits inhibitory action in secretory cells, including central (35) and SCG neurons (36), chromaffin cells of the adrenal medulla (37), ß-cells of the pancreas (38), as well as the PC12 (39, 40) and CHO (41) secretory cell lines. Relatedly, Tomosyn is found to be colocalized to presynaptic terminals alongside numerous other proteins that are important for the exocytic process, including Syntaxin1a, VAMP2, Bassoon, Synaptophysin, and vGluT1 (36, 42-45). This is notable because it suggests a conserved need, across organ systems and species, for a brake to balance facilitative and constitutive secretory mechanisms. Interestingly, Tomo-1 protein has also been found to associate with synaptic vesicles (42-44) and the plasma membrane of insulin-secreting adipocytes (46), bovine adrenal chromaffin cells (37), and the PC12 cell line (37, 40). Furthermore, Tomo-2 was identified in dendrites of mammalian hippocampal neurons (47). This diversity in Tomo-1 expression highlights the need for a more complete understanding of its actions and mechanisms beyond that which is currently

known regarding its presynaptic inhibition. An open question following the finding of postsynaptic Tomosyn by Barak et al. (47) is how it may act there to influence synaptic physiology or plasticity. Indeed, we have here further identified that Tomo-1 colocalizes with the postsynaptic scaffolding protein PSD95 in hippocampal neuronal culture and is also expressed and serves a regulatory role within dendritic spines. This finding is significant because, not only is it a new characterization of Tomo-1 expression, we have further recognized a mechanism by which the Tomo-1-dependent density of dendritic spines is regulated, namely by HRD1. At present however, a physiological effect of spine density regulation remains elusive.

Currently identified inhibitory mechanisms of Tomo-1 stem from its C-terminal SNARE domain competitively inhibiting VAMP and Munc18 from binding with reactive Syntaxin1a *in vitro* (48, 49), in C. elegans (43), in chromaffin cells (37), and in SCG neurons (49). However, its N-terminal WD40 repeat domain also appears to have the capacity for sequestering SNARE complexes (50). Ultimately, Tomo-1 decreases the priming and fusion of RRP vesicles in neurons (50-52). This biochemically-driven model casts Tomo-1 as a rather passive inhibitor of vesicle priming and concomitant release. However, the integration of present findings supports the addition of a more functional understanding of how Tomo-1 influences synaptic physiology and plasticity. The completely novel finding that Tomo-1 protein level is regulated by the UPS positions it as the prime candidate inhibitory presynaptic effector of the targeted retrograde action following activity-induced postsynaptic upregulation of mTORC1/BDNF. Furthermore, we are the first to identify effects of Tomo-1 on dendritic morphology, which occurred in

a SNARE domain-independent fashion. This promotes fresh consideration of the mechanisms by which Tomo-1 actions are implemented.

There are reports of regulatory mechanisms contributing to the action of Tomo-1 and orthologues, however most are still in reference to its inhibitory effects and/or its SNARE domain (49, 53-55). These include conformational changes of the tail domain influencing overall protein structure and binding affinity of Tomo-1 for partners such as VAMP (56), Munc13 (43), and Rab3 small GTPases (51, 57, 58). Our unique findings offer a shift in focus for identifying Tomo-1 regulatory mechanisms and their influence over neurotransmission. That is, we suggest additional consideration is warranted in the focus of Tomo-1 research – evaluation of the variations in intrinsic protein properties (such as conformation) and SNARE-specific mechanisms (and their influence on effector interactions) should also include thorough examination of upstream Tomo-1 regulatory mechanisms. For example, the post-translational modification of Tomo-1 is becoming recognized as critical in contributing to the cell biological pathways sensing and rectifying neuronal activity (51) as well as those controlling the amount of Tomo-1 present in neurons (59). Indeed, there are multiple reports from our lab and others indicating the importance of PTMs in regulating Tomosyn protein action, including SUMOylation (40, 60) and phosphorylation (36, 41, 51, 61). However, to date, there is only one report on the regulation of Tomosyn protein level. It was shown that exogenously expressed Tomo-2 protein degradation by HRD1 was facilitated following its phosphorylation in the heterologous HEK293FT cell line (61). The hypothesis that controlling Tomo-2 level has relevance *in vivo* was substantiated by the fact that

glucose-stimulated insulin secretion in pancreatic ß-cells significantly increased the rate of Tomo-2 turnover.

Previous work on HRD1's roles in primary cells centered around its non-secretory ERAD processes and its gross localization to specific brain regions in mice (62-64) and the post-mortem brains of human AD patients (6, 65-67). Results presented herein exemplify the previously hypothesized, but largely unknown, significance of HRD1 action in the regulation of neuronal activity. Notably, one study employed the use of chemically-differentiated neurons from P19 cells following retinoic acid treatment to examine the effect of HRD1 in culture and determined HRD1 has neuroprotective effects in response to tunicamycin-induced ER stress and influences dendrite outgrowth during development (68). Our results build on this foundation by indicating a similar role in primary neurons and further indicate a mechanism by which the effects are mediated. The neurodevelopmental importance of HRD1 was initially identified because HRD1 null mouse embryos were found to be inviable due to death *in utero* (1). This result contrasts those from its orthologue, HRD1p, being dispensable in yeast. However, it is still an open question how HRD1 contributes to the development and integration of neurons and synapses, other than its regulation of Tomo-1 to control dendritic spine morphogenesis in mammalian excitatory neurons of the hippocampus. Relatedly, the mTORC1/BDNF pathway has been linked to morphological adaptations, such as those observed in postsynaptic dendritic spines during LTP induction (69, 70). In addition, it appears that LTP and homeostatic upregulation, though both utilizing postsynaptic mTORC1 and upregulated protein translation, can be induced by different cellular

mechanisms. Though many questions remain to be answered, our work suggests that the ubiquitination of synaptic proteins does not only alter presynaptic release and receptor cycling to modulate the strength of individual boutons, but also controls the number of synapses linking neurons into networks, as indicated by dendritic spine count. This evidence highlights the necessity for parsing out feed-forward- and feedback-based cellular mechanisms, most notably the UPS and its upstream activation, in the implementation of modulating synaptic morphology and plasticity. Overall, our findings fit with our initial hypothesis in the sense that we indeed found Tomo-1 to be under the control of the UPS in neurons. Furthermore, this level of control influenced cell morphology in a way we expect to contribute downstream of these increased synaptic locations.

4.2 Limitations and Future Directions

Chapter 2

The importance of the UPS in regulating protein levels through targeted degradation is widely recognized in eukaryotic cells. This is partially illustrated by the substantial number of human diseases related to alterations in proteostasis (71). However, careful examination of individual cell-types, tissue regions, physiological conditions, and activity parameters is further required to better understand how Tomo-1 degradation affects neuronal function. The approaches utilized in acquiring Chapter 2 data do not differentiate between hippocampal neuron sub-types, primarily due to the dissociated cell culture approach. However, a number of specific targeting approaches

were implemented to ensure results obtained on the UPS-mediated regulation of Tomo-1 occurs in neurons and not glial cells, as outlined in the results and materials and methods sections therein. Due to the lack of identification of individual neuronal sub-types, which are known to differentially express a plethora of important proteins and undergo varying forms of plasticity (72, 73), our conclusions are limited to those neurons which we were able to specifically resolve (general for biochemistry, pyramidal for imaging). Furthermore, it is at present unknown if any of the recognized effects also occur across developmental stages, such as the differentiation of neurons and the biogenesis and integration of dendrites and synapses. Data acquisition occurred between the noted timepoints in reference to animal age at primary cell harvesting as well as number of days *in vitro* following dissociation and plating. Greater resolution in how these degradation effects are differentially implemented by neurons during various stages of maturity and plasticity state requires careful examination of a repeated measures/timecourse approach.

The high level of sequence and structural homology between the three Tomo-1 splice isoforms in mammals (40, 74) is also a limiting factor to some degree, in that there are, at present, no commercially available isoform-specific antibodies. Therefore, it is unclear which isoforms of Tomo-1 may be preferentially targeted and regulated, including their localization, effector affinity, and resulting downstream effects. However, it is reported that the s- and m-Tomo-1 isoforms (for small and medium) are brain-specific, as evidenced by RT-PCR of Tomo-1 mRNA, and highly enriched at synapses (35, 75). Relatedly, it is presently unknown if and how the related Tomo-2 protein may

act endogenously within these neurons. Tomo-1 and Tomo-2 have regions of overlapping and non-overlapping expression in the intact hippocampus likely also within individual compartments of various neurons (47). Therefore, there is the potential for differential expression, as well as supplemental, redundant, and/or competitive actions of Tomo-1 and Tomo-2 in mediating some of the results outlined in Chapter 2. Again, specific targeting of Tomo-1 was implemented wherever possible, with verified antibodies and proof-of-principal empirical testing, as described in the results and materials and methods sections.

Resulting from the general limitations of the biochemical analysis of neuronal lysate samples, our ubiquitination studies do not allow for spatially resolving the subcellular regional location of Tomo-1 interaction with HRD1, its ubiquitination, nor its degradation. Notable exceptions include all fixed- and live-cell imaging experiments, including the proximity-ligation assay for Tomo-1/HRD1 interaction *in situ*. Otherwise, results generated in Chapter 2 cannot be specifically attributed to synapses, or even axons or dendrites, though given HRD1's integral ER membrane localization, they are presumed to occur at subcellular regions with some sort of ER present. Therefore, the additional implementation of high-resolution imaging and biochemical enrichment strategies is a logical next step for further conclusions of this research topic. Imaging approaches, including Dendra2-Tomo-1 fusion protein expression via sparse transfection as in chapter 2, would allow for timelapse imaging of proteostasis while affording the additional control of tracking both translation and degradation rates with subcellular specificity. This approach could be expanded further in the implementation

of UPS-specific pharmacological manipulations, Tomo-1 disruptions including K-R ubiquitination mutations and loop domain deletions, and electrically- or chemically-induced plasticity. Findings gathered from these experiments should yield additional insights into both how and where Tomo-1 is controlled during its action on synaptic activity and morphological plasticity. Further biochemical approaches and analyses are also warranted to probe the detailed mechanisms utilized in the proteostatic regulation of Tomo-1 and its relationship with effector proteins following post-translational modifications including ubiquitination and phosphorylation. For example, differential centrifugation and neuro/synaptosomes preparation would promote the identification of Tomo-1 ubiquitination sites *in vivo* from neurons under various conditions, which is critical to determining if the synaptic population of Tomo-1 is specifically targeted versus the total and could be carried out vis SDS-PAGE and mass spectrometry analyses.

The study of Tomo-1 proteostasis is currently in its infancy. Indeed, there are no known *in vivo* variations of Tomo-1 protein expression level modulation reported in neurons with which to compare our novel HRD1-mediated observations. The importance of this consideration cannot be overstated, as numerous synaptic proteins are reported to have relatively long half-lives (76, 77), which can be drastically altered upon perturbing proteasomal activity (78). Furthermore, determination of steady-state Tomo-1 levels in specific brain regions, cell-types, specific activity paradigms, is needed to identify both the physiological scale of our observed Tomo-1 protein level changes, and consequentially, its relevance to tuning Tomo-1 level within that dynamic range. Relatedly, our interpretations of the proteasome activity-dependent alterations in Tomo-

1 protein level rely on the assumption that the decrease in UPS activity is the primary cause of Tomo-1's increased proteostasis. Although this is the most straightforward interpretation of the data, we did not empirically determine degradation rates themselves to identify specific changes. However, we do find increased Tomo-1 protein level upon inhibiting the E3 ligase HRD1 and by inhibiting the catalytic activity of the 26S proteasome with two different pharmacological agents, adding specificity to this system. Nonetheless, the topic of neuronal and synaptic protein lifetimes has become a recent topic of quantitative investigation (77-78). Results appear to indicate that simple pharmacological treatments modulating the UPS can prompt unanticipated effects in protein production rates, in addition to degradation, which may confound our interpretation. It would be quite useful to now make relevant synaptic protein lifetime measurements. Indeed, there is evidence in the literature regarding the protein lifetime of Tomo-1 being quite extensive. Tomo-1 half-life was reported via stable isotope labeling with amino acids in cell culture (SILAC) to be approximately 94 hours, with an approximate 136-hour lifetime (76, supplemental data tables). Although protein biosynthesis rates themselves were not examined, the effects following use of proteasome inhibitors were found to be complementary to those of our HRD1 KD condition, which resulted in a specific increase in Tomo-1 protein in our similar hippocampal culture system. Thus, we hypothesize that KD of HRD1, as an E3 targeting Tomo-1, to be more selective when compared to global pharmacological inhibition of the proteasome, especially given the rather acute 4-hour timescale of our proteasome blockade treatment. However, ultimately, an increase in Tomo-1

biosynthetic activity could be linked to reduced UPS-mediated degradation or actions of proteasome blockers and thus are limited in further conclusions. This requires empirical determination via complementary methods, which would allow for the specific influences of HRD1 interaction, ubiquitination, and proteasomal degradation on the gross and specific sub-populations of Tomo-1 to be evaluated under various physiologically-relevant paradigms such as plasticity induction.

Given that HRD1 is heavily reported to interact with numerous partner proteins in accomplishing its degradative tasks (79-81) it will be worthwhile to probe for the necessity and effect of these mechanistically-related adapting and stabilizing proteins. The present study did not determine if or which partner and effector proteins are required by or facilitate HRD1's regulation of Tomo-1 levels *in vivo,* which will be required prior to examination of potential resultant changes in synaptic physiology. We did however identify which UPS-related proteins are minimally required for HRD1-mediated degradation of Tomo-1 *in vitro*, which include the mammalian E1 UBE1, the E2 UBE2D2 (also known as UbcH5b), the E3 HRD1, mammalian Ubiquitin, and ATP. However, the HRD1 provided has the ER-transmembrane region deleted to inhibit potential aggregation. Furthermore, critical regulation of total or specific HRD1 target substrates may presumably be influenced by the protein compliment of the multi-protein retrotranslocon complex and its correlated adaptors and effector proteins.

Relatedly, we could not differentiate between ubiquitin chain linkage-types/variations created by HRD1 on Tomo-1, *in vivo* or *in vitro*. Fascinatingly, specific mono- and poly-ubiquitin chain linkages, of which there are dozens predicted, are

increasingly implicated in the specific targeting of various substrates to their fates, notably including receptor internalization, nuclear localization, and proteasomal or lysosomal degradation (82-84). This knowledge will be important for the advancement of our understanding of Tomo-1-specific degradation by HRD1, but also the generalizable interpretation of these ubiquitin chain classes and their specific influences over synaptic and neuronal cell biology. Overexpression of the relatively well-characterized ubiquitin mutants, including the K48R and K63R variants, would be particularly useful in examining this aspect of Tomo-1 regulation.

Lastly, our present study was not designed to determine if the Tomo-1 or HRD1 influences on spines was primarily implemented by modulating their morphogenesis, stability, retraction, or other temporally labile properties. Though all of the spine imaging reported in Chapter 2 was undertaken on single live neurons, we did so in individual sessions. It is extensively reported that dendritic spine dynamics and structural plasticity vary greatly following a number of conditions and treatments (85). Furthermore, we did not specifically examine potential effects on specific morphologically-defined dendritic spine sub-types (i.e. mushroom, filopodia) or effects of shaft branching. However, upon examination, we did not identify significant differences in the distribution of spines proximal or distal to the soma through the measured dendrite lengths. A repeat examination of Tomo-1 and HRD1 effects on the density and finer morphological characteristics of dendritic spines would greatly benefit from a timelapse imaging approach in examination of the onset, timecourse, and stability of spine density alterations. These results would be directly applicable to hypothesis generation for

downstream/emergent effects of intrinsic neuronal or network excitability and potential for induction of various physiologically-induced plasticities. At present, we can only speculate that the observed increase in dendritic spine density, defined as spine count over a given distance, directly correlates with concomitant effects on synapse number, distribution, sub-type proportion, and/or activity and plasticity.

Chapter 3

The ubiquitination of protein substrates at specific lysine residues is key to their targeted degradation. E3 ligases are the main mediator of protein targeting and often the individual residue targeting for ubiquitination. In the case of HRD1, as a RING-type E3, this process occurs in conjunction with its cognate upstream E2 conjugating enzyme (86). The target lysine residue is presumed to be poly-ubiquitinated alongside E4 conjugation factor proteins via either pre-constructed or salvaged chains (87) or iterative elongation initiating from the mono-ubiquitinated lysine. Our assays were unable to determine by which method poly-ubiquitination of Tomo-1 by HRD1 occurs upstream of its degradation.

Gathering this information would be highly facilitated by more sensitive proteomic analysis, but moreover, by increased Tomo-1 protein expression and yield from intact neurons, as opposed to heterologous cell lines, for use in follow-up *in vitro* and *in vivo* assays. Toward this end, we have successfully inserted the WT and 12xKR constructs created and utilized in Chapter 3 into the lentiviral YFP-tagged vector utilized in Chapter 2 for higher neuronal expression and greater yield during purification. These constructs

will be of immediate use in repeating the MS/MS experimental approaches following affinity-purification, rather than the lower yield Tomo-1 antibody-based IP purification, which indicated no reliable ubiquitination sites from neuronal samples. Furthermore, the inclusion of SILAC labeling for pulse-chase techniques and analysis should also prove worthwhile in the determination of relevant Tomo-1 ubiquitination events and sites *in vivo*. Tomo-1 antibody-based IPs also showed moderate levels of non-specific, presumably unrelated proteins in purified samples. The stronger and more specific biotin-streptavidin affinity in conjunction with the neuron-specific expression of the WT and 12xKR mutants should increase the probability of successful ubiquitination site identification from neuronal Tomo-1. This should then allow for comparison of WT and mutant (e.g. individual single site K-R mutants which were generated alongside the 12xKR) constructs. Finally, these ubiquitination sites would serve as initial points of focus for the testing of relevant physiological conditions under which Tomo-1 degradation may naturally be modulated. Those may include specific activity paradigms, homeostatic or Hebbian plasticity induction, and alongside co-manipulation of Taco-1 effector molecules. These naturally-occurring variable conditions are hypothesized to also include cross-talk between PTMs (e.g. PO_4, SUMO, targeted ubiquitination by other E3s). The research objectives of potential future experiments related to the findings outlined in this dissertation appear endless, and it will be quite interesting to see where hypothesis-driven examination leads the field of UPS-mediated synaptic regulation.

Final Remarks

In summary, the collective work comprising this dissertation provides novel indications that Tomo-1, a potent negative regulator of presynaptic release, interacts with and is ubiquitinated and targeted for proteasomal degradation by the E3 ligase HRD1 (Chapter 2). Furthermore, these findings reveal that HRD1 modulates Tomo-1 protein abundance in neurons, an interaction which appears to cooperatively regulate the density of postsynaptic dendritic spines. Relatedly, HRD1 is capable of ubiquitinating Tomo-1 at multiple specific lysine residues *in vitro* (Chapter 3), though which may be important for its targeted degradation and/or plasticity induction *in vivo* remains to be determined. These findings may prove useful in the future if integrated with related results regarding Tomo-1 and the UPS implications in the proteinopathy and protein aggregation associated effects apparent in neurological and neurodegenerative diseases such as Autism Spectrum Disorders, Alzheimer's Disease, and Parkinson's Disease.

Figure 4.1: Schematic model overviewing UPS-mediated Tomo-1 degradation.

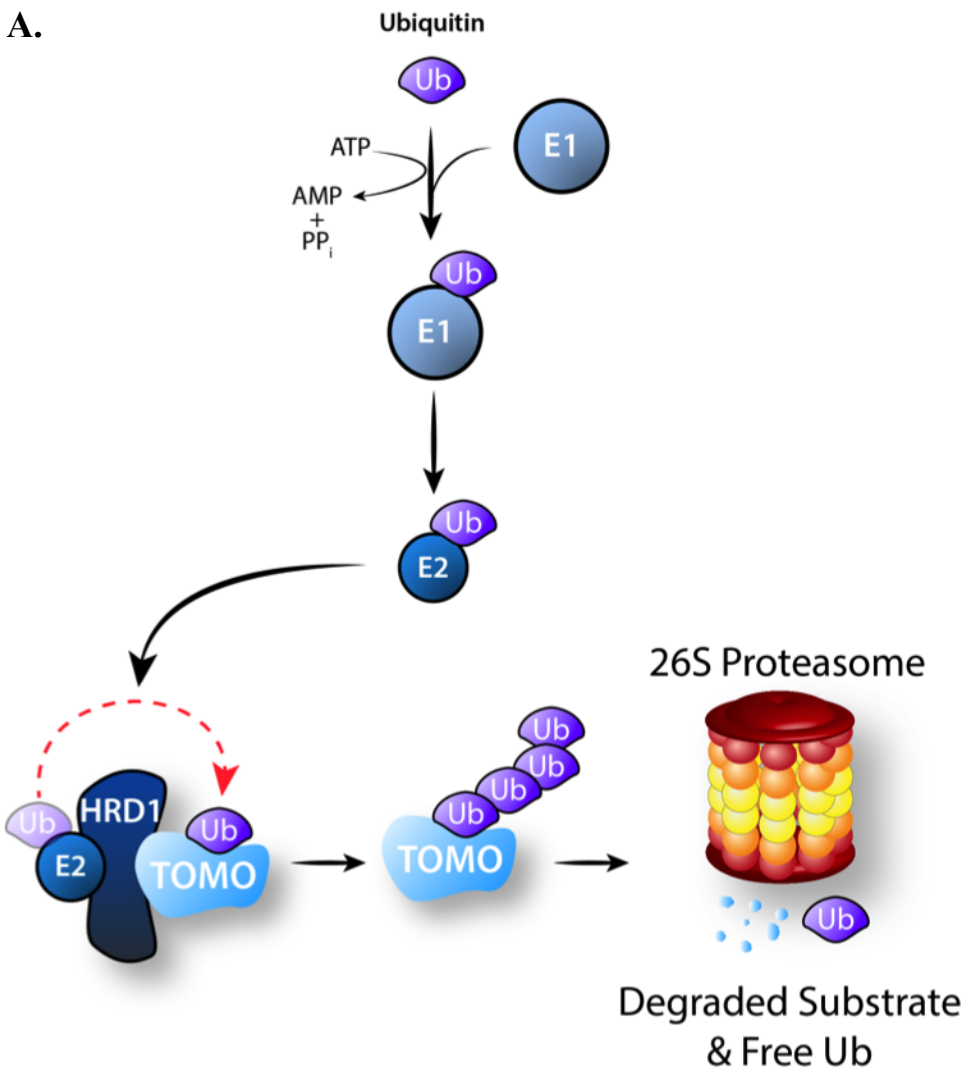

Figure 4.1: Schematic model overviewing UPS-mediated Tomo-1 degradation.

A, Simplified cartoon model outlining the various UPS-related components and actions hypothesized to control Tomo-1 degradation in neurons. Ubiquitin molecules are activated by an E1 enzyme through an ATP-dependent process and transferred to a cognate E2 conjugating enzyme. This E2-ubiquitin then complexes with HRD1, which prompts the ubiquitin transfer to Tomo-1 as the target protein substrate. At present, it is unclear if this process occurs in an iterative fashion to accomplish ubiquitin chain elongation or if a pre-formed poly-ubiquitin chain may be transferred directly onto Tomo-1 by the E2-HRD1 complex. Once poly-ubiquitinated, the Tomo-1 is then targeted and subject to degradation by the 26S proteasome complex, which subsequently cleaves the protein into polypeptide fragments and free ubiquitin molecules.

4.4 Bibliography

1. Yagishita, N., Ohneda, K., Amano, T., Yamasaki, S., Sugiura, A., Tsuchimochi, K., Shin, H., Kawahara, K. I., Ohneda, O., Ohta, T., Tanaka, S., Yamamoto, M., Maruyama, I., Nishioka, K., Fukamizu, A., and Nakajima, T. (2005) Essential Role of Synoviolin in Embryogenesis. *Journal of Biological Chemistry*. **280**, 7909–7916

2. Maeda, T., Marutani, T., Zou, K., Araki, W., Tanabe, C., Yagishita, N., Yamano, Y., Amano, T., Michikawa, M., Nakajima, T., and Komano, H. (2009) An E3 ubiquitin ligase, Synoviolin, is involved in the degradation of immature nicastrin, and regulates the production of amyloid beta-protein. *FEBS J.* **276**, 5832–5840

3. Qi, X., Okuma, Y., Hosoi, T., Kaneko, M., and Nomura, Y. (2004) Induction of murine HRD1 in experimental cerebral ischemia. *Molecular Brain Research*. **130**, 30–38

4. Omura, T., Kaneko, M., Okuma, Y., Orba, Y., Nagashima, K., Takahashi, R., Fujitani, N., Matsumura, S., Hata, A., Kubota, K., Murahashi, K., Uehara, T., and Nomura, Y. (2006) A ubiquitin ligase HRD1 promotes the degradation of Pael receptor, a substrate of Parkin. *J Neurochem*. **99**, 1456–1469

5. Yang, H., Zhong, X., Ballar, P., Luo, S., Shen, Y., Rubinsztein, D. C., Monteiro, M. J., and Fang, S. (2007) Ubiquitin ligase Hrd1 enhances the degradation and suppresses the toxicity of polyglutamine-expanded huntingtin. *Experimental Cell Research*. **313**, 538–550

6. Kaneko, M., Koike, H., Saito, R., Kitamura, Y., Okuma, Y., and Nomura, Y. (2010) Loss of HRD1-Mediated Protein Degradation Causes Amyloid Precursor Protein Accumulation and Amyloid- Generation. *Journal of Neuroscience*. **30**, 3924–3932

7. Regehr, W. G., Carey, M. R., and Best, A. R. (2009) Activity-Dependent Regulation of Synapses by Retrograde Messengers. *Neuron*. **63**, 154–170

8. Henry, F. E., McCartney, A. J., Neely, R., Perez, A. S., Carruthers, C. J. L., Stuenkel, E. L., Inoki, K., and Sutton, M. A. (2012) Retrograde Changes in Presynaptic Function Driven by Dendritic mTORC1. *Journal of Neuroscience*. **32**, 17128–17142

9. Penney, J., Tsurudome, K., Liao, E. H., Elazzouzi, F., Livingstone, M., Gonzalez, M., Sonenberg, N., and Haghighi, A. P. (2012) TOR is required for the retrograde regulation of synaptic homeostasis at the Drosophila neuromuscular junction. *Neuron*. **74**, 166–178

10. Jakawich, S. K., Nasser, H. B., Strong, M. J., McCartney, A. J., Perez, A. S.,

Rakesh, N., Carruthers, C. J. L., and Sutton, M. A. (2010) Local Presynaptic Activity GatesHomeostatic Changes in Presynaptic Function Driven by Dendritic BDNF Synthesis. *Neuron*. **68**, 1143–1158

11. Henry, F. E., Wang, X., Serrano, D., Perez, A. S., Carruthers, C. J. L., Stuenkel, E. L., and Sutton, M. A. (2018) A unique homeostatic signaling pathway links synaptic inactivity to postsynaptic mTORC1. *J. Neurosci.* 10.1523/JNEUROSCI.1843-17.2017

12. Davis, G. W., and Müller, M. (2015) Homeostatic control of presynaptic neurotransmitter release. *Annu. Rev. Physiol.* **77**, 251–270

13. Ma, X. M., and Blenis, J. (2009) Molecular mechanisms of mTOR-mediated translational control. *Nat Rev Mol Cell Bio*. **10**, 307–318

14. Switon, K., Kotulska, K., Janusz-Kaminska, A., Zmorzynska, J., and Jaworski, J. (2017) Molecular neurobiology of mTOR. *Neuroscience*. **341**, 112–153

15. Lindskog, M., Li, L., Groth, R. D., Poburko, D., Thiagarajan, T. C., Han, X., and Tsien, R. W. (2010) Postsynaptic GluA1 enables acute retrograde enhancement of presynaptic function to coordinate adaptation to synaptic inactivity. *Proceedings of the National Academy of Sciences*. **107**, 21806–21811

16. Santos, A. R., Mele, M., Vaz, S. H., Kellermayer, B., Grimaldi, M., Colino-Oliveira, M., Rombo, D. M., Comprido, D., Sebastiao, A. M., and Duarte, C. B. (2015) Differential Role of the Proteasome in the Early and Late Phases of BDNF-Induced Facilitation of LTP. *Journal of Neuroscience*. **35**, 3319–3329

17. Li, Q., Korte, M., and Sajikumar, S. (2015) Ubiquitin-Proteasome System Inhibition Promotes Long-Term Depression and Synaptic Tagging/Capture. *Cereb. Cortex*. **26**, 2541–2548

18. Alvarez-Castelao, B., and Schuman, E. M. (2015) The Regulation of Synaptic Protein Turnover. *Journal of Biological Chemistry*. **290**, 28623–28630

19. Hegde, A. N., and DiAntonio, A. (2002) Ubiquitin and the synapse. *Nat Rev Neurosci*. **3**, 854–861

20. Tai, H.-C., and Schuman, E. M. (2008) Ubiquitin, the proteasome and protein degradation in neuronal function and dysfunction. *Nat Rev Neurosci*. **9**, 826–838

21. Rinetti, G. V., and Schweizer, F. E. (2010) Ubiquitination acutely regulates presynaptic neurotransmitter release in mammalian neurons. *Journal of Neuroscience*. **30**, 3157–3166

22. Jarome, T. J., and Helmstetter, F. J. (2014) Protein degradation and protein synthesis in long-term memory formation. *Front Mol Neurosci*. **7**, 61

23. Colledge, M., Snyder, E. M., Crozier, R. A., Soderling, J. A., Jin, Y., Langeberg, L. K., Lu, H., Bear, M. F., and Scott, J. D. (2003) Ubiquitination regulates PSD-95 degradation and AMPA receptor surface expression. *Neuron*. **40**, 595–607

24. Moriyoshi, K., Iijima, K., Fujii, H., Ito, H., Cho, Y., and Nakanishi, S. (2004) Seven in absentia homolog 1A mediates ubiquitination and degradation of group 1 metabotropic glutamate receptors. *Proc. Natl. Acad. Sci. U.S.A.* **101**, 8614–8619

25. Marangoudakis, S., Andrade, A., Helton, T. D., Denome, S., Castiglioni, A. J., and Lipscombe, D. (2012) Differential ubiquitination and proteasome regulation of Ca(V)2.2 N-type channel splice isoforms. *J. Neurosci.* **32**, 10365–10369

26. Zemoura, K., and Benke, D. (2014) Proteasomal Degradation of -Aminobutyric AcidB Receptors Is Mediated by the Interaction of the GABAB2 C Terminus with the Proteasomal ATPase Rtp6 and Regulated by Neuronal Activity. *Journal of Biological Chemistry*. **289**, 7738–7746

27. Widagdo, J., Guntupalli, S., Jang, S. E., and Anggono, V. (2017) Regulation of AMPA Receptor Trafficking by Protein Ubiquitination. *Front Mol Neurosci*. **10**, 461–10

28. Ehlers, M. D. (2003) Activity level controls postsynaptic composition and signaling via the ubiquitin-proteasome system. *Nat. Neurosci.* **6**, 231–242

29. Lin, A. W., and Man, H.-Y. (2013) Ubiquitination of neurotransmitter receptors and postsynaptic scaffolding proteins. *Neural Plast.* **2013**, 432057–10

30. Speese, S. D., Trotta, N., Rodesch, C. K., Aravamudan, B., and Broadie, K. (2003) The ubiquitin proteasome system acutely regulates presynaptic protein turnover and synaptic efficacy. *Curr. Biol.* **13**, 899–910

31. Lazarevic, V., Schöne, C., Heine, M., Gundelfinger, E. D., and Fejtova, A. (2011) Extensive remodeling of the presynaptic cytomatrix upon homeostatic adaptation to network activity silencing. *Journal of Neuroscience*. **31**, 10189–10200

32. Yao, I., Takagi, H., Ageta, H., Kahyo, T., Sato, S., Hatanaka, K., Fukuda, Y., Chiba, T., Morone, N., Yuasa, S., Inokuchi, K., Ohtsuka, T., MacGregor, G. R., Tanaka, K., and Setou, M. (2007) SCRAPPER-Dependent Ubiquitination of Active Zone Protein RIM1 Regulates Synaptic Vesicle Release. *CELL*. **130**, 943–957

33. Takagi, H., Setou, M., Ito, S., and Yao, I. (2012) SCRAPPER regulates the thresholds of long-term potentiation/depression, the bidirectional synaptic plasticity in hippocampal CA3-CA1 synapses. *Neural Plast.* **2012**, 352829–7

34. Koga, K., Yao, I., Setou, M., and Zhuo, M. (2017) SCRAPPER Selectively Contributes to Spontaneous Release and Presynaptic Long-Term Potentiation in the Anterior Cingulate Cortex. *Journal of Neuroscience*. **37**, 3887–3895

35. Ashery, U., Bielopolski, N., Barak, B., and Yizhar, O. (2009) Friends and foes in synaptic transmission: the role of tomosyn in vesicle priming. *Trends Neurosci.* **32**, 275–282

36. Baba, T., Sakisaka, T., Mochida, S., and Takai, Y. (2005) PKA-catalyzed phosphorylation of tomosyn and its implication in Ca2+-dependent exocytosis of neurotransmitter. *The Journal of Cell Biology*. **170**, 1113–1125

37. Gladycheva, S. E., Lam, A. D., Liu, J., D'Andrea-Merrins, M., Yizhar, O., Lentz, S. I., Ashery, U., Ernst, S. A., and Stuenkel, E. L. (2007) Receptor-mediated regulation of tomosyn-syntaxin 1A interactions in bovine adrenal chromaffin cells. *J. Biol. Chem.* **282**, 22887–22899

38. Zhang, W., Lilja, L., Mandic, S. A., Gromada, J., Smidt, K., Janson, J., Takai, Y., Bark, C., Berggren, P.-O., and Meister, B. (2006) Tomosyn is expressed in beta-cells and negatively regulates insulin exocytosis. *Diabetes*. **55**, 574–581

39. Hatsuzawa, K., Lang, T., Fasshauer, D., Bruns, D., and Jahn, R. (2003) The R-SNARE motif of tomosyn forms SNARE core complexes with syntaxin 1 and SNAP-25 and down-regulates exocytosis. *J. Biol. Chem.* **278**, 31159–31166

40. Williams, A. L., Bielopolski, N., Meroz, D., Lam, A. D., Passmore, D. R., Ben-Tal, N., Ernst, S. A., Ashery, U., and Stuenkel, E. L. (2011) Structural and functional analysis of tomosyn identifies domains important in exocytotic regulation. *Journal of Biological Chemistry*. **286**, 14542–14553

41. Nagano, K., Takeuchi, H., Gao, J., Mori, Y., Otani, T., Wang, D., and Hirata, M. (2015) Tomosyn is a novel Akt substrate mediating insulin-dependent GLUT4 exocytosis. *Int. J. Biochem. Cell Biol.* **62**, 62–71

42. Fujita, Y., Shirataki, H., Sakisaka, T., Asakura, T., Ohya, T., Kotani, H., Yokoyama, S., Nishioka, H., Matsuura, Y., Mizoguchi, A., Scheller, R. H., and Takai, Y. (1998) Tomosyn: a syntaxin-1-binding protein that forms a novel complex in the neurotransmitter release process. *Neuron*. **20**, 905–915

43. McEwen, J. M., Madison, J. M., Dybbs, M., and Kaplan, J. M. (2006) Antagonistic

regulation of synaptic vesicle priming by Tomosyn and UNC-13. *Neuron*. **51**, 303–315

44. Takamori, S., Holt, M., Stenius, K., Lemke, E. A., Grønborg, M., Riedel, D., Urlaub, H., Schenck, S., Brügger, B., Ringler, P., Müller, S. A., Rammner, B., Gräter, F., Hub, J. S., De Groot, B. L., Mieskes, G., Moriyama, Y., Klingauf, J., Grubmüller, H., Heuser, J., Wieland, F., and Jahn, R. (2006) Molecular Anatomy of a Trafficking Organelle. *CELL*. **127**, 831–846

45. Barak, B., Okun, E., Ben-Simon, Y., Lavi, A., Shapira, R., Madar, R., Wang, Y., Norman, E., Sheinin, A., Pita, M. A., Yizhar, O., Mughal, M. R., Stuenkel, E., van Praag, H., Mattson, M. P., and Ashery, U. (2013) Neuron-specific expression of tomosyn1 in the mouse hippocampal dentate gyrus impairs spatial learning and memory. *Neuromolecular Med.* **15**, 351–363

46. Widberg, C. H., Bryant, N. J., Girotti, M., Rea, S., and James, D. E. (2003) Tomosyn interacts with the t-SNAREs syntaxin4 and SNAP23 and plays a role in insulin-stimulated GLUT4 translocation. *J. Biol. Chem.* **278**, 35093–35101

47. Barak, B., Williams, A., Bielopolski, N., Gottfried, I., Okun, E., Brown, M. A., Matti, U., Rettig, J., Stuenkel, E. L., and Ashery, U. (2010) Tomosyn expression pattern in the mouse hippocampus suggests both presynaptic and postsynaptic functions. *Front Neuroanat*. **4**, 149

48. Masuda, E. S., Huang, B. C., Fisher, J. M., Luo, Y., and Scheller, R. H. (1998) Tomosyn binds t-SNARE proteins via a VAMP-like coiled coil. *Neuron*. **21**, 479–480

49. Yamamoto, Y., Mochida, S., Kurooka, T., and Sakisaka, T. (2009) Reciprocal intramolecular interactions of tomosyn control its inhibitory activity on SNARE complex formation. *J. Biol. Chem.* **284**, 12480–12490

50. Sakisaka, T., Yamamoto, Y., Mochida, S., Nakamura, M., Nishikawa, K., Ishizaki, H., Okamoto-Tanaka, M., Miyoshi, J., Fujiyoshi, Y., Manabe, T., and Takai, Y. (2008) Dual inhibition of SNARE complex formation by tomosyn ensures controlled neurotransmitter release. *The Journal of Cell Biology*. **183**, 323–337

51. Cazares, V. A., Njus, M. M., Manly, A., Saldate, J. J., Subramani, A., Ben-Simon, Y., Sutton, M. A., Ashery, U., and Stuenkel, E. L. (2016) Dynamic Partitioning of Synaptic Vesicle Pools by the SNARE-Binding Protein Tomosyn. *Journal of Neuroscience*. **36**, 11208–11222

52. Gracheva, E. O., Burdina, A. O., Holgado, A. M., Berthelot-Grosjean, M., Ackley, B. D., Hadwiger, G., Nonet, M. L., Weimer, R. M., and Richmond, J. E. (2006)

Tomosyn Inhibits Synaptic Vesicle Priming in Caenorhabditis elegans. *PLoS Biol.* **4**, e261–12

53. Lehman, K., Rossi, G., Adamo, J. E., and Brennwald, P. (1999) Yeast homologues of tomosyn and lethal giant larvae function in exocytosis and are associated with the plasma membrane SNARE, Sec9. *The Journal of Cell Biology*. **146**, 125–140

54. Gangar, A., Rossi, G., Andreeva, A., Hales, R., and Brennwald, P. (2005) Structurally Conserved Interaction of Lgl Family with SNAREs Is Critical to Their Cellular Function. *Current Biology*. **15**, 1136–1142

55. Hattendorf, D. A., Andreeva, A., Gangar, A., Brennwald, P. J., and Weis, W. I. (2007) Structure of the yeast polarity protein Sro7 reveals a SNARE regulatory mechanism. *Nature*. **446**, 567–571

56. Yamamoto, Y., Fujikura, K., Sakaue, M., Okimura, K., Kobayashi, Y., Nakamura, T., and Sakisaka, T. (2010) The tail domain of tomosyn controls membrane fusion through tomosyn displacement by VAMP2. *Biochemical and Biophysical Research Communications*. **399**, 24–30

57. Rossi, G., Watson, K., Demonch, M., Temple, B., and Brennwald, P. (2014) In vitro Reconstitution of Rab-dependent Vesicle Clustering by the Yeast Lethal Giant Larvae/Tomosyn Homolog, Sro7. *Journal of Biological Chemistry*. 10.1074/jbc.M114.595892

58. Watson, K., Rossi, G., Temple, B., and Brennwald, P. (2015) Structural basis for recognition of the Sec4 Rab GTPase by its effector, the Lgl/tomosyn homologue, Sro7. *Molecular Biology of the Cell*. **26**, 3289–3300

59. Saldate, J. J., Shiau, J., Cazares, V. A., and Stuenkel, E. L. (2017) The ubiquitin-proteasome system functionally links neuronal Tomosyn-1 to dendritic morphology. *Journal of Biological Chemistry*. 10.1074/jbc.M117.815514

60. Geerts, C. J., Jacobsen, L., van de Bospoort, R., Verhage, M., and Groffen, A. J. A. (2014) Tomosyn Interacts with the SUMO E3 Ligase PIASγ. *PLoS ONE*. **9**, e91697–8

61. Bhatnagar, S., Soni, M. S., Wrighton, L. S., Hebert, A. S., Zhou, A. S., Paul, P. K., Gregg, T., Rabaglia, M. E., Keller, M. P., Coon, J. J., and Attie, A. D. (2014) Phosphorylation and degradation of tomosyn-2 de-represses insulin secretion. *Journal of Biological Chemistry*. **289**, 25276–25286

62. Omura, T., Kaneko, M., Tabei, N., Okuma, Y., and Nomura, Y. (2008)

Immunohistochemical localization of a ubiquitin ligase HRD1 in murine brain. *J. Neurosci. Res.* **86**, 1577–1587

63. Mei, J., and Niu, C. (2010) Alterations of Hrd1 expression in various encephalic regional neurons in 6-OHDA model of Parkinson's disease. *Neurosci. Lett.* **474**, 63–68

64. Kawada, K., Kaneko, M., Nomura, Y., Mimori, S., Hamana, H., Ogita, K., Murayama, T., Fujino, H., and Okuma, Y. (2011) Expression of the Ubiquitin Ligase HRD1 in Neural Stem/Progenitor Cells of the Adult Mouse Brain. *J Pharmacol Sci*. **117**, 208–212

65. Hou, H.-L., Shen, Y.-X., Zhu, H.-Y., Sun, H., Yan, X.-B., Fang, H., and Zhou, J.-N. (2006) Alterations of hHrd1 expression are related to hyperphosphorylated tau in the hippocampus in Alzheimer's disease. *J. Neurosci. Res.* **84**, 1862–1870

66. Saito, R., Kaneko, M., Okuma, Y., and Nomura, Y. (2010) Correlation between decrease in protein levels of ubiquitin ligase HRD1 and amyloid-beta production. *J Pharmacol Sci*. **113**, 285–288

67. Shen, Y. X., Sun, A. M., Fang, S., Feng, L. J., Li, Q., Hou, H. L., Liu, C., Wang, H. P., Shen, J. L., Luo, J., and Zhou, J. N. (2012) Hrd1 Facilitates Tau Degradation and Promotes Neuron Survival. *Curr. Mol. Med.* **12**, 138–152

68. Kawada, K., Iekumo, T., Saito, R., Kaneko, M., Mimori, S., Nomura, Y., and Okuma, Y. (2014) Aberrant neuronal differentiation and inhibition of dendrite outgrowth resulting from endoplasmic reticulum stress. *J. Neurosci. Res.* **92**, 1122–1133

69. Kumar, V., Zhang, M.-X., Swank, M. W., Kunz, J., and Wu, G.-Y. (2005) Regulation of dendritic morphogenesis by Ras-PI3K-Akt-mTOR and Ras-MAPK signaling pathways. *J. Neurosci.* **25**, 11288–11299

70. Henry, F. E., Hockeimer, W., Chen, A., Mysore, S. P., and Sutton, M. A. (2017) Mechanistic target of rapamycin is necessary for changes in dendritic spine morphology associated with long-term potentiation. *Mol Brain*. **10**, 63

71. Labbadia, J., and Morimoto, R. I. (2015) The biology of proteostasis in aging and disease. *Annu. Rev. Biochem.* **84**, 435–464

72. Malenka, R. C., and Bear, M. F. (2004) LTP and LTD: an embarrassment of riches. *Neuron*. **44**, 5–21

73. Turrigiano, G. (2012) Homeostatic Synaptic Plasticity: Local and Global

Mechanisms for Stabilizing Neuronal Function. *Cold Spring Harbor Perspectives in Biology*. **4**, a005736–a005736

74. Groffen, A. J. A., Jacobsen, L., Schut, D., and Verhage, M. (2005) Two distinct genes drive expression of seven tomosyn isoforms in the mammalian brain, sharing a conserved structure with a unique variable domain. *J Neurochem*. **92**, 554–568

75. Yokoyama, S., Shirataki, H., Sakisaka, T., and Takai, Y. (1999) Three splicing variants of tomosyn and identification of their syntaxin-binding region. *Biochemical and Biophysical Research Communications*. **256**, 218–222

76. Cohen, L. D., Zuchman, R., Sorokina, O., Müller, A., Dieterich, D. C., Armstrong, J. D., Ziv, T., and Ziv, N. E. (2013) Metabolic Turnover of Synaptic Proteins: Kinetics, Interdependencies and Implications for Synaptic Maintenance. *PLoS ONE*. **8**, e63191–20

77. Cohen, L. D., and Ziv, N. E. (2017) Recent insights on principles of synaptic protein degradation. *F1000Res*. **6**, 675–12

78. Hakim, V., Cohen, L. D., Zuchman, R., Ziv, T., and Ziv, N. E. (2016) The effects of proteasomal inhibition on synaptic proteostasis. *The EMBO Journal*. **35**, 2238–2262

79. Hwang, J., Walczak, C. P., Shaler, T. A., Olzmann, J. A., Zhang, L., Elias, J. E., and Kopito, R. R. (2017) Characterization of protein complexes of the endoplasmic reticulum-associated degradation E3 ubiquitin ligase Hrd1. *Journal of Biological Chemistry*. **292**, 9104–9116

80. Schoebel, S., Mi, W., Stein, A., Ovchinnikov, S., Pavlovicz, R., DiMaio, F., Baker, D., Chambers, M. G., Su, H., Li, D., Rapoport, T. A., and Liao, M. (2017) Cryo-EM structure of the protein-conducting ERAD channel Hrd1 in complex with Hrd3. *Nature Publishing Group*. **548**, 352–355

81. Schulz, J., Avci, D., Queisser, M. A., Gutschmidt, A., Dreher, L.-S., Fenech, E. J., Volkmar, N., Hayashi, Y., Hoppe, T., and Christianson, J. C. (2017) Conserved cytoplasmic domains promote Hrd1 ubiquitin ligase complex formation for ER-associated degradation (ERAD). *Journal of Cell Science*. **130**, 3322–3335

82. Kaiser, P., and Wohlschlegel, J. (2005) Identification of Ubiquitination Sites and Determination of Ubiquitin-Chain Architectures by Mass Spectrometry. in *Methods in Enzymology*, pp. 266–277, Methods in Enzymology, Elsevier, **399**, 266–277

83. Collins, G. A., and Goldberg, A. L. (2017) The Logic of the 26S Proteasome.

CELL. **169**, 792–806

84. Kwon, Y. T., and Ciechanover, A. (2017) The Ubiquitin Code in the Ubiquitin-Proteasome System and Autophagy. *Trends in Biochemical Sciences*. **42**, 873–886

85. Patterson, M., and Yasuda, R. (2011) Signalling pathways underlying structural plasticity of dendritic spines. *Br. J. Pharmacol.* **163**, 1626–1638

86. Jackson, P. K., Eldridge, A. G., Freed, E., Furstenthal, L., Hsu, J. Y., Kaiser, B. K., and Reimann, J. D. (2000) The lore of the RINGs: substrate recognition and catalysis by ubiquitin ligases. *Trends in Cell Biology*. **10**, 429–439

87. Koegl, M., Hoppe, T., Schlenker, S., Ulrich, H. D., Mayer, T. U., and Jentsch, S. (1999) A novel ubiquitination factor, E4, is involved in multiubiquitin chain assembly. *CELL*. **96**, 635–644